COMPUTERIZED POWDER METALLURGY (P/M) FORGING TECHNIQUES

SEPTEMBER 1980

S. PILLAY
H. A. KUHN

TECHNICAL REPORT

UNIVERSITY OF PITTSBURGH

ENGINEERING DIRECTORATE
ROCK ISLAND ARSENAL
ROCK ISLAND, ILLINOIS 61299

DISPOSITION INSTRUCTIONS:

Destroy this report when it is no longer needed. Do not return it to the originator.

DISCLAIMER:

The findings of this report are not to be construed as an official Department of the Army position unless so designated by other authorized documents.

UNCLASSIFIED
SECURITY CLASSIFICATION OF THIS PAGE *(When Data Entered)*

REPORT DOCUMENTATION PAGE

READ INSTRUCTIONS BEFORE COMPLETING FORM

1. REPORT NUMBER: EN-80-02	2. GOVT ACCESSION NO.
3. RECIPIENT'S CATALOG NUMBER	
4. TITLE *(and Subtitle)*: COMPUTERIZED POWDER METALLURGY (P/M) FORGING TECHNIQUES	5. TYPE OF REPORT & PERIOD COVERED: Technical Report - Final
6. PERFORMING ORG. REPORT NUMBER	
7. AUTHOR(s): Suresh Pillay; Howard Kuhn	8. CONTRACT OR GRANT NUMBER(s): DAAA08-78-C-0013
9. PERFORMING ORGANIZATION NAME AND ADDRESS: University of Pittsburgh, Pittsburgh, PA 15261	10. PROGRAM ELEMENT, PROJECT, TASK AREA & WORK UNIT NUMBERS
11. CONTROLLING OFFICE NAME AND ADDRESS: Engineering Directorate, Rock Island Arsenal, Rock Island, IL 61299	12. REPORT DATE: September 1980
	13. NUMBER OF PAGES
14. MONITORING AGENCY NAME & ADDRESS*(if different from Controlling Office)*	15. SECURITY CLASS. *(of this report)*: Unclassified
	15a. DECLASSIFICATION/DOWNGRADING SCHEDULE

16. DISTRIBUTION STATEMENT *(of this Report)*

Approved for public release; distribution unlimited.

17. DISTRIBUTION STATEMENT *(of the abstract entered in Block 20, if different from Report)*

18. SUPPLEMENTARY NOTES

19. KEY WORDS *(Continue on reverse side if necessary and identify by block number)*

1. Computer-aided design
2. Preform design
3. Powder metallurgy
4. Powder forging

20. ABSTRACT *(Continue on reverse side if necessary and identify by block number)*

Forging of sintered powder preforms is an attractive manufacturing alternative to conventional forging as it combines the cost and material saving advantages of conventional, press-and-sinter, powder metallurgy and the property enhancement of forging. The preforms contain a dispersion of voids, and forging of such materials into finished shapes must be accomplished such that no defects are formed and all residual porosity is eliminated. These objectives can be achieved through the proper design of the powder preform. The design currently is accomplished through a lengthy trial-and-error procedure.

DD FORM 1 JAN 73 1473 EDITION OF 1 NOV 65 IS OBSOLETE

UNCLASSIFIED
SECURITY CLASSIFICATION OF THIS PAGE *(When Date Entered)*

Empirical design rules have been established, from simple model experiments, to facilitate the proper design of preforms. Application of these rules to complex components requires an understanding of the behavior of porous materials with respect to densification, flow and fracture and the effects of die design, lubrication and temperature.

An interactive computer-aided design approach was developed to facilitate the design and evaluation of preforms. The design was accomplished in two phases. The first phase described the part to be forged together with a schematic subdivision of the part into regions. The second phase involved the specification of trial preform shapes for the part. The program evaluated the input shape for densification and non-aggravating metal flow. This was accomplished by recognizing characteristic deformation modes in the input shape for which available design rules have been programmed. By interactively manipulating the preform shape, a proper preform may be obtained rapidly. The program determines the size and mass distribution required in the preform to achieve full densification.

The present program was implemented for non-axisymmetric parts with a reasonably complex geometry. The procedure developed was applied to a weapon component wherein the designed preform was trial forged and metallurgically evaluated. The success of the forging encourages further study to extend the accuracy and capabilities of the present approach to other part configurations.

FOREWORD

This report was prepared by Professor Howard Kuhn and Dr. Suresh Pillay of the University of Pittsburgh, Pittsburgh, PA in compliance with Contract No. DAAA08-78-C-0013 under the direction of the Engineering Directorate, Rock Island Arsenal, Rock Island, Illinois, with Mr. Mukesh Solanki as Project Engineer.

This project was accomplished as part of the US Army Manufacturing Technology Program and was administered by the US Army Industrial Base Engineering Activity. The primary objective of this program is to develop, on a timely basis, manufacturing processes, techniques, and equipment for use in production of Army material.

TABLE OF CONTENTS

1.0 PROBLEM DEFINITION AND SCOPE

1.1 Introduction

Powder forging is a hybrid process in which preforms made by conventional press-and-sinter powder metallurgy (P/M) techniques are hot forged in closed impression dies. The process is not new; although production of structural parts via the powder forging route is very recent. The earliest application of this process, circa 1910, was the development of tungsten wires and filaments hot forged from pressure compacted, pre-sintered tungsten.[1]*

During the last few years, the automotive industry expanded the use of conventional press-and-sinter methods to parts with increasingly larger dimensions and strength. The requirements of size and strength quickly exceeded the capacity of the conventional process. Residual porosity was the main cause for the degradation of strength levels. To meet the required property standards, the feasibility of appending the hot forging process to the standard P/M process sequence of pressing and sintering was investigated. This resulted in a significant reduction in the level of residual porosity and, consequently, improvement in the strength levels. However, the dynamic properties of impact and

---

*Parenthetical references placed superior to the line of text refer to the bibliography.

fatigue strength fell short of those in conventional cast or wrought materials.

Considerable enhancement of dynamic property levels were obtained when significant amounts of plastic deformation and lateral flow were permitted during hot forging. Powder preform forging, then, gained attention as a viable alternate route for the production of high strength parts. The process successfully combined the advantages of conventional powder metallurgy, viz, high production rates superior material utilization as a result of elimination of much or all finish machining ability to form complex components with excellent surface finish in one forging blow, and the property enhancement of true forging.

The requirement of lateral metal flow during densification of a porous compact introduces two adverse conditions that make the powder preform process somewhat complex and difficult to control. Firstly, the porosity is in the form of voids which provide ample sites for the occurrence of fracture. Secondly, as in the case of conventional forging, excessive material flow leads to pronounced die wear. For a successful process, suitable process parameter selection is required so that metal flow is controlled between the lower limit to fully densify the porous preform for acceptable properties and the upper limit for fracture and excessive die wear. Proper preform design is the single most important parameter, and this has been

demonstrated in numerous earlier studies.[2-4]

Rational design of powder preforms for complex shapes requires knowledge of densification, flow and fracture behavior of the material, and the effects of die design, lubrication and temperature on this behavior. Preform design guidelines have been established for commonly occurring axisymmetric parts.[4] These guidelines were developed from relatively simple model experiments, and successfully applied to specific parts. However, in the present development of powder forging, the design of preforms to forge into complex parts is done by extensive trial-and-error effort. This trial-and-error effort is usually the rate limiting step in the development of the powder forging process.

1.2 Problem Definition

The current research program is directed towards a rational design of preforms for powder forging, without the extensive laboratory trial-and-error effort. A Computer Aided Design (CAD) approach is followed, with the aim of reducing the lead time from the inception of the process to successful prototype forging. To demonstrate the validity and evaluate the merit of this approach, reasonable goals have been set. Specifically, the goals are to (i) develop a general approach, as far as possible, to input the data regarding the shape of the finished part and material, (ii)

develop a preform design scheme for the part, (iii) design the preform for a specific part using the CAD approach, (iv) forge the preform designed in step (iii), and (v) critique the merit and limitations of this approach.

The success of CAD of preforms for powder forging depends upon the availability of quantitative information at various phases of the design. At the present state of development, this information is scant. Available information, in the form of empirical guidelines, is predominantly for axisymmetric shapes. The specific part is a weapon component and is non-axisymmetric. The preform for this part is to be designed using the proposed CAD approach and evaluated. Applicable results of axisymmetric parts, together with limited information generated during the course of this program are used to formulate the preform design scheme. The accuracy of the design process, then, is restricted by the amount of data that is presently available. Further research is needed to improve the design strategy. A goal of the current program is also to explicitly define the avenues of future activity.

The current work is organized as follows:

(i) Review of the process parameters for the powder forging process, and identify the effects of each parameter on the overall process.

(ii) Review the state of analytical techniques pertaining to deformation of sintered powder compacts.

(iii) Definition of a logical basis for an interactive computer-aided design approach. This is followed by the implementation of the basis.

(iv) Actual design of a preform for the weapon component, together with prototype forging and evaluation.

2.0 SINTERED POWDER FORGING: OVERVIEW OF PROCESS PARAMETERS

2.1 Introduction

The pictorial production route for the manufacture of powder forgings is illustrated in Figure 1. The pictorial manufacturing route for a typical conventional hot forging is also included for comparison.[5] In the conventional forging route, the hot billet is usually subjected to a succession of blows, in a series of dies, to develop the final shape. Subsequent machining operations follow to produce the finished part, Figure 2. In the powder forging route, the loose powder is compacted to a preform which is sintered and hot forged, in one forging blow, in one set of dies, to produce the finished part which may require little or no subsequent machining. This results in a reduction of the actual forging cost and great improvement in press utilization. The major reasons why this is possible are:

(1) The forging characteristics of a hot powder preform differ significantly from those of a wrought billet.

(2) Metal can be located in the preform where it is required, and hence material redistribution during forging is minimized.

(3) The absence of flash reduces the forging load required.

The success of a powder forging depends upon the proper location of metal in various regions of the preform. This

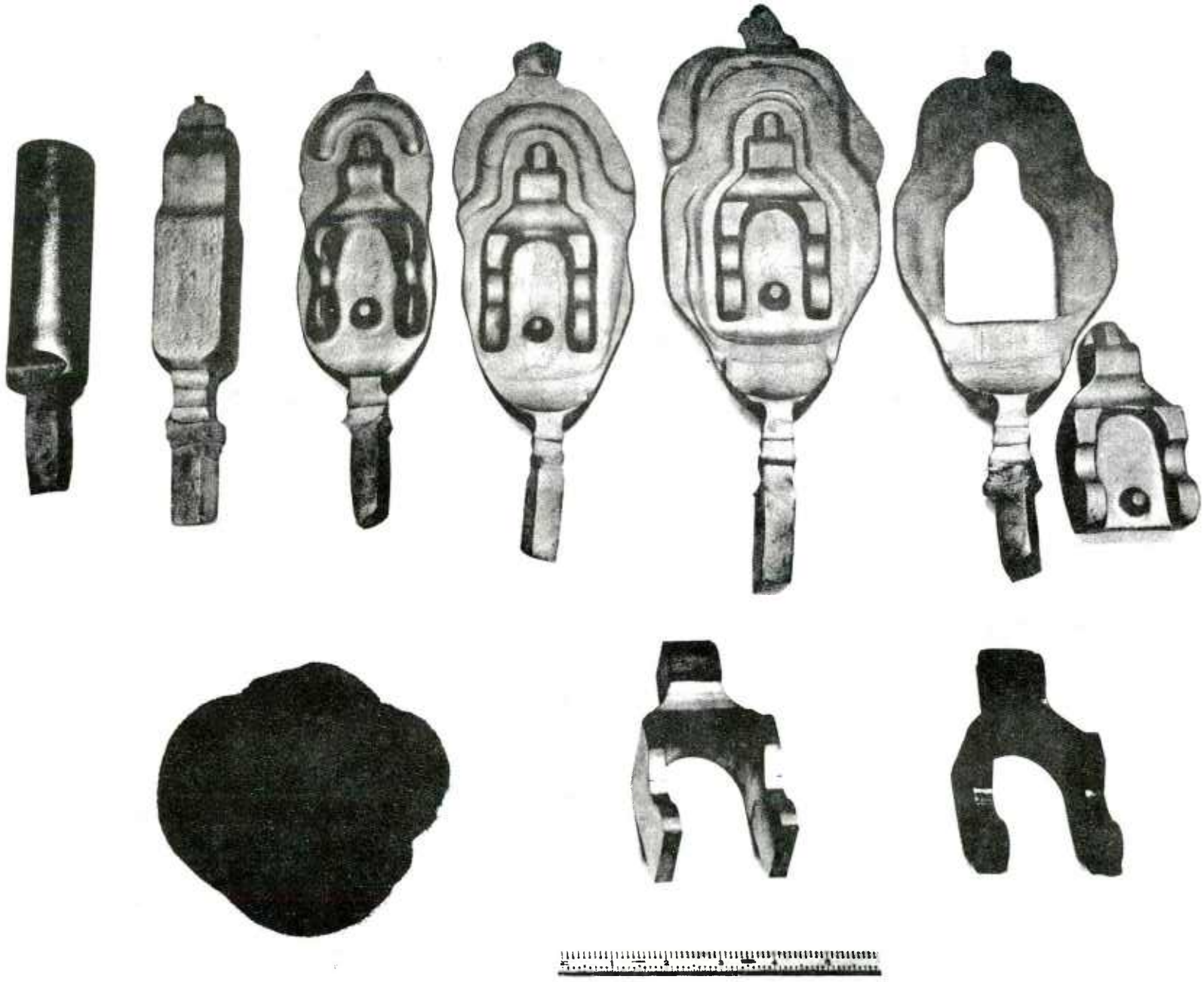

Figure 1. Pictorial comparison of conventional forging and powder forging processes.(5)

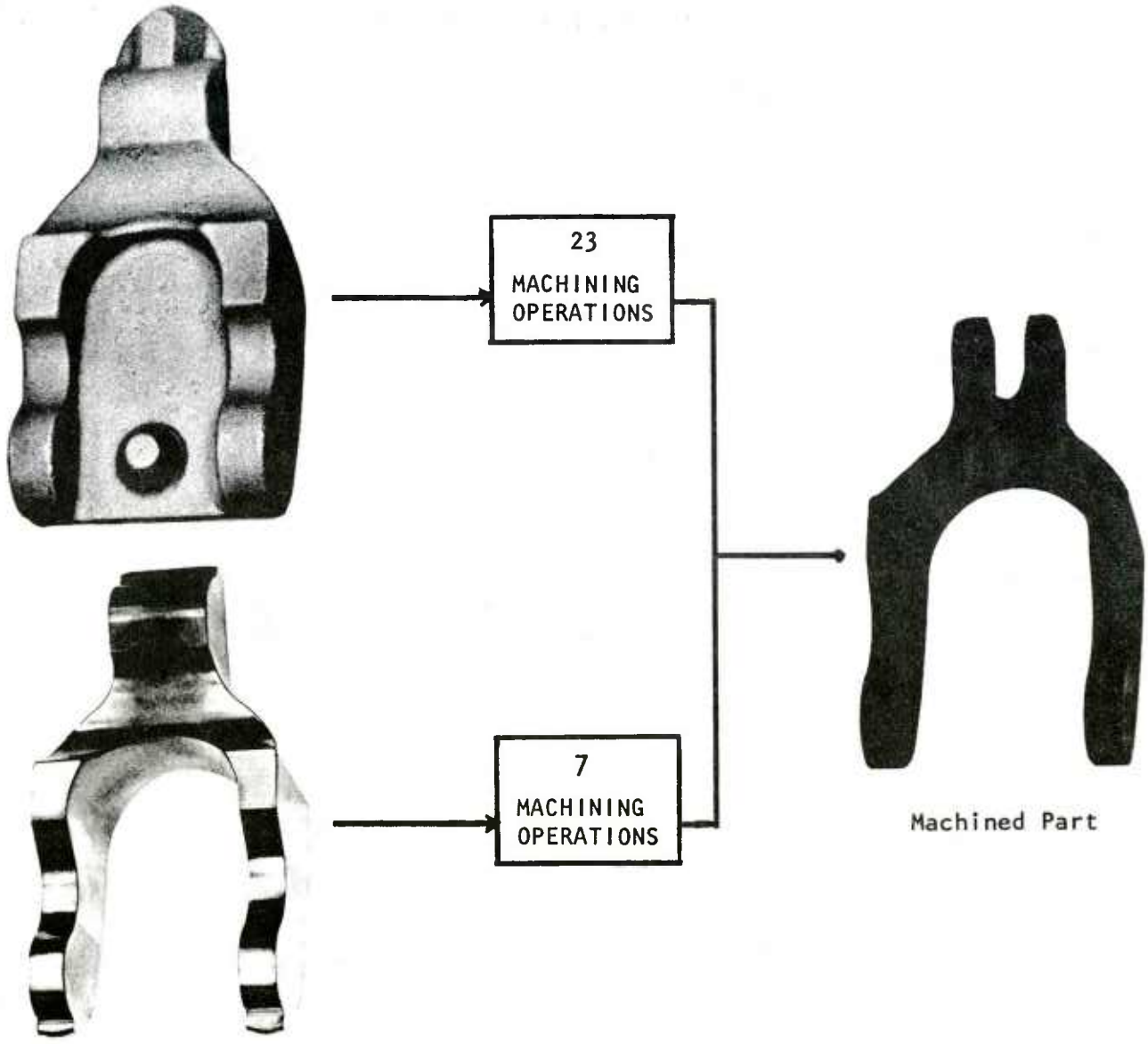

Figure 2. Comparison of number of required machining operations for conventionally and P/M forged parts.(5)

influences the metal flow during the forging stage and the structural homogeniety of the finished part. The ductility of porous preforms is severely limited due to porosity, hence fracture is a severe problem. Consequently, preform design is critical.

Two options for hot working the porous preform are available, namely,

(i) the preform has a form that corresponds closely to the finished part. In this case, hot working is essentially simple compaction with very little metal flow. This process is termed "hot repressing".

(ii) the preform has a very simple shape but correct weight and most of the shape detail is developed during forging by metal flow. This process is of interest to the current investigation because it imparts better properties to the finished part than hot repressing.

2.2 Mechanical Properties

Production of structural components from powder, on a competitive basis vis-a-vis wrought products, requires that the final material be free of residual porosity. This, however, is not a sufficient condition to guarantee optimal resistance to crack propagation in impact or cyclic loading. The mode of densification has an important bearing on this aspect.[6]

In hot repressing of porous preforms, there is little or no metal flow in the lateral direction to the applied pressure. Densification ensues as a result of simple pore flattening. In the absence of relative motion between the collapsed pore surfaces, oxides or other contaminant layers on the internal surfaces of the pores mitigate against the development of a strong mechanical bond across the interface. This results in poor dynamic properties for the finished part. In upset forging, where lateral metal flow is permitted, the presence of relative motion between collapsing pore surfaces leads to rupturing of the oxide layers. This promotes the possibility of a sound metallurgical bond.(7)

Static properties, viz, tensile strength and ductility, are comparable to wrought products in preforms that are fully densified by either repressing or upset forging. The enhancement of Izod values obtained by upset forging is shown, in Figures 3 and 4, for varying degrees of lateral metal flow. Like toughness, fatigue strength is also increased by the presence of lateral metal flow.(8)

The effect of initial preform density on the forging process is evident. If material flow were the only consideration, maximum toughness is to be expected at some intermediate level of initial preform density. The rationale is that at low initial preform densities, much of the material flow serves only to close up porosity without significant shear and interparticle movement. Conversely, at

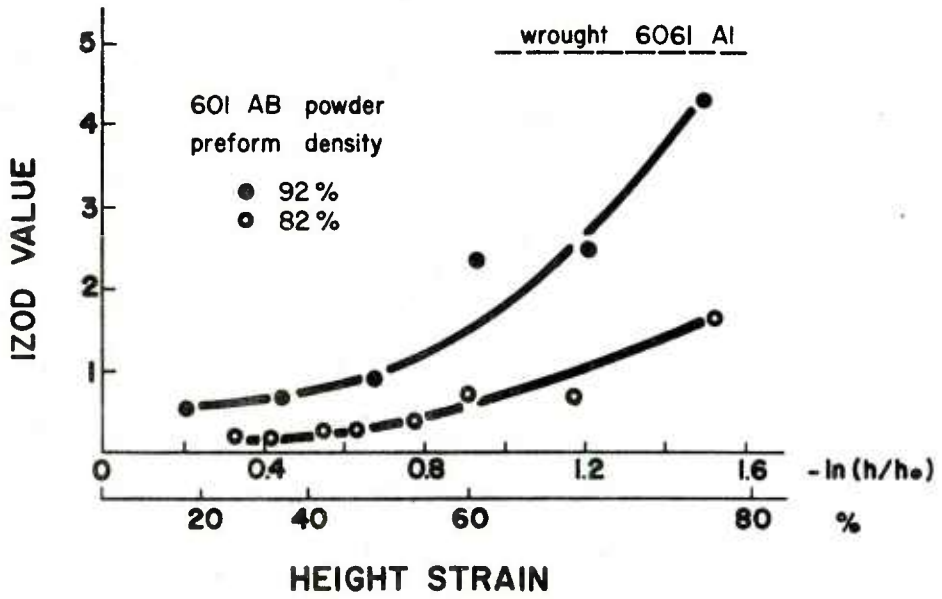

Figure 3. Impact resistance of 601AB aluminum alloy, hot forged to full density as a function of height strain (and hence lateral flow). (3)

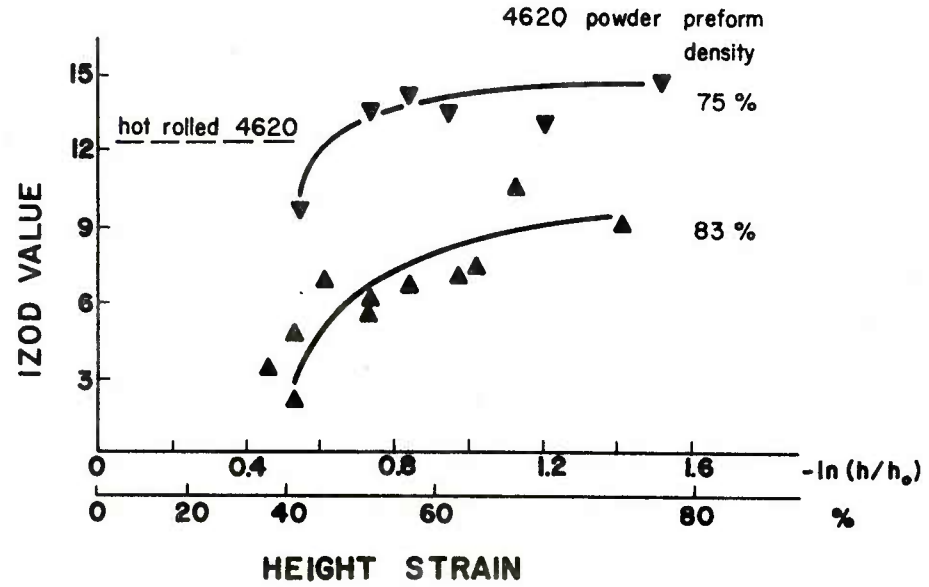

Figure 4. Impact resistance of 4620 steel alloy, hot forged to full density as a function of height strain.(3)

too high a starting value of preform density, insufficient deformation is imparted to the preform, for interparticle displacements, to promote integrity of bonding across collapsed pore surfaces.

Superimposed on metal flow, effect(s) of phenomena intrinsic to the material are also exhibited. In the case of aluminum alloy powders, preforms with lower initial densities have greater pore surface area per unit volume and hence higher levels of the tenacious oxide film. Consequently, preforms of 92% initial density result in higher levels of toughness than those of 82% initial density. By comparison, it is the lower initial preform density (75% cf 85% theoretical) that results in optimum toughness in low alloy steel powder forgings. This is attributed to the fact that the lower density preform have a significantly larger amount of interconnected porosity; during sintering, the oxide reducing gas can penetrate to a greater extent resulting in a lower final oxide content.[3] Toughness achieves a saturation value after about 50% height reduction for the steel powder, whereas, for the aluminum alloy powders no saturation behavior is exhibited.

2.3 Workability

Sintered powder preforms typically consist of 10-30% porosity in the form of voids at the interstices between

powder particles. These voids act as sites for crack initiation and aid in crack propagation during deformation. Consequently, the ductility of preforms is severely restricted.

In order to assess the extent of deformation that may be imparted to a material prior to fracture, the concept of workability or formability was introduced. This concept was first put forth for sheet metal working,[9] and then extended to bulk forming processes.[10]

Workability is defined as the degree of deformation that can be achieved in a particular metal working process without fracture. In general, workability depends upon the local conditions of stress, strain, strain-rate and temperature in combination with material characteristics. The stress and strain rate in a material undergoing deformation is not uniform, but varies from point to point. This, in turn, is determined by process parameters associated with die design, preform geometry and lubrication. Control of these parameters is used to produce conditions favorable for enhanced deformation prior to fracture.

These concepts may be qualitatively expressed as

$$\text{Workability} = f(\text{material}) \times g(\text{process})$$

where, in this relationship, 'f' is a function of the basic ductility of the material and 'g' is a function of the stress system imposed by the process, in particular, the secondary tensile stresses generated during deformation. Thus, a

workability analysis would include (i) a fracture criterion, 'f', expressing the stress and/or strain states at fracture as a function of the strain-rate and temperature; and (ii) a description of the local stress, strain, strain-rate, temperature histories, 'g', at potential fracture sites in the material during deformation. The workability analysis consists of comparing the local conditions existing in the material, for a given set of process variables, to the limiting conditions expressed by a fracture criterion.

The determination of the material function applicable to a broad range of stress and strain states is critical to a workability analysis. Lee and Kuhn[11] successfully determined such a criterion from upset tests on circular cylinders. The upset test is particularly flexible as by varying (i) the cylinder aspect ratio (height to diameter ratio) and (ii) the lubrication at the die contact surfaces, the barrelling severity and hence the secondary tensile stresses developed on the bulge surface can be varied over a wide range. The results are shown in Figure 5. Strain paths are obtained from grid measurements taken at the bulge surface on an equitorial diametral plane. The strain paths are process dependent and their terminal points, determined by visual observation of fracture, appear to lie on a straight line with a slope of one-half. This linear relationship has been demonstrated for a variety of materials, including sintered powder materials, both during

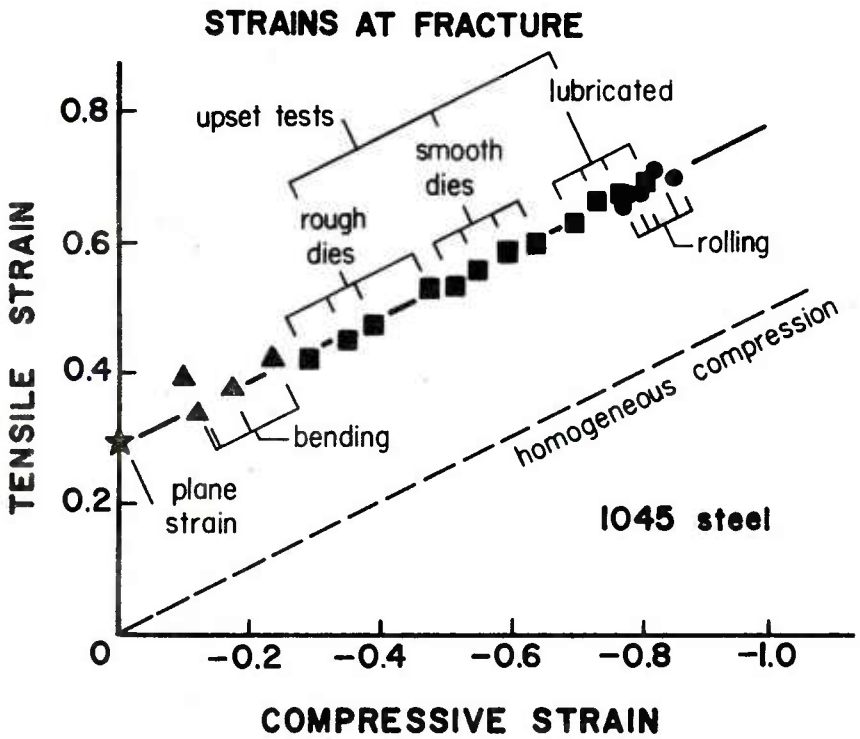

Figure 5. Experimental fracture strains in bulk forging of wrought 1045 steel. (11)

hot and cold forging.[3] The intercept of the line with the tensile strain axis changes in accordance with the inherent ductility of the material.

The workability limit diagram ,Figure 5, applies for free surface fracture. The presence of hydrostatic pressure tends to retard the initiation of fracture. It has been shown[4] that the workability diagram is raised, towards larger deformation to fracture, in the presence of hydrostatic pressure.

2.4 Fracture

A variety of fractures and defects occur in a sintered powder forging process. Their location and occurrence are, in general, controlled by the process parameters. Typical fractures that occur, are illustrated in Figure 6 and, may be classified as follows:

2.4.1 Free Surface Fracture

This type of fracture occurs on the expanding free surface of a deforming preform, before contact with the die walls. The cracks developed on the bulge surface of an upset cylinder is typical of this type of fracture. The occurrence is attributed to the secondary tensile stresses developed due to friction at the die/workpiece interface.

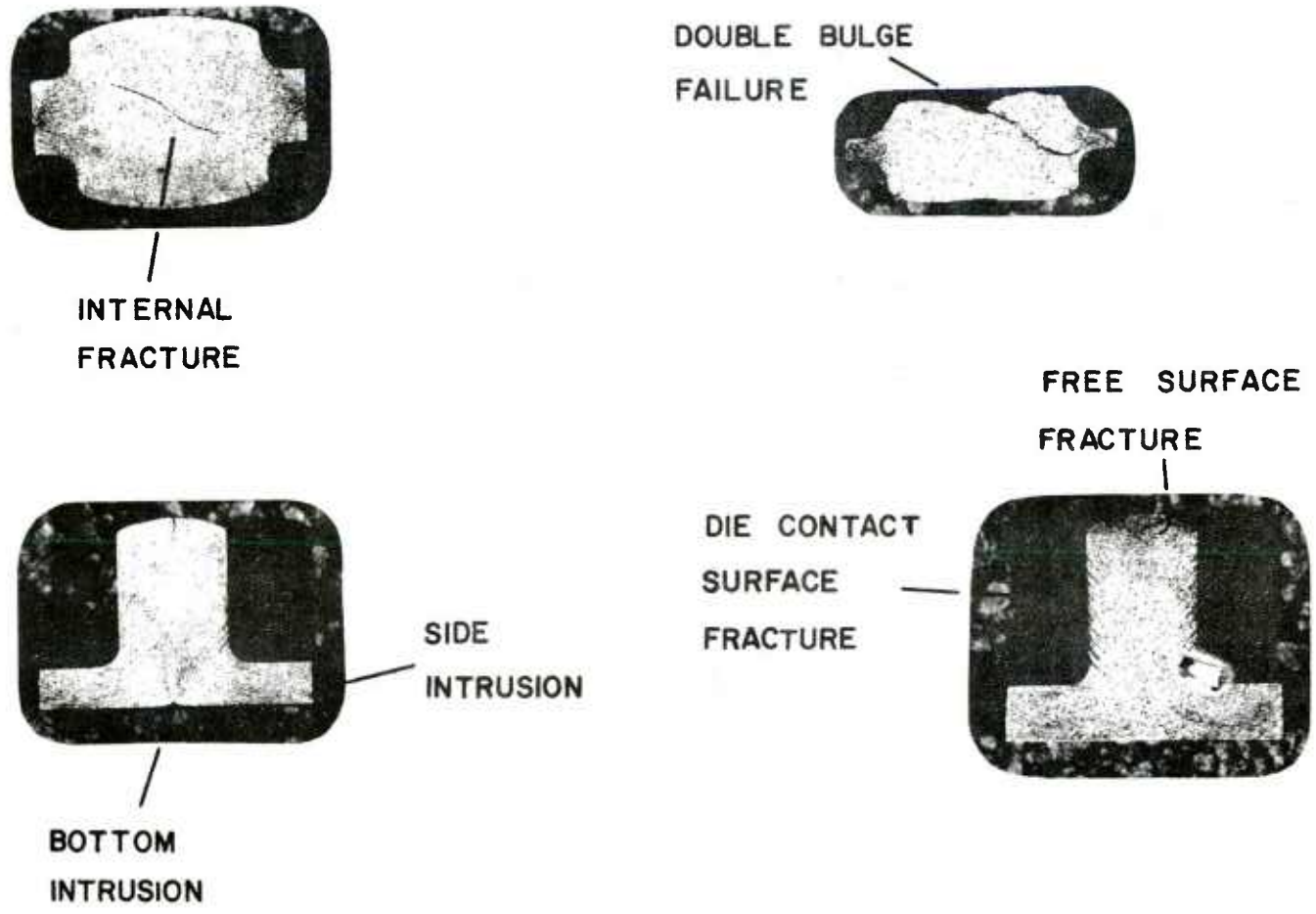

Figure 6. Fracture and defects in cold extrusion of sintered 601AB aluminum alloy preforms.

2.4.2 Die Contact Surface Frature

This class of fracture occurs at the die/workpiece interface. A common location for the initiation is in the vicinity of a punch or die corner where metal flow changes direction. They do not usually propagate throughout the workpiece, but does severely detract from the surface finish.

Fundamental studies on hub extrusion by Suh[4] show that a concentration of shear deformation combined with tension or low values of hydrostatic pressure in the vicinity of a corner lead to the initiation of this fracture. Non-uniform lubrication, also, plays a role. The occurrence may be suppressed by providing generous radii and uniform lubrication at these sites, as both contribute to reducing the magnitude of tensile stresses.

2.4.3 Internal Fracture

Unlike free surface and die contact fractures, internal fractures occur inside the workpiece and rarely penetrate to the surface. As a result, they may go undetected and possibly lead to catastrophic failures during service. Central bursts during extrusion are an example of this class of fractures.

The center of double hub extrusions is a potential site for an internal fracture. Experimental studies of Suh[4]

indicate that the occurence of internal fracture correlate with the geometry of the deformation zone. Die lubrication has little effect.

2.4.4 Intrusion Defects

Intrusion defects, although not fractures, also occur during forging. They manifest as a surface disturbance, and detract from a uniform surface finish. The occurrence of these defects are generally geometry related, with lubrication having little effect.

2.5 Fracture Prevention

A comprehensive study of fractures and their prevention for simple axisymmetric powder forgings is presented elsewhere.[4] As mentioned in the earlier sections, deformation zone geometry, and consequently the preform geometry, have an important bearing on the likelihood of fracture. Due to the limited ductility of a porous preform, control of metal flow becomes critical. The metal flow that occurs under actual conditions is determined by the preform shape and its relation to the shape of the dies. A subtle change in the preform shape can significantly alter the metal flow and the likelihood of fracture. This fact is illustrated in Figure 7.

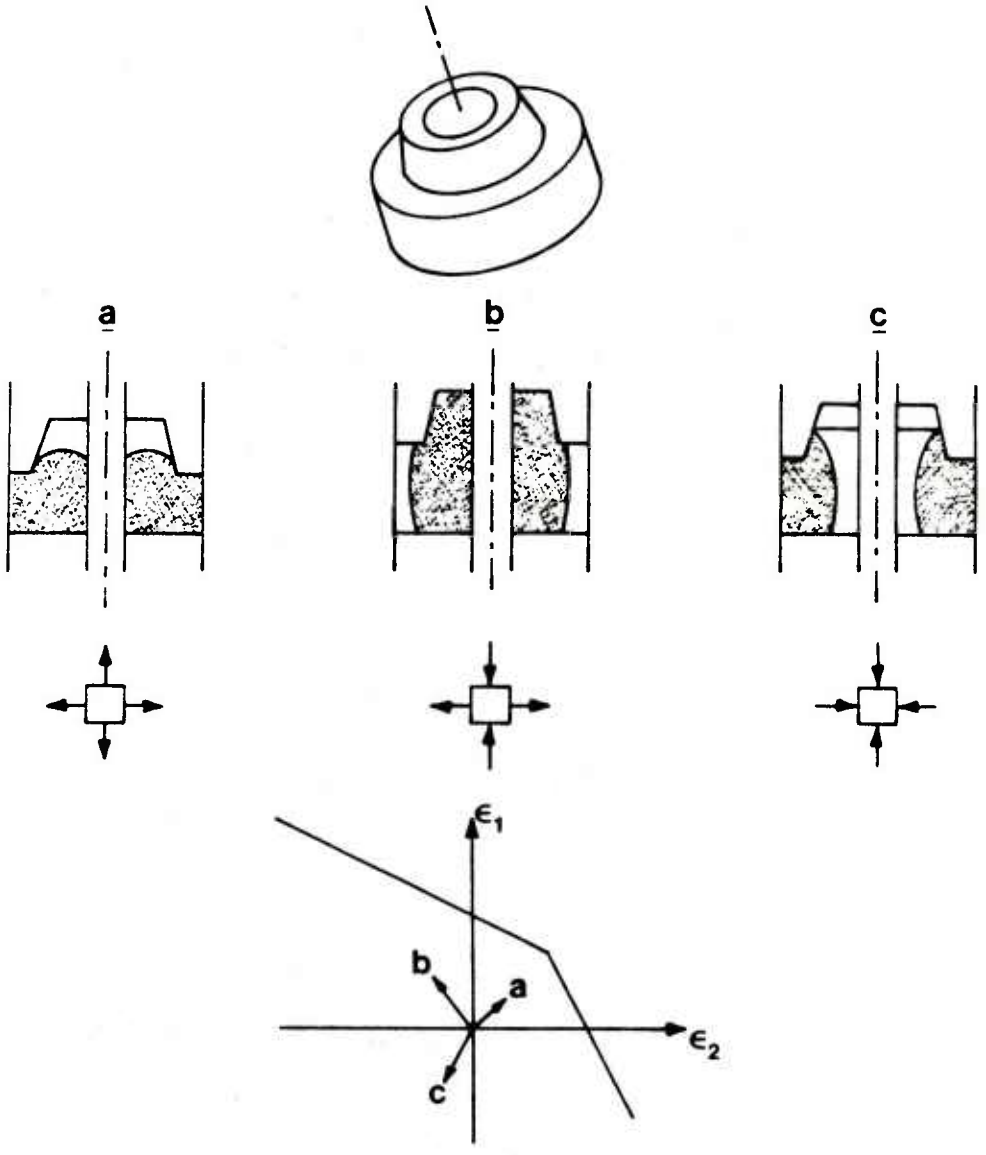

Figure 7. Preform options for forging an axisymmetric component consisting of a flange and hub with central hole.(3)

The component forged is axisymmetric, consisting of a hub, a flange and a central hole. Three preform options may be pursued. Option 1 is to have the preform fill the flange, so that the hub is formed by back extrusion. Option 2 is to have the preform fill the hub, so that the flange is formed by radially outward metal flow. Finally, option 3 is an intermediate shape, where metal flow is directed radially inward toward the mandrel and up into the hub.

The likelihood of free surface fracture in each of these preform options may be examined by studying the strain states at the free surface along with the workability diagram, Figure 5. Typical strain states which occur are shown in Figure 7. In preform option 1, the strain path is located in the first quadrant, the biaxial strain state being developed due to frictional constraint at the mandrel and the hub surfaces, and fracture is a strong possibility. In preform option 2, the strain path is in the second quadrant, hence a larger deformation to fracture may be expected. In option 3, the strain state developed is biaxial compression and fracture is remote.

Thus from qualitative arguments based on observation of simple model experiments, a workable preform geometry may be inferred. Experiments have verified that preform option 3, in the above example, results in a defect free forging, whereas the other two preform options exhibit the fractures as expected.[3]

2.6 Lubrication and Temperature Effects

Friction at the interfaces between the deforming preform and the dies leads to a non-homogenous deformation and, consequently, results in non-uniform densification. The effect of lubrication on densification is shown in the macrographs, Figure 8, for an upset forged cylinder. In the unlubricated case, the void patterns are markedly different in various regions due to variation in the stress state. The lubricated case indicates a more uniform void distribution indicative of a more uniform densification.

The degree of non-uniformity in densification has important practical implications, particularly in the case of hot forging. A typical powder forging process generally involves some flow till the free surfaces of the preform contact with the die walls. If lubrication is poor, the free surface develops enlarged voids. When the hot deforming preform contacts the relatively cooler die walls; the flow stress is increased due to die chill and it becomes more difficult to close up the voids with increasing pressure. As a result, it is common to find residual porosity at the surfaces of hot forged components. A provision for good lubrication is beneficial in the sense that it allows for a more uniform densification and pore flattening.

Good lubrication also results in lower forging loads during the upset forging stage. From a workability point of

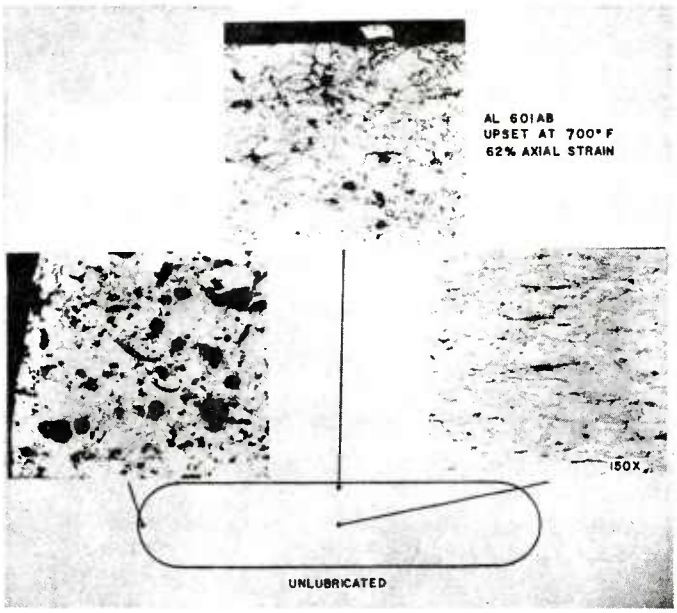

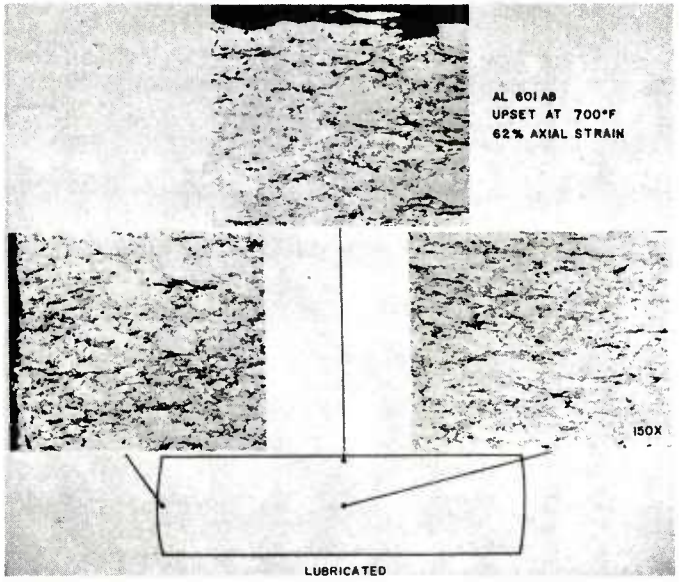

Figure 8. Macrographs of densification characteristics of 601AB aluminum alloy powder preforms upset without and with lubrication.(3)

view, lubrication affects the strain path which, in turn, determines the deformation to fracture. Good lubrication leads to larger deformation to fracture.

2.7 Discussion

The aim of a successful powder forging process is towards the production of a uniformily densified, defect free part with the available press capacity. A brief summary of the process and the parameters were described in the earlier sections. It is evident that the complexity of the forging process, with its complex interplay of parameters, precludes exact quantification. As a result, considerable experience is required for process designers to achieve their goal. Proper preform design is the key to a successful process. Guidelines and recommendations have been generated over the years, and these form the basis for the present and future work.

Prior to the actual design of a preform, prerequisite information is required regarding its compaction from loose powder. Mechanical property requirements in the finished part suggest a minimum initial preform density. The experimental evidence, referenced in section 2.2, indicate that for low-alloy steel powders, an initial preform density of 78-80% theoretical is optimum. Compaction of the preform to the required density may be achieved either by die compaction or isostatic compaction, the choice of the

compaction process being determined by the geometry of the preform. For die compaction, compaction pressures in the range of 40-50tsi[5] are required. This requirement, together with the available press capacity, limit the plan area of the preform that may be compacted.

Prevention of fracture during powder forging is the prime consideration for preform design. Proper preform shape and size is required to obtain a controlled metal flow to avoid fracture and undensified regions. In the case of hot repressing, lateral flow is negligible and fracture is not a severe problem. However, the distribution of mass in the preform, especially in regions of changing geometry, is critical to achieve a uniformily densified part. Considerable trial-and-error effort is required to determine this mass distribution for a complex part.[5] In powder forging, the presence of flow and the possibility of fracture add considerably to the uncertainities. Shape and size of the preform become interrelated where the shape controls the fracture likelihood and the size controls the mass distribution.

The workability analysis, in principle, has been successfully applied to preform design for simple configurations.[4] The material function, 'f', was determined from upset tests conducted at the desired forging temperature. The process function, 'g', however, was experimentally addressed by strain measurements at potential

fracture sites. Fracture likelihood was then inferred.

A quantitative prediction of fracture, with respect to process parameters, is a complex task. A detailed analytical simulation of the deformation, together with a fracture criterion, at potential sites, appears to be the approach. To this end, the state of analytical development is reviewed and assessed in the following chapter.

3.0 ANALYTICAL TECHNIQUES FOR FORGING OF SINTERED POWDER PREFORMS

3.1 Introduction

In the development of the theoretical mechanics of plastic deformation of any material, it is first necessary to establish a criterion of yielding and then a flow rule from which the relations between stress and strain are derived. For plastic deformation of a conventional, full density, cast and wrought material, the von Mises yield criterion and the resulting Levy-Mises stress-strain equations are applicable.

Densification accompanying deformation of a sintered powder material leads to the violation of the fundamental assumption of incompressibility of classical plasticity theory. Therefore, the yield criterion for porous materials must include the effect of hydrostatic stress.

Kuhn et al (12) and Shima[13] derived the yield criterion following an experimental approach. Shima assumed the yield function for a sintered porous material to be a linear combination of the yield function of the incompressible matrix and the hydrostatic stress. The constants were determined from uniaxial compression tests and correlated to the relative density, ρ , of the porous compact. From studies on uniaxial compression tests, Kuhn[14] observed a correlation between the plastic Poisson's ratio, ν , and the

relative density ρ. The empirical relation

$$\nu = 0.5\rho^{a} \qquad (3\text{-}1)$$

was exhibited for the density range $0.7 < \rho < 1.0$. The exponent 'a' varied between 1.92 and 2.0, and was insensitive to material and temperature. As densification progresses, the plastic Poisson ratio approaches 0.5, which is the value for conventional fully dense materials. The yield criterion was presented as

$$f = \{ 3J_2' - (1 - 2\nu) J_2 \}^{\frac{1}{2}} \qquad (3\text{-}2)$$

A comparitive study of various yield criteria published on porous materials was presented by Honess.[14] This study demonstrated that equation (3-2) correlated best with various experiments. On this basis, the present analytical effort exclusively uses equations (3-1) and (3-2).

3.2 Basic Equations

3.2.1 Yield Behavior

The yield criterion represented by equation (3-2), in three dimensional stress space, is an ellipsoid whose major axis coincides with the direction of the hydrostatic stress vector. The intersection of the yield surface with the π-plane is a circle. As densification progresses, the yield

surface expands predominantly along the hydrostatic stress direction. In the limit, when ν approaches Ø.5, the ellipsoid degenerates to the classical Mises cylinder. This is schematically illustrated in Figure 9.

3.2.2 Flow Rule

In conventional plasticity theory, the flow rule is obtained from the normality between the incremental strain vector and the yield surface. Assuming that this is valid in the case of sintered powder materials, we have

$$d\varepsilon_{ij} = d\lambda \cdot df/d\sigma_{ij} \tag{3-3}$$

Substituting (3-2) into (3-3), in component form, we have

$$\begin{aligned} d\varepsilon_{11} &= (d\lambda/f)\ \{\ \sigma_{11} - \nu(\ \sigma_{22} + \sigma_{33}\ )\} \\ d\varepsilon_{22} &= (d\lambda/f)\ \{\ \sigma_{22} - \nu(\ \sigma_{33} + \sigma_{11}\ )\} \\ d\varepsilon_{33} &= (d\lambda/f)\ \{\ \sigma_{33} - \nu(\ \sigma_{11} + \sigma_{22}\ )\} \end{aligned} \tag{3-2a}$$

The term $(d\lambda/f)$ is evaluated by defining the equivalent stress, $\bar{\sigma}$, and the incremental equivalent strain, $d\bar{\varepsilon}$, for the porous compact. Following Hill,[15] the effective stress is given by

$$\{\ \frac{(1+\nu)}{3}\ \{\ (\sigma_{11}-\sigma_{22})^2+(\sigma_{22}-\sigma_{33})^2+(\sigma_{33}-\sigma_{11})^2\ \} + \frac{1-2\nu}{3}(\sigma_{11}+\sigma_{22}+\sigma_{33})^2\} \tag{3-4}$$

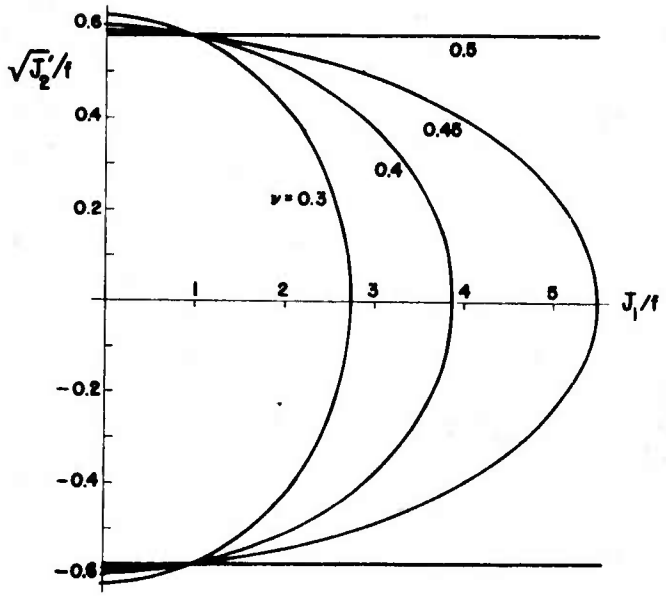

Figure 9. Yield locus predicted by plasticity theory for porous materials. Axes represent the second invariant of the stress deviator(shear) and the first invariant of the stress tensor(hydrostatic pressure). (3)

The plastic work done per unit volume of the compact is

$$\bar{\sigma}d\bar{\varepsilon} = \sigma_{11}d\varepsilon_{11} + \sigma_{22}d\varepsilon_{22} + \sigma_{33}d\varepsilon_{33} \tag{3-5}$$

Using (3-3a) and (3-4), the incremental equivalent strain is obtained as

$$\left\{ \frac{1}{3(1+\nu)} \left\{ (d\varepsilon_{11}-d\varepsilon_{22})^2+(d\varepsilon_{22}-d\varepsilon_{33})^2+(d\varepsilon_{33}-d\varepsilon_{11})^2 \right\} + \frac{(1-2\nu)}{3}(d\varepsilon_{11}+d\varepsilon_{22}+d\varepsilon_{33})^2 \right\}^{\frac{1}{2}} \tag{3-6}$$

and

$$(d\lambda/\mathbf{f}) = (d\bar{\varepsilon}/\bar{\sigma}) \tag{3-7}$$

3.2.3 Densification

The densification of the porous compact is determined through conservation of mass. In general, during deformation, density gradients may develop in the domain of the compact. The equation of conservation of mass is given by

$$\partial\rho/\partial t + u_k \, \partial\rho/\partial x_k + \rho\partial u_k/\partial x_k = 0 \tag{3-8}$$

where u_k : components of the velocity vector.

x_k : coordinates of a point.

k : is the summation index.

3.3 Application to Simple deformations

The plasticity theory developed above has been applied to predict the densification and deformation of a porous compact in simple applications, namely, frictionless uniaxial compression, plane strain compression, repressing and hydrostatic compression. The results are presented in Reference 3, and good predictive capability was demonstrated, establishing the soundness of the theory and its underlying principles. In the above applications, frictional constraint at the die surfaces is zero or does not influence the deformation hence, the densification is uniform. As a result, equation (3-8) may be simplified and cast in an incremental form

$$-d\rho/\rho = d\varepsilon_{11} + d\varepsilon_{22} + d\varepsilon_{33} \qquad (3\text{-}8a)$$

The govering equations can be integrated in closed form with this simplification. However, when friction at the die surfaces contributes to non-uniform densification, a closed form solution to simple deformations is not feasible. Numerical techniques have to be resorted to, and this constitutes the main effort of this chapter.

3.4 Approximate Techniques

Exact solutions to conventional plasticity problems are lacking except for very simple, idealized deformations.

Approximate techniques were developed, which are listed in order of increasing sophistication and effort, as follows:

(1) Slab or Equilibrium Analysis.

(2) Upper Bound Techniques.

(3) Finite Element Method.

The slab analysis can predict the effect of interface friction and other process parameters on the total forging load. The upper bound technique minimizes the deformation energy resulting from an assumed, kinematically admissible, velocity field and yields a closer approximation to the total forging load. Both techniques are incapable of detailed prediction of stress and strain distributions. The finite element method can predict distributions of stress and strain in the deforming material. However, applications are presently limited to simple geometries due to the extensive computational effort and complexities in the numerical procedures. This method is currently being researched intensely.

With the objective of developing comparable approximate techniques for sintered powder materials, two techniques are presented. The first is the slab analysis, which is capable of predicting approximations to the total load and density distributions in the presence of friction at the die walls. The second technique is a hybrid scheme, based on an energy bounding principle but, numerically similar to the finite element method. This scheme was first introduced, for

conventional fully dense materials, by Lee and Kobayashi.[16] Applications are presently limited to simple geometries for purposes of evaluation.

3.5 Slab Analysis for Axisymetric Upset Forging

3.5.1 Development of Equations

The underlying assumptions for the slab analysis are:[17]

(i) Stress on a plane or surface normal to the flow direction is a principal stress. Hence, for an infinitesmal element parallel to this plane, the deformation element is considered homogenous.

(ii) The presence of external friction or shear does not modify the internal stress distribution.

Consider the upsetting of a compact whose cross-section, shown in Figure 1Ø, is a trapezoid. For an infinitesmal element, the radial stress, σ_r, is developed due to the frictional shear on the punch interfaces. Under the assumption of homogenous deformation, σ_r, does not vary with axial position. Assuming that the hoop stress, σ_θ, is equal to the radial stress, the yield criterion, (3-2), simplifies to

$$Y^2 = (\sigma_r - \sigma_z)^2 + (1-2\nu)(\sigma_r + 2\sigma_r\sigma_z) \quad . \qquad (3\text{-}9)$$

where Y = yield strength of the compact at density ρ .

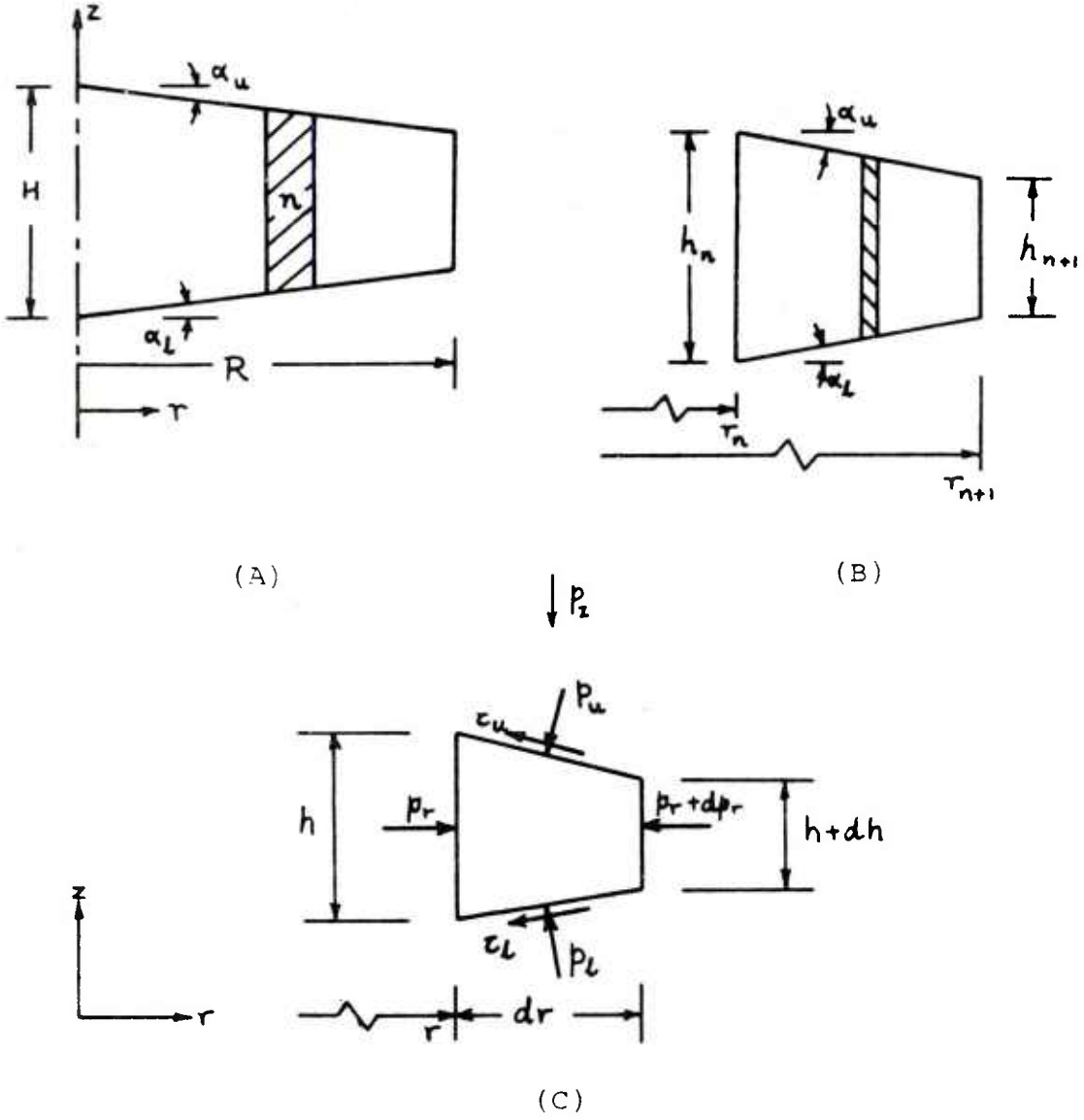

(A) Trapezoidal cross section showing zone subdivision.

(B) Geometry of n^{th} zone with infinitesmal element.

(C) Stresses acting on infinitesmal element.

Figure 10. Geometry of axisymmetric component with a trapezoidal cross-section for Slab analysis.

σ_z = applied normal stress.

The flow equations, (3-3a), expressed in terms of strain rates are:

$$\dot{\varepsilon}_r = (\dot{\lambda}/Y)\{\sigma_r - \nu(\sigma_r + \sigma_z)\}$$

$$\dot{\varepsilon}_z = (\dot{\lambda}/Y)\{\sigma_z - 2\nu\sigma_r\} \qquad (3\text{-}10)$$

The radial velocity, u_r, at the radial position r, is

$$u_r = u_0 + \int_{r_0}^{r} \dot{\varepsilon}_z (\dot{\varepsilon}_r/\dot{\varepsilon}_z)dr \qquad (3\text{-}11)$$

where u_0= radial velocity at $r = r_0$.

The densification rate, (3-8), assuming density as a function of radial position, is

$$\partial\rho/\partial t = -\rho\dot{\varepsilon}_z\{1 + 2(\dot{\varepsilon}_r/\dot{\varepsilon}_z)\} + u_r\,\partial\rho/\partial r \qquad (3\text{-}12)$$

The distribution of the radial stress, σ_r, is obtained from equilibrium considerations of an infinitesmal element. From Appendix A, we have

$$d\sigma_r/dr = -\{(\sigma_z-\sigma_r)(\tan\alpha_u+\tan\alpha_l) - (\tau_u\mathrm{Sec}^2\alpha_u+\tau_l\mathrm{Sec}^2\alpha_l)\}/h$$

$$r = r_{n+1} \;;\; \sigma_r = (\sigma_r)_{r=r_{n+1}} \qquad (3\text{-}13)$$

3.5.2 Solution of Equations

Equations (3-9) to (3-13) together with (3-1) form the set of equations for an incremental numerical procedure. This was implemented on a digital computer and the upset of a circular cylinder was simulated for various values of aspect ratios and interface friction.

The cross-section was descretized into n slabs. Density and velocities are specified at the sides flanking each slab. The density is assumed to vary linearly within each element. For a given axial strain-rate, $\dot{\varepsilon}_z$, assumed constant, equation (3-13) coupled with (3-9) is numerically integrated from the outermost slab towards the interior by a fourth order Runge-Kutta scheme. Eqaution (3-9) then furnishes σ_z, whence the ratio $(\dot{\varepsilon}_r / \dot{\varepsilon}_z)$ is evaluated from (3-10). Integrating (3-11), the radial velocity distribution for the current increment is obtained with the densification computed from (3-12). For a time increment Δt, the density and positions of the slabs are updated and the procedure repeated.

Numerical instabilities were encountered in the above procedure for the cases of high interface and/or low aspect ratios. For low values of friction, the procedure was stable and yielded results consistent with experimental trends. This prompted a closer look on the influence of friction on the algorithm.

For a circular cylinder, $\alpha_u = \alpha_l = \emptyset$. Assuming that $\tau_u = \tau_l = mk$, where m is the friction factor and k the shear yield strength of the compact, equation (3-13) may be integrated to yield

$$\sigma_r / Y = -\{ m/(H/D) \} \{1 - (r/R)\} / \sqrt{3} \qquad (3\text{-}14)$$

It is evident that (σ_r / Y) is directly proportional to 'm' and inversely to (H/D). High values of m and low values of (H/D) result in large values of (σ_r / Y), these being the situations when the algorithm is unstable.

Solving the yield criterion, (3-9), explicitly for (σ_z / Y), we have,

$$\sigma_z / Y = 2\nu\sigma_r / Y - \{ 1 - 2(\sigma_r / Y)^2 (1+\nu)(1-2\nu) \}^{\frac{1}{2}} \qquad (3\text{-}15)$$

This is plotted in Figure 11 for various values of ν. We infer that as (σ_r / Y) decreases linearly from zero, as suggested by (3-14), (σ_z / Y) attains a maximum negative value. The maximum value is easily derived to be

$$(\sigma_z / Y)_{max} = (\sigma_r / Y)^* (1-\nu)/\nu$$
$$(\sigma_r / Y)^* = -\nu / \{(1-\nu^2)(1-2\nu)\}^{\frac{1}{2}} \qquad (3\text{-}16)$$

It can be shown that (3-16) corresponds to the stresses on a circular disk under a repress deformation.

The strain-rate ratio, (3-10), changes sign in the vicinity of the stress state (3-16) according to

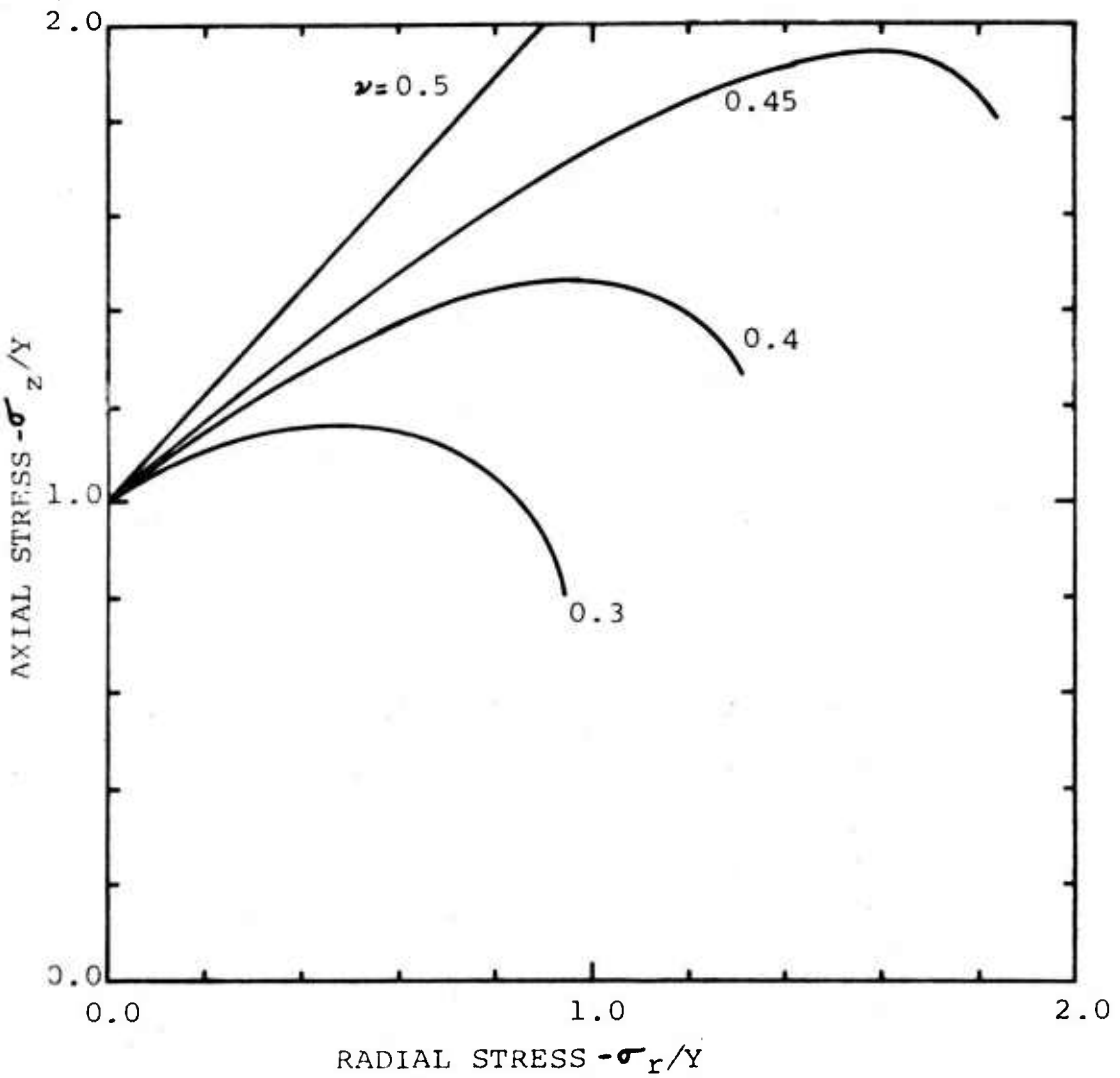

Figure 11. Variation of radial stress vs. axial stress for disk upset as predicted by the yield criterion.

$$\dot{\varepsilon}_r/\dot{\varepsilon}_z \begin{cases} < 0 & ; \ \sigma_r/Y < (\sigma_r/Y)^* \\ = 0 & ; \ \sigma_r/Y \quad (\sigma_r/Y)^* \\ > 0 & ; \ \sigma_r/Y > (\sigma_r/Y)^* \end{cases} \tag{3-17}$$

Suppose that the disk has a low aspect ratio and is deformed under a large frictional constraint. For material flow directed radially outward, the radial stress varies linearly and monotonically from zero at the rim to a finite value at the center. The strain-rate ratio is negative at the rim, consistent with an outward flow, and increases toward the center. Suppose at some interior point, $r=r^*$, $(\dot{\varepsilon}_r/\dot{\varepsilon}_z)$ is zero. Then for any position $r<r^*$, $(\dot{\varepsilon}_r/\dot{\varepsilon}_z)$ is positive implying that the flow is radially inward. This would imply a reversal in the direction of interfacial shear and result in a decrease in $(-\sigma_r/Y)$. This contradicts the hypothesis that $(-\sigma_r/Y)$ is always increasing. Hence, we conclude that $(-\sigma_r/Y) \geq (-\sigma_r/Y)^*$, which implies that the radial stress distribution (3-14) is strictly given by

$$\sigma_r/Y \begin{cases} = -\{m/(H/D)\}\{1-r/R\}/\sqrt{3} \\ = (\sigma_r/Y)^* \quad ; \ 0 < r < r^* \end{cases} \tag{3-14a}$$

Physically, this means that for extreme case of porous parameters, there are two zones of deformation. An outer zone undergoing upset deformation surrounding an inner zone undergoing a pure repress deformation. It can be shown that as the deformation progresses, the ensuing densification of the repress core results in the core shrinking to zero, whence the entire disk then undergoes an upset deformation.

The inclusion of equation (3-14a) into the numerical procedure resulted in a stable procedure for all conditions of process parameters.

3.5.2 Results for Disk Upset

Available experimental data on upsetting of disks under different conditions of lubrication and aspect ratios are shown in Figures 12 and 13. The overall densification, Figure 12, is enhanced with deformation under high frictional constraint and for low aspect ratios, respectively. The density gradients at various levels of deformation, Figure 13, are consistent with the macrographs of Figure 8.

Results of simulation by the slab analysis, under conditions approximate to the experiments, are shown in Figures 14, 15 and 16. The friction condition, qualitatively defined in the experimental data as 'lubricated' and 'unlubricated', is specified in the analysis by a constant interfacial shear. The friction factor, m, for the shear specification was chosen as 0.2 and 0.5 for the lubricated

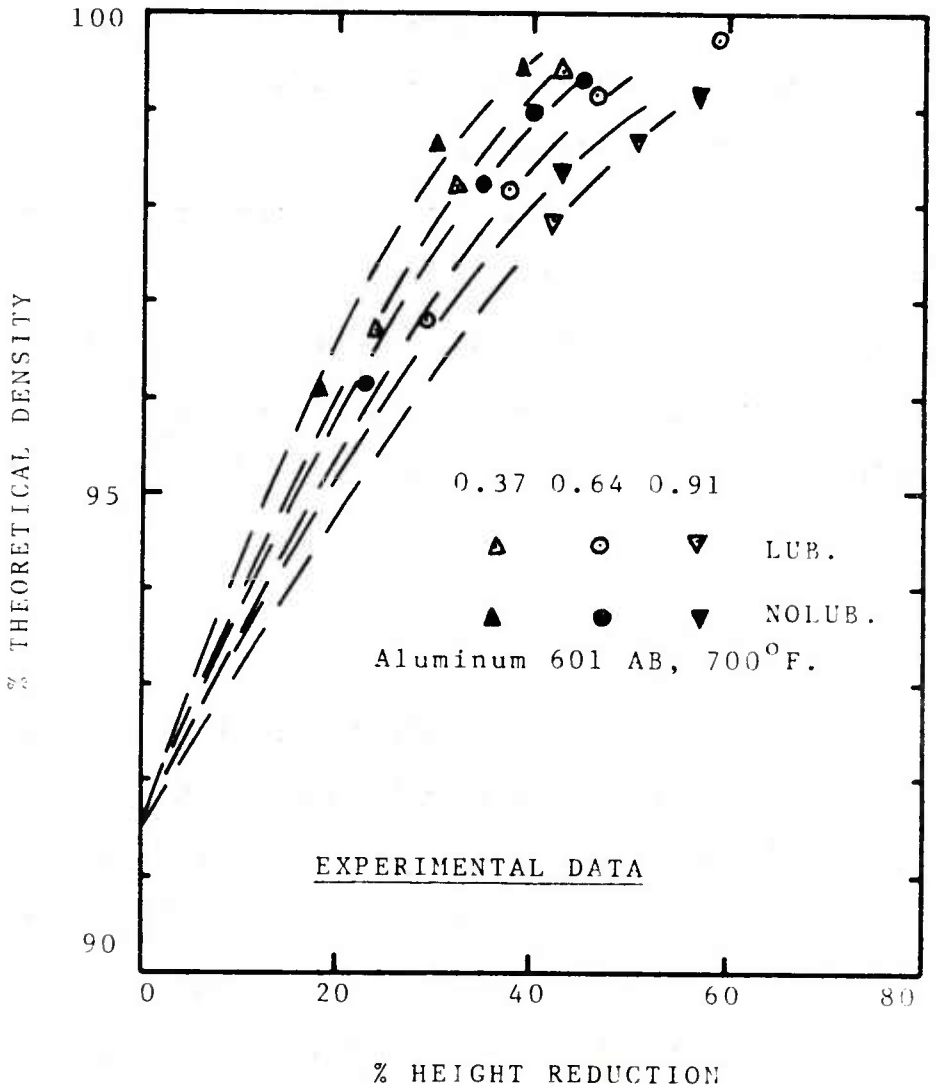

Figure 12. Experimental data on overall densification in disk upset of 601AB aluminum alloy powder preforms for various aspect ratios and lubrication. (3)

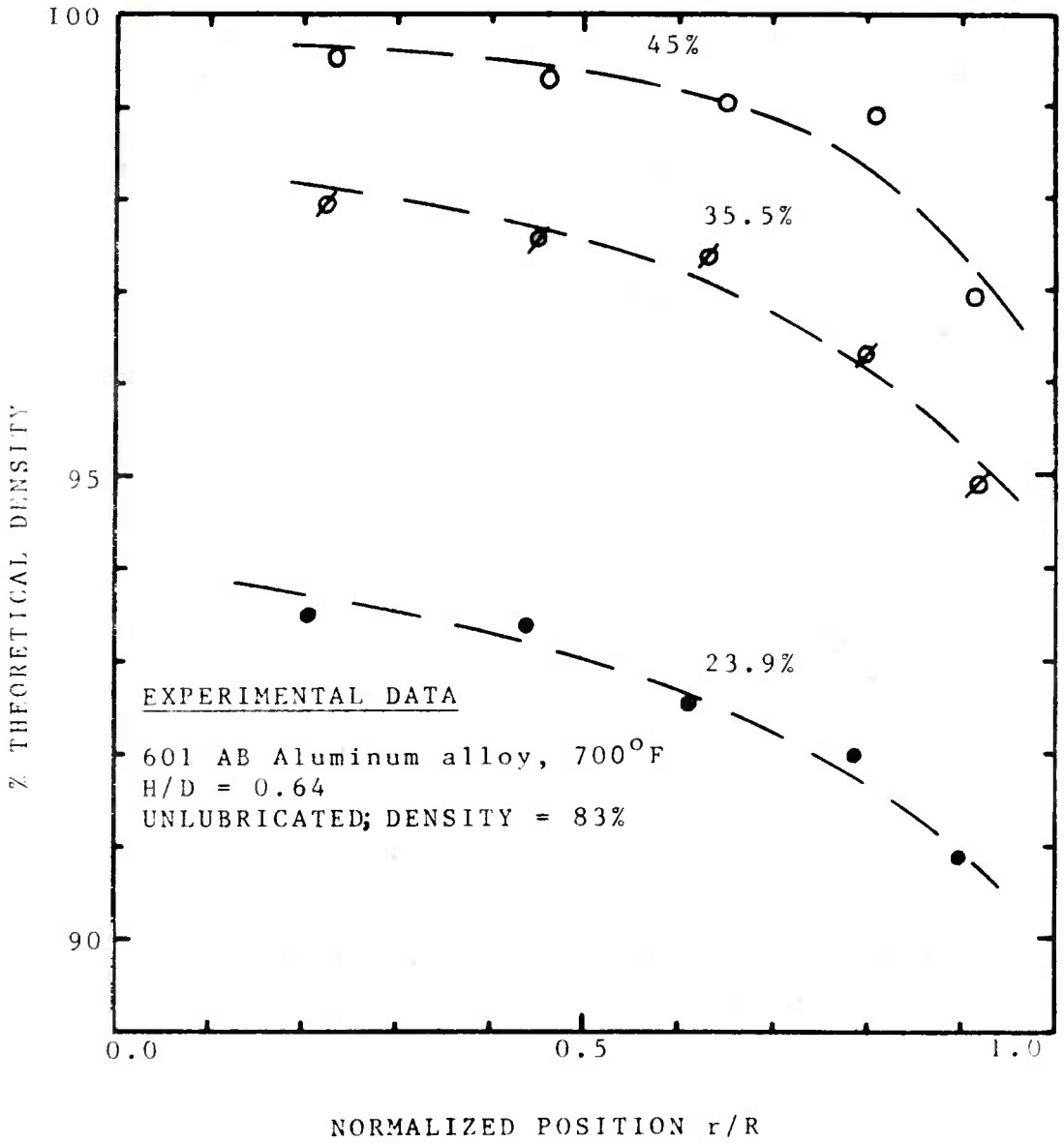

Figure 13. Densification profile as measured across an upset 601AB aluminum alloy powder disk preform.(3)

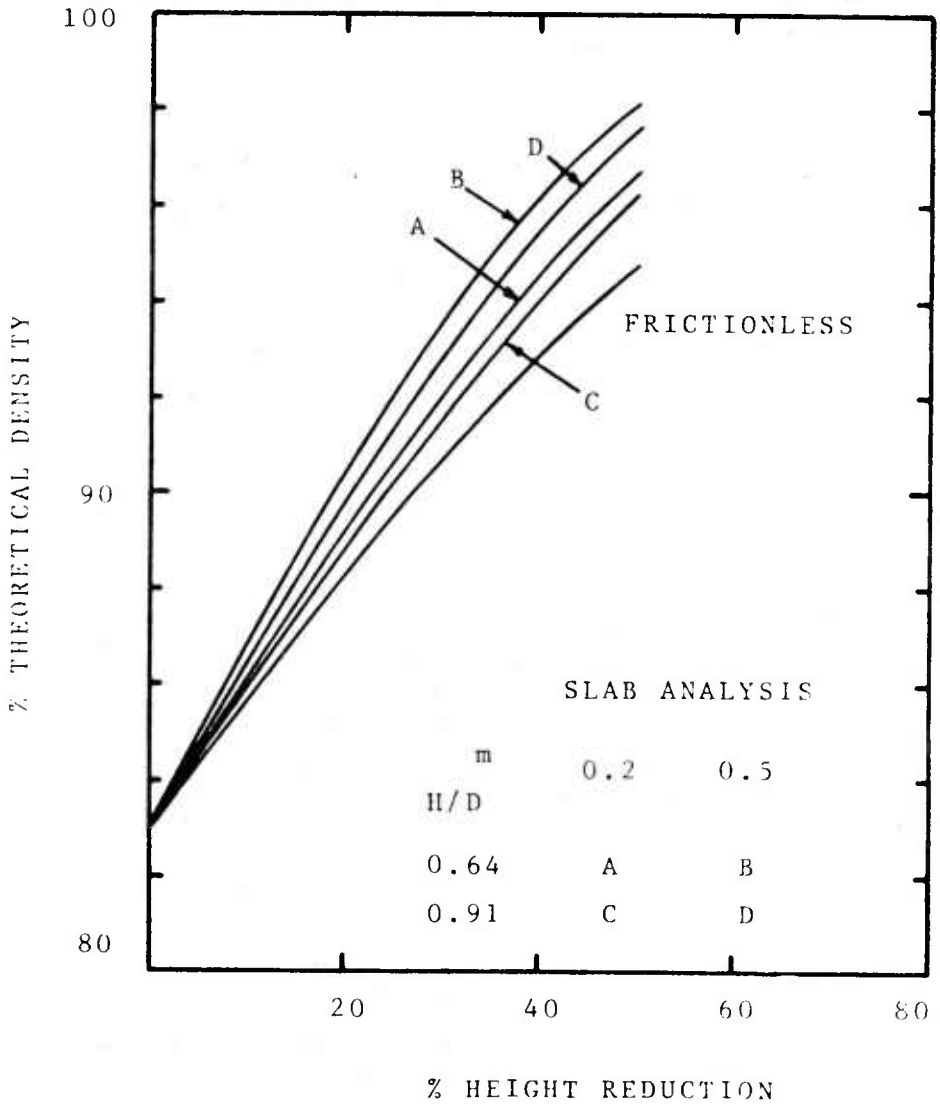

Figure 14. Overall densification calculated by Slab analysis for upset of 601AB aluminum alloy powder disk preforms at various aspect ratios and lubrication.

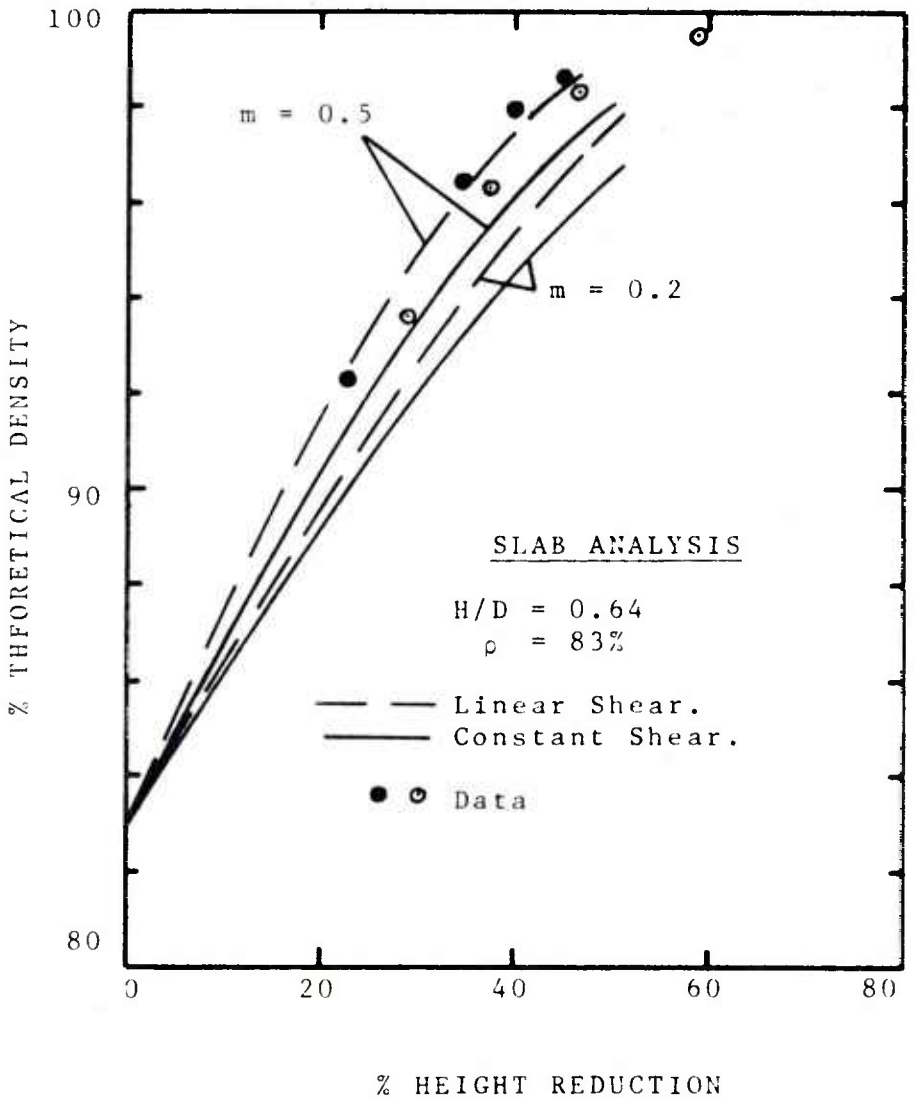

Figure 15. Comparison of overall densification calculated by Slab analysis with experimental data for upset of 601AB aluminum alloy powder disk preforms.

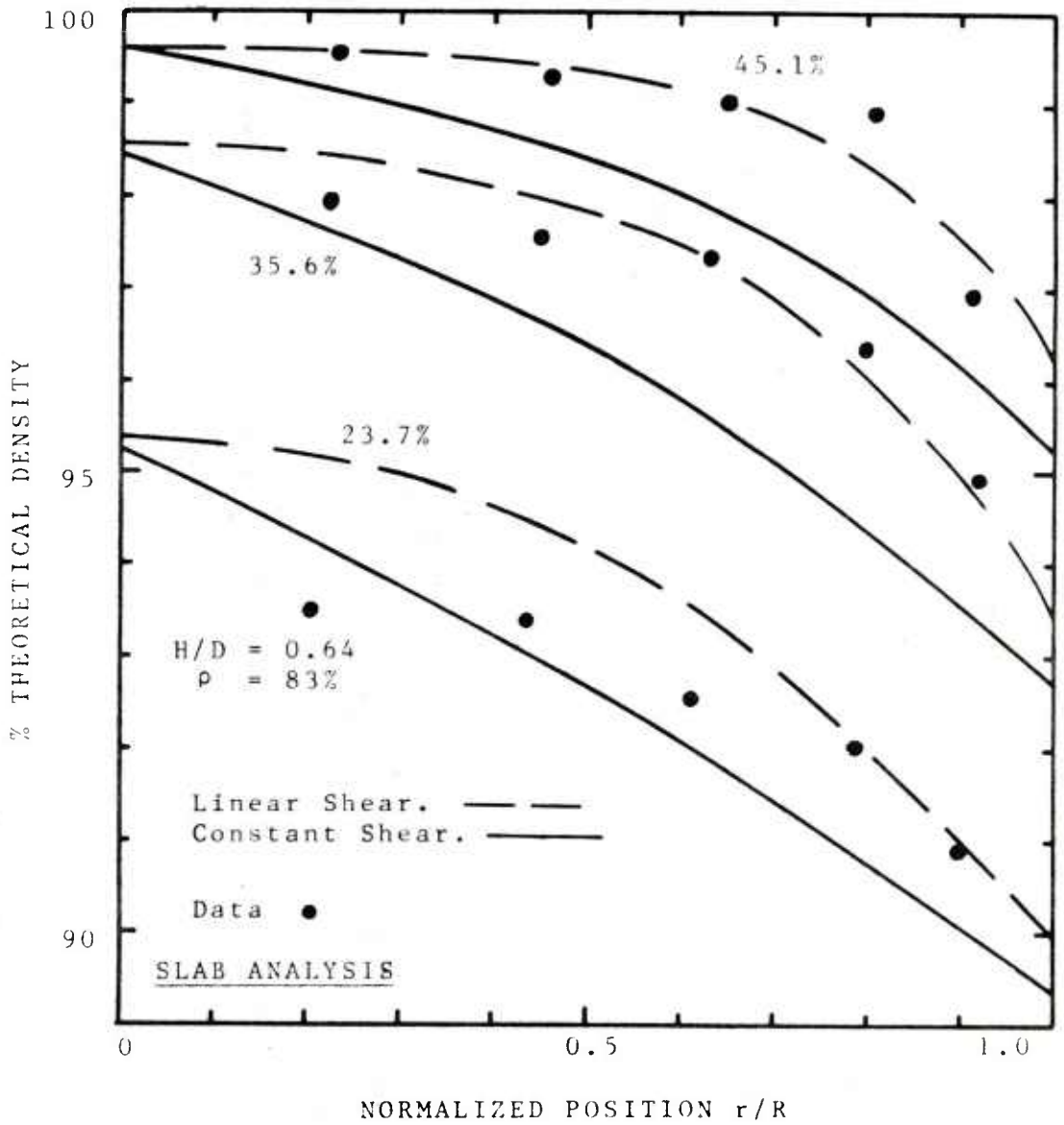

Figure 16. Comparison of densification profiles calculated by Slab analysis with experimental profiles for upset of 601AB aluminum alloy powder disk preforms.

and unlubricated conditions, respectively.

Trends in the overall densification with deformation as predicted by the slab analysis, Figure 14, are consistent with experimental observation. Figure 15 illustrates a typical comparison with experimental data. The analysis underestimates the actual overall densification. This may be the result of an underestimation of the friction factor.

Figure 16 illustrates the comparison of the density gradient predicted by the analysis with the experimental data. There exists a marked difference, which immediately raises questions on the validity of the slab analysis. The data indicates that the density is fairly uniform in the central regions and falls off towards the rim, whereas the analysis yields an almost linear density distribution. The uniform density at the central regions indicate the presence of a core under repress deformation, but for the process conditions selected this is false.

Rooyen and Backofen[18] attempted to experimentally determine the distribution of interfacial shear for the upsetting of Aluminum disks. Their observation was that the interfacial shear was not constant but increased toward the rim of the disk. The variation was complex and not quantifiable.

Variation in the frictional constraint at the interface influences the densification behavior of a porous compact. Interfacial friction generates the radial pressure (cf

equation 3-14), the variation of which results in density gradients. If we assume that the frictional shear is distributed linearly and increasing towards the periphery of the disk, the radial pressure distribution becomes parabolic (as opposed to linear for a constant shear). This would result in the densification being dampened near the core of the disk, as suggested by the data. To determine the extent of the change that would result, a linear shear specification was imposed. The shear was zero at the center and with a slope such that the average shear was equal in magnitude to the constant shear that was specified earlier.

The results are shown in Figure 16 by the broken line. The density distribution predicted resembles the data closely, especially at the higher reductions. The effect on the overall densification , Figure 15, is marginal, but tends towards a better agreement with the data.

3.6 Energy Method for Axisymmetric Upset

3.6.1 Derivation of the Functional

Consider a deforming porous body in a fully plastic state. Let S_u denote the surface where velocities are prescribed and S_F the surface where tractions are specified. For this body of volume V, let the following be defined:

$\underset{\sim}{U}$: prescribed velocity vector on S_u .

$\underset{\sim}{F}$: prescribed traction vector on S_F .

$\dot{\varepsilon}_{ij}$: actual strain-rate field satisfying compatibility.

σ_{ij}: equilibrium stress field satisfying boundary conditions.

u_i^* : any velocity field that satisfies the prescribed boundary conditions.

$\dot{\varepsilon}_{ij}^*$: strain-rate field derived from u_i^* .

σ_{ij}^*: stress field derived from $\dot{\varepsilon}_{ij}^*$ via the flow rule and satisfying the yield criterion.

σ_{eq}: equivalent stress derived from components of σ_{ij}^* .

$\dot{\varepsilon}_{eq}$: equivalent strain-rate field derived from components of $\dot{\varepsilon}_{ij}^*$.

n_j : components of unit outward normal to surface.

The principle of maximum plastic work for a concave -to-origin yield locus is given by[19]

$$\int_V (\sigma_{ij}^* - \sigma_{ij})\, \dot{\varepsilon}_{ij}^*\, dV > 0 \qquad (3\text{-}18)$$

By the principle of virtual work, we have

$$\int_V \sigma_{ij}\, \dot{\varepsilon}_{ij}^*\, dV = \int_{S_F} \underset{\sim}{F}.\underset{\sim}{u}^* dS + \int_{S_u} (\sigma_{ij} n_j) U_i\, dS$$

Using equation (3-18) we have,

$$\Phi = \int_V \sigma_{ij}^* \dot{\varepsilon}_{ij}^*\, dV - \int_{S_F} \underset{\sim}{F}.\underset{\sim}{u}^* dS > \int_{S_u} (\sigma_{ij} n_j) U_i\, dS \qquad (3\text{-}19)$$

Following Hill[20]

$$\int_V \sigma_{ij}\dot{\varepsilon}_{ij}\,dV = \int_{S_F} \underset{\sim}{F}.\underset{\sim}{u}\,dS + \int_{S_u} (\sigma_{ij}n_j)U_i\,dS \qquad (3\text{-}20)$$

Hence, from (3-19) and (3-20)

$$\int_V \sigma^*_{ij}\dot{\varepsilon}^*_{ij}\,dV - \int_{S_F} \underset{\sim}{F}.\underset{\sim}{u}^*\,dS > \int_V \sigma_{ij}\dot{\varepsilon}_{ij}\,dV - \int_{S_F} \underset{\sim}{F}.\underset{\sim}{u}\,dS$$

$$= \int_{S_u} (\sigma_{ij}n_j)U_i\,dS$$

The functional, in terms of equivalent stress and strain-rate, is then given by

$$\Phi = \int_V \sigma_{eq}\dot{\varepsilon}_{eq}\,dV - \int_{S_F} \underset{\sim}{F}.\underset{\sim}{u}\,dS \qquad (3\text{-}21)$$

3.6.2 Solution of Equations

We seek to determine the kinematically admissible velocity field $\underset{\sim}{u}^*$, from a class of velocity fields satisfying the prescribed boundary conditions, that minimizes the functional Φ. The stress field σ^*_{ij}, then is an upper bound on the actual stress field σ_{ij}, as σ^*_{ij} need not necessarily satisfy the equilibrium conditions.

To obtain a solution for the kinematically admissible velocity that minimizes the functional Φ, we use the finite element procedure of Lee and Kobayashi.[16] The axisymmetric domain is descretized into M elements. The velocity field, u*, is approximated in terms of the

velocities at the nodal points, $\underset{\sim}{v}$, by

$$\underset{\sim}{u}^* = G\underset{\sim}{v} \tag{3-22}$$

The strain-rate field is derived as

$$\dot{\underset{\sim}{e}} = B\underset{\sim}{u}^* \tag{3-23}$$

The functional Φ is approximated as

$$\Phi = \sum_{m=1}^{M} \phi^{(m)} = \sum_{m=1}^{M} \{ \int_{V^{(m)}} \sigma_{eq}\dot{\varepsilon}_{eq}\, dV - \int_{S_F^{(m)}} F.u^*\, dS \} \tag{3-24}$$

The equivalent strain-rate, $\dot{\varepsilon}_{eq}$, is then derivable as

$$\dot{\varepsilon}_{eq}^2 = \frac{2}{3(1+\nu)} \dot{\underset{\sim}{\varepsilon}}^T A \dot{\underset{\sim}{\varepsilon}} + \frac{1}{3(1-2\nu)} \dot{\underset{\sim}{\varepsilon}}^T I \dot{\underset{\sim}{\varepsilon}} \tag{3-25}$$

where I is the identity matrix, A is a constant matrix.

Substituting (3-22, 23, 24) into (3-25), we have

$$\Phi = \sum_{m=1}^{M} \{ \int_{V^{(m)}} \sigma_{eq} (\underset{\sim}{v}^T X \underset{\sim}{v})^{\frac{1}{2}}\, dV - \int_{S_F^{(m)}} \underset{\sim}{F}^T G \underset{\sim}{v}\, dS \} \tag{3-26}$$

where $X = B^T AB + B^T IB$

Minimizing Φ with respect to the nodal point velocities,

$$\partial\Phi/\partial\underset{\sim}{v} = \sum_{m=1}^{M} \{ \int_{V^{(m)}} \sigma_{eq} (\underset{\sim}{v}^T X \underset{\sim}{v})^{-\frac{1}{2}} X\underset{\sim}{v}\, dV - \int_{S_F^{(m)}} G^T \underset{\sim}{F}\, dS \} \tag{3-27}$$

This represents a system of non-linear equations in the nodal point velocities. The solution determines the velocity field that minimizes the functional. This solution may be obtained either by the Newton-Raphson method or by linearization of equation (3-27).[16] The latter is accomplished by assuming that at the n-th iteration, the velocity vector is given by

$$\underset{\sim}{v}_{(n)} = \underset{\sim}{v}_{(n-1)} + \Delta\underset{\sim}{v}_{(n)} \tag{3-28}$$

The linearization procedure and the resulting linear system of equations in $\Delta\underset{\sim}{v}_{(n)}$ is detailed in Appendix B. Schematically, the system of equations is

$$\sum_{m=1}^{M} \sigma_{eq}{}^{P}{}_{(n-1)}\, \Delta\underset{\sim}{v}_{(n)} + \sum_{m=1}^{M} \sigma_{eq}{}^{H}{}_{(n-1)}\, \underset{\sim}{\Gamma} - \sum_{m=1}^{M} \underset{\sim}{\Gamma} = 0 \tag{3-29}$$

The iteration procedure for an increment of deformation is started by assuming a trial velocity field. This is iterated till the velocity iterate, $\Delta\underset{\sim}{v}$, is less than a prescribed tolerance.

Once a converged velocity field is obtained for an increment, the strain-rate distribution may be obtained from (3-23). Stress distribution is obtained by inverting the flow rule. Note, however, that this inversion is valid only for sintered powder materials.

3.6.3 Results for Disk Upset

As an initial application of the energy method, the disk is descretized into elements which are slabs. This element configuration was chosen to provide a check for the results of the slab analysis. For a more detailed analysis, the element may be a quadrilateral,[16] in which case even the attendent bulging of the free surface may be obtained.

The element equations and material characterization are given in Appendix B. The velocity field is approximated by a linear interpolation of the velocities of the element sides. Density is also assumed to vary linearly within the element. For the first deformation increment, the assumed trial velocity field was that of uniaxial frictionless compression. For subsequent increments, the converged velocity field of the previous increments is used. The number of iterations required to meet the specified error tolerance depend upon how close the assumed velocity field is to the actual velocity field. The convergence criteria was specified as

$$||\Delta \underline{v}||/||\underline{v}|| < 1.0 \times 10^{-4}$$

where $||\Delta \underline{v}||$, $||\underline{v}||$ are the Euclidean vector norms. On the average, a converged velocity field was obtained in 6-8 iterations for the first increment, and the subsequent iterations required 2-3 iterations.

The deformation of the disk was simulated under the same conditions that were used in the slab analysis. Interface

shear was specified as constant in one set of computations, and varying linearly in another set. The computed density distributions for both shear specifications are shown in Figure 17 along with the experimental data.

The predictions are similar, both qualitatively as well as quantitatively, to that of the slab analysis. This result is not surprising for the type of element chosen. For the case of zero interfacial shear, both techniques yield results that are identical and agree with the results for uniaxial frictionless compression.

The predicted overall densification is also similar. The predicted forging load is slightly higher for the energy method when compared to that of the slab method. The good correlation between the results for the same set of conditions establishes the correctness of the algorithms and the computations.

3.7 Discussion

Two numerical techniques, applicable to sintered powder materials, were presented in the above sections and applied to the uniaxial compression of a cylinder with interfacial frictional constraint. The predicted results are consistent with experimental observations. The pros and cons of both techniques are compared with respect to accuracy, computational effort and limitations. The candidacy of both

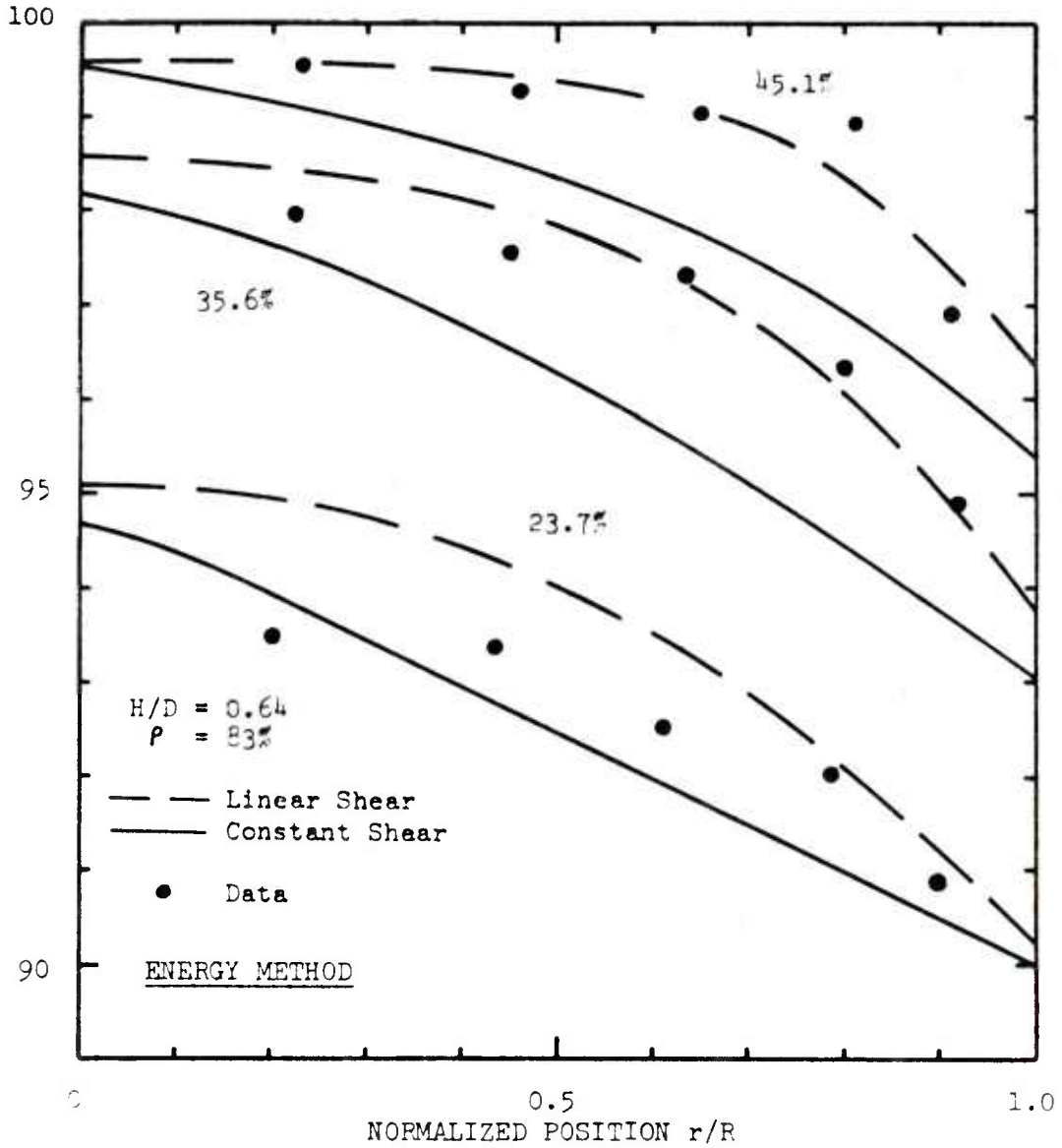

Figure 17. Comparison of densification profiles calculated by Energy method with experimental profiles for upset of 601AB aluminum alloy powder disk preforms.

for analytical process modeling is discussed in the following paragraphs.

The slab analysis, by virtue of its underlying assumptions, is incapable of predicting the local states of stress and strain during deformation. In the case of wrought materials, the primary advantage is in obtaining quick estimates of the forging load. The assumption of homogenous deformation, valid strictly in the case of frictionless compression, is not valid in reality. This assumption, however, considerably simplifies the mathematics required to obtain an expression for the forging load. In the case of sintered powder materials, the resulting non-uniform densification precludes the possibility of an explicit expression for the forging load.

The energy method, on the other hand, does not assume a homogenous deformation. Yet, the results of the slab analysis and the energy method compare very well. Figure 18 illustrates the typical computed radial and hoop strain-rates for the slab analysis and the energy method. The assumption of homogenous deformation seems to lead to strain-rates that are an average of the radial and hoop strain-rate values of the energy method.

The energy method has the potential ability to describe the stress and strain distribution within a deforming material. The present element chosen, however, results in a considerable oversimplification and as a result does

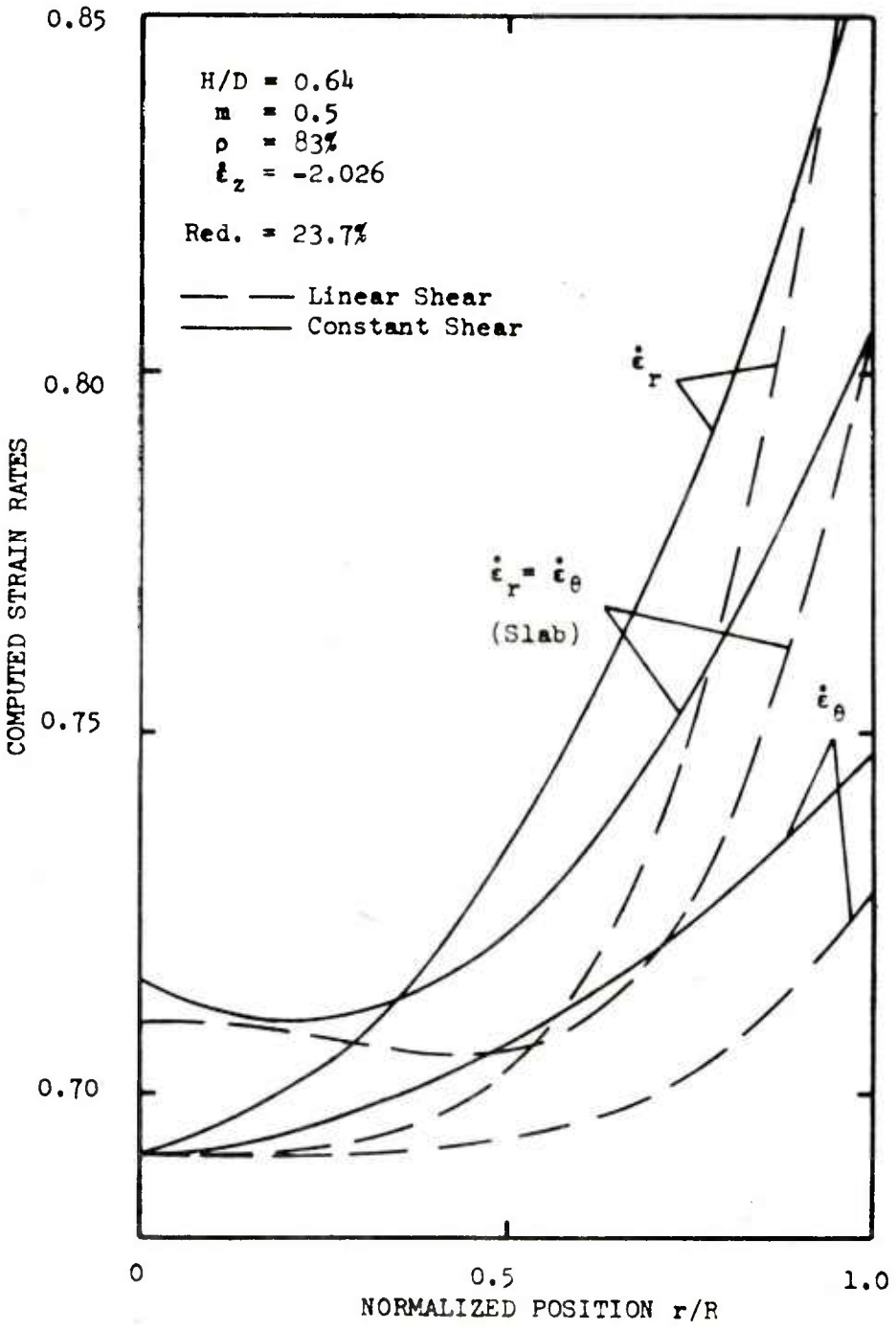

Figure 18. Comparison of radial and hoop strain-rates calculated from the Energy method with strain-rates of the Slab analysis.

injustice to the capability of the technique. As mentioned earlier, this element was chosen primarily to evaluate the merit of the technique and provide for evaluating the slab analysis. A quadrilateral element, with bilinear velocity interpolation, is the simplest configuration that would provide the detailed description of the deformation. This extension is a subject for future activity.

To compare the computaional effort and accuracy of the techniques, the process conditions were made similar. Ten slabs were used in both cases and the increment of deformation was chosen to be equivalent to an axial strain of 0.01. This choice is a trade off between the computational effort and errors, to reach a specific height reduction.

For the slab analysis, errors were measured by the difference between the computed mass at each increment and the original mass of the cylinderical preform. For the deformation increment chosen, the error was held to less than 1% , for a height reduction of 50%. Increasing the number of slabs does not contribute in any positive way to the results, but only increases the computational effort. Hence, some judgement needs to be exercised regarding the choice of the deformation increment and the number of slabs. The slab analysis is limited in its capability of process modeling.

The energy method, being an iterative process, is by far a better technique. For the slab type element chosen, the computational effort is approximately of the same order. No

attempt was made to optimize the number of elements as it is recognized that the slab element does not exploit the capability of this method. It needs to be cautioned that in going from a slab type element to a quadrilateral element will result in a large increase in computation. This increase can be justified by the detailed results that is potentially obtainable.

When full densification is approached, numerical difficulties may arise. Specifically, this occurs because as full density is approached, the Poisson's ratio tends to 0.5 and some terms in the equations may become very large. This problem can be avoided if full density is assumed to be 99.95% theoretical. It was numerically verified that as full density is approached, the volumetric strain-rate tends to zero, i. e., the incompressibility condition is approximately satisfied. The significance of this is clear when one compares the current method for sintered powder materials at 99.95% density with the companion method for wrought materials of Lee and Kobayashi.[16] For wrought materials, the incompressibility condition is absorbed into the functional by means of a Lagrange multiplier. This is computed for each element, for each iteration, and increases the number of equations to be solved by the number of elements in the descretized domain. The Lagrange multiplier was shown to be equivalent to the hydrostatic stress. To compute the stress distribution, the deviatoric stresses are

calculated from the strain-rates and the hydrostatic stress is added. For sintered powder materials, the stress distribution is obtainable by directly inverting the flow rule. Thus, for large scale problems, considerable savings in computations and as well as storage can be realized. The accuracy deficiencies, if any, needs to be assessed.

An interesting result of the present analytical effort was the influence of interfacial friction on the process modeling. Considerable research was done in the last two decades to understand and quantify the effect of friction in metalworking processes. Current practice is to assume the Coulomb model or the constant friction factor (Amoton's Law), the latter being preferred because of the mathematical simplifications that result without appreciable differences in the forging load. A quantitative average estimate of the friction factor is obtained by the ring test,[21] where changes in the geometry of the ring are used as an indicator of the magnitude of friction. However, it was noted in the present work that changing the frictional shear distribution has a pronounced influence on the densification profiles but virtually no change in the deformed geometry. The change in the forging load was also marginal, as shown in Figure 19. Perhaps the ring test for a sintered powder material would shed more light on a technique for assessing friction factors. The energy method, with the slab type element would be a good approach to take to assess ring deformation.

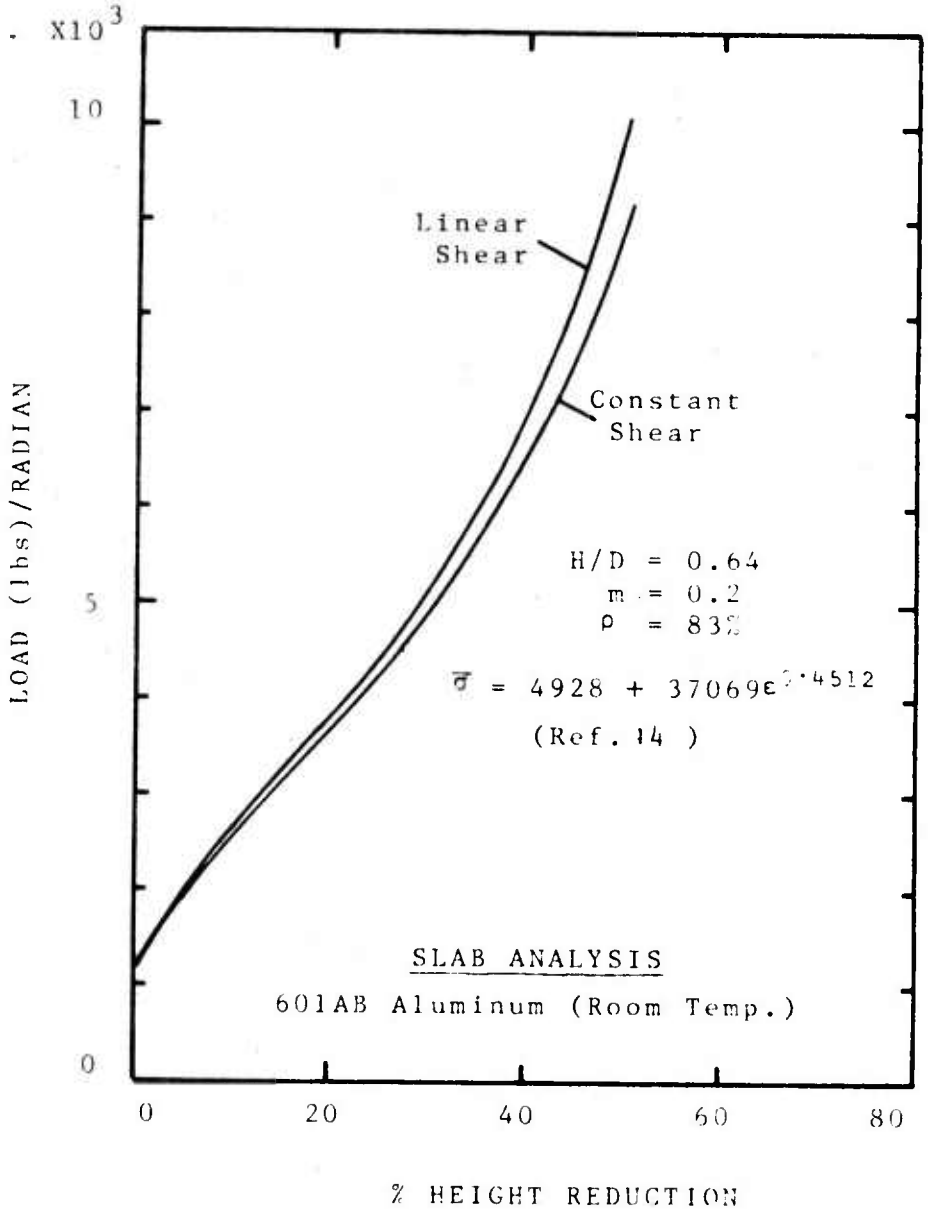

Figure 19. Calculated forging load for upset of 6061AB aluminum alloy powder disk preforms.

It is premature at this time to seek an analytical approach to the workability question. Even for the case of a simple cylinder, additional research activity is required. Firstly, upgrading the energy method to a quadrilateral element and secondly, address the question of interfacial shear specification. Then applications to more complex geometries need to be pursued. Hence, one may conclude that for the present, the prevention of fracture in sintered powder forging will have to be on an empirical level.

4.0 COMPUTER-AIDED DESIGN OF PREFORMS

4.1 Introduction

The importance of preform design was realized at a very early stage in the development of powder forging. An early example is the forging of differential side pinion gears,[22] where a partial bevel preform, determined from experimental results using plasticine, successfully led to a sound forging. Subsequently, the influence of preform shape on material flow, residual porosity and occurrence of flaws was further emphasized in the forging of specific axisymmetric parts.[23, 24] An experimental approach was pursued in these works, where the actual preform was developed after a study of the mechanics of deformation and defect formation in a limited series of model experiments. Kuhn et. al.[2, 25-27] pursued this approach in some detail, the result of which is the establishment of preform design as the single most important parameter in powder forging. Empirical guidelines for the prevention of defects for a variety of simple shapes were also obtained.

The application of these concepts to a complex forging has been successful, but is quite tedious.[2] Firstly, an understanding of metal flow, densification and fracture behavior of preforms, acquired primarily with experience, is required to determine the shape of the preform. Secondly,

the preform is to be sized so as to maintain the desired shape, provide adequate mass distribution in various regions and maintain the proper weight control. The latter task is time consuming and prone to human errors, particularly in the case of complex shapes.

Accurate determination of volumes lends itself easily to computerization. The computerization of the mechanics, however, is not straight forward. If this is achieved, the design of powder preform forging processes may be accomplished by those who are unfamiliar with the details. Development of the computer-aided design approach was motivated by this need. This original contribution is aimed towards exploitation of powder forging as the technology for the new decade.

4.2 Review of CAD in Manufacturing

The use of computers in manufacturing is growing rapidly, primarily due to increased productivity and superior quality control that is achieved. The earliest use of computers was in Numerical Control(NC) Machining. The NC language, APT (Automated Programmed Tool), was developed for this purpose. APT is used to define the part geometry and the necessary machine tool control commands to drive a cutting tool to produce the part. APT developed over a decade to encompass more complex part geometries; requiring trained

personnel to implement its sophisticated capabilities. In parallel, machine tool builders developed the necessary hardware to complement the advances. APT was designed to aid machining technology, and it ably does so.

The application of similar technology to precision forging was attempted by researchers at Battelle Columbus Laboratories.[29-31] A modular approach is followed, where representative cross-sections are isolated; preforms are designed using established practices and then assembled in a building block fashion to yield the preform for a complex part. One approach is limited to a class of structural components of a rib-web type, where any representative cross-section is an assembly of basic L shapes. The preform for a L shape is defined as having a specific but different L shape, which is sized to maintain a constant area equal to the area of the finished L. Limited or no user intervention is required in this design scheme. The analysis is done on a cross-section basis, primarily because analytical techniques are currently only available for plane-strain or axisymmetric deformations. The major obstacle, in the work, is the part description and the determination of representative cross-sections. APT is used for this purpose.

Preform design for powder forging has a different set of rules compared to those for conventional forging. For non-axisymmetric structural components, the use of the L shaped module is not feasible due to unequal densification

that occurs in the rib and web. The current trial-and-error practice of preform design identifies "regions" in the part, and the preform is obtained by distributing the material in various regions. The density of the material in the regions need not be the same, depending on whether the forging is accomplished by repressing or not.

The earlier chapters summarized the powder forging process and the parameters that affect the process. The state of analytical techniques was also examined, for possible application to the current work. In the following sections, the question of computer-aided preform design for powder forging is addressed.

4.3 Basic Considerations for Preform Design

Structural forgings, in general, have complex geometries which result in complex metal flow. Certain elementary or generic metal flow patterns can be identified, which collectively result in a complex flow. Each of these generic flow patterns are result of a unique combination of the preform shape with respect to the die profiles.

Each generic flow pattern has associated with it unique characteristics regarding defect and fracture likelihood, ease of forging etc. Once these generic elements are established in a complex forging, a rational preform design procedure may be effected.

4.3.1 Forging Direction Specification

The choice of forging direction affects the producibility of the part by powder forging. In general, the choice must be such that the part may be ejected from the dies after forging. If the part geometry does not permit ejection, modifications of part geometry have to be done to permit ejection. For example, a part with undercuts, reverse tapers etc. cannot be ejected. For purposes of forging, this is removed by appropiate modifications, and then handled by subsequent machining.

Guide lines for the choice of forging direction are as follows:

(i) The part must be ejectable from the dies after forging.

(ii) The plan area of the part in the forging plane, which is defined as any plane normal to the forging direction, is the largest.

(iii) The maximum part height in the forging direction be within the limits suggested by the press manufacturer. It is recommended to be less than 0.8 times the press stroke.

4.3.2 Region Definition

To illustrate the definition of regions, consider the simple part configurations in Figure 20. The axisymmetric hub-flange as well as the rib-web part have the same cross-section. The terms rib-web and hub-flange are

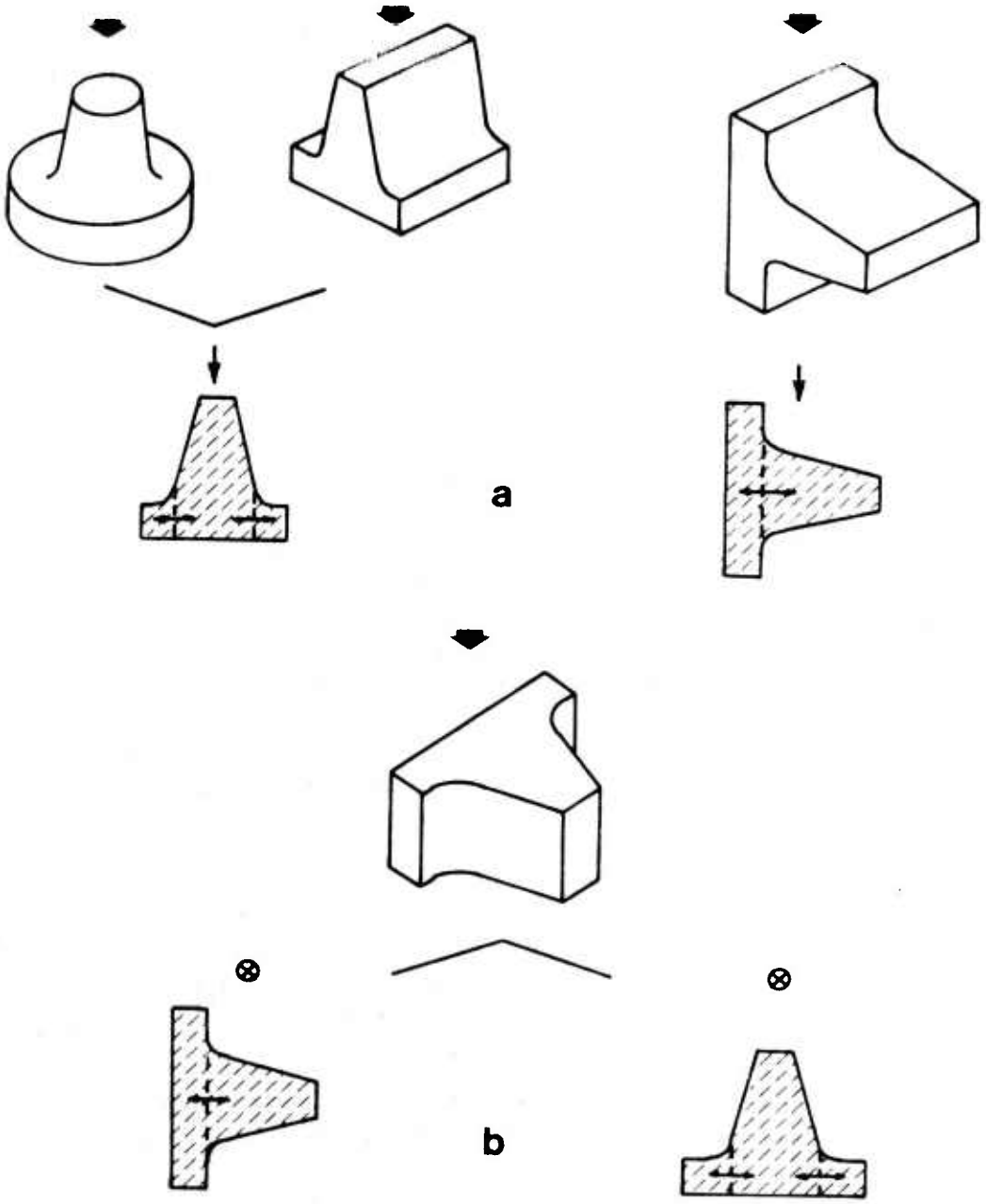

Figure 20. Illustration of region definition for simple part configurations.

identified with respect to a forging direction and the geometry. These terms may correspondingly be defined by profile changes in the cross-section. The demarkation is approximately shown by the broken lines in Figure 20.

For a part that is powder forged, the part simplification is termed "region subdivision". The terms rib-web, hub-flange lose significance and are called as regions. Hence, for a cross-section, the region subdivision criterion is based on significant changes in the profile.

In the present work, the region interfaces, viz, the surfaces that are common to a pair of adjacent regions, are approximated as planes. These are oriented such that any inter-region metal flow, that is postulated, occurs approximately in a direction normal to the interface.

The plane of the cross-section, called the definition plane, may have two orientations with respect to the forging plane. Firstly, it may be normal to the forging plane, Figure 20a. In this case, the interfaces may be unambiguously determined to be parallel to the forging direction at locations of significant profile change. Secondly, the definition plane may be parallel to the forging plane. In this case, Figure 20b, two possible interface combinations are indicated. Either choice is permissible; but the choice will affect the preform design, as will be elaborated in subsequent sections.

4.3.3 Generic Metal Flow Patterns

Various combinations of metal flow across interfaces, together with the specified forging direction may be used to define generic metal flow patterns. These patterns are equivalent to basic deformation modes. They are illustrated in Figure 21.

Figures 21a and 21b represent a back-extrusion and forward extrusion mode respectively. In either case, the interface metal flow is into the region, with the preform deformation is in a direction opposite to or in the same direction as the ram motion. In Figure 21c, the interface flow is reversed, and we have a lateral extrusion mode. Note that in Figures 21a-21c, the definition plane is normal to the forging plane.

In Figure 21d, the definition plane is parallel to the forging plane. The inter-region metal flow shown represents a lateral extrusion. The flow direction is inconsequential, and if reversed will also result as a lateral extrusion. To contrast with the lateral extrusion mode of Figure 21c, the orientation of the definition plane with respect to the forging plane is used. In Figure 21c, the definition plane is normal to the forging plane, hence the mode is called the normal lateral extrusion mode. In Figure 21d, the definition plane is parallel to the forging plane, hence the mode is called the parallel lateral extrusion mode.

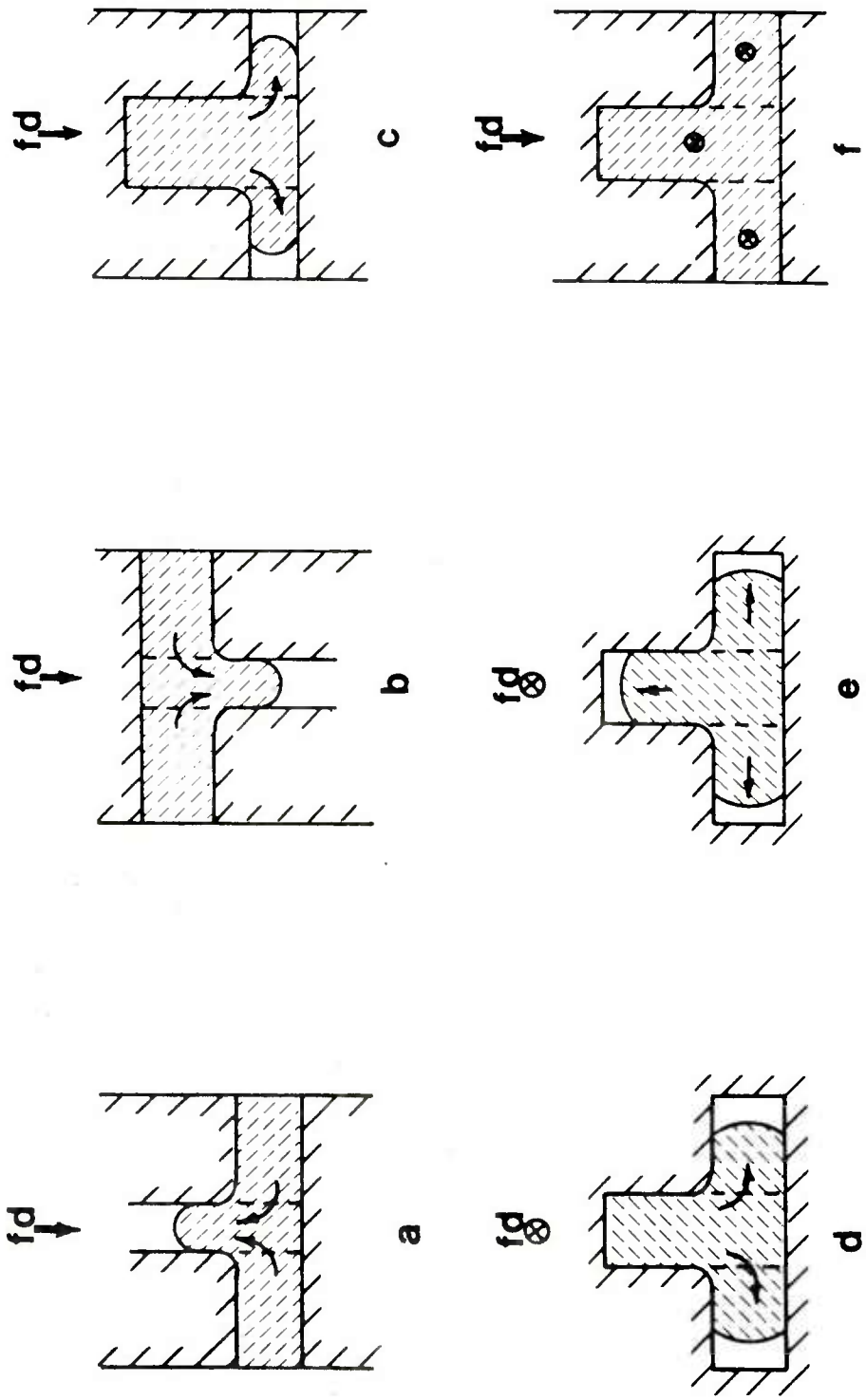

Figure 21. Generic metal flow patterns in powder forging.

In Figure 21e, there is effectively no interface metal flow. Deformation is constrained to occur within each region. Such a mode is termed the parallel upset mode. Figure 21f, analogously represents the normal upset mode, where in this case the preform is free to deform in a direction normal to the plane of the paper. This is possible only for a non-axisymmetric part. For axial symmetry, the configuration will result in a repress deformation.

The metal flow patterns which occur in various regions depend upon profile differences between the preform with respect to the rigid tooling. In regions where clearances exist between the preform and tooling profiles, metal flow must be present so that the clearances are closed during forging. Hence, clearances may be explicitly defined to influence the metal flow during forging.

In extrusion modes, inter-region metal flow is present across interfaces. The extent of flow is dictated by the mass deficiencies that have to be accounted for. On the other hand, in upset deformation modes, there is no substantial metal flow across interfaces. Hence, all deformation is confined within the region. The mass of material in the preform for the upset region will correspond to the finished mass in the region.

4.3.4 Assessment of Fracture Potential

For the generic deformation modes, a qualitative assessment of fracture likelihood and their potential sites may be done to determine optimum preform shapes. These optimum shapes may then be quantified with process parameters, via experimental modeling techniques, to develop guide lines. This approach was pursued in detail for back extrusion of hub-flange and cup configurations. [3,4]

We now restrict our attention specifically to non-axisymmetric shapes that exhibit the deformation modes, as shown in Figure 21. Non-axisymmetric shapes are best formed by restricting metal flow to one direction. Unrestricted flow results in early fracture, due to the poor workability of sintered powder preforms. Restricting flow provides for some compression effects, which inhibit fracture initiation.

For the deformation modes in Figures 21a-21e, metal flow is permitted in the definition plane. Consequently, flow constraint is imposed in a direction normal to the definition plane. Conversely, in Figure 21f, there is no flow possible in the definition plane, and hence, flow is permitted to occur in a direction normal to the definition plane. If no flow is explicitly permitted in any direction in Figure 21f, a repress deformation is obtained as a special case.

In back and forward extrusion modes, the expanding free surface is susceptible to fracture due to friction at the side walls. For no-draft extrusion, there is no compression generated by the side walls to inhibit the possible growth of tensile stresses.

The vicinity of the fillet undergoes rapid changes in deformation intensity as the material moves from under the punch into the rib, where it does not undergo any futher plastic deformation. Die contact surface fracture is a possibility if the radius is small.

For the cases of normal and parallel lateral extrusion, die contact surface fracture is less probable due to the presence of compression in the fillet. Free surface fracture is also suppressed at the expanding surfaces due to the presence of compression. Intrusion defect formation is unlikely for these modes.

For the upset modes, there is no appreciable flow in the vicinity of the fillet to initiate die contact surface fracture. Free surface fracture is the only type of fracture that is likely.

4.4 Experimental Criteria for Fracture Prevention

Of all the generic modes of deformation encountered, back extrusion is likely to exhibit greater fracture problems. The influence of process parameters and preform

options were studied in a parallel experimental program.[32,33] Relavent information is summarized in the following paragraphs.

4.4.1 Experimental Conditions

The experimental process conditions for sintered powder forging of single rib and opposed rib configurations are given in Table 1. The material was aluminum alloy 6061AB and 6061AC of initial density approximately 85% theoretical. Copper dispersed in oil was the lubricant.

The deformation was done cold. The preforms were 0.75 inches square and flat. Each preform was split at a central plane and grid marks were etched. The two halves were assembled and forged, thus providing a deformed grid pattern.

4.4.2 Summary of Results

Free surface fracture occurs during very early stages of rib formation in the forging of both single rib and opposed rib shapes. The occurrence was not affected to any great degree by the size of the fillet radii or the initial preform aspect ratio. The % reduction in area, i. e., the rib thickness, was the only significant parameter which affects to any noticable degree. The trend is towards earlier fracture with increasing % reduction in area (thinner ribs).

Table 1. Experimental process conditions for single and opposed rib forging.

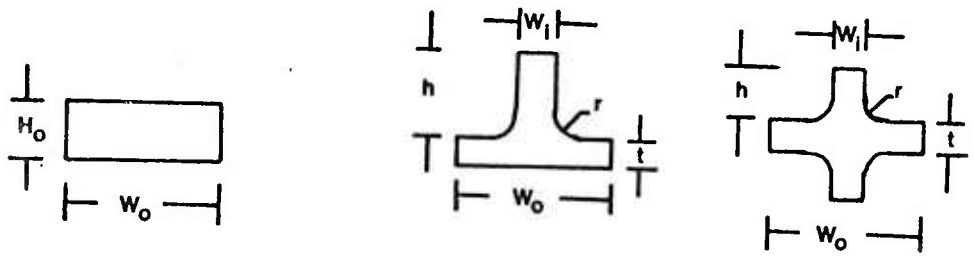

$$\%R = (1 - w_i/w_o) \times 100\%$$

Material : 601AB, 601AC aluminum alloy powder.
Preform density : 85% theoretical.
Lubricant : Copper dispersed in oil.
Temperature : Room temperature.
Preform aspect ratios (H_o/w_o) : 0.6, 0.5, 0.4, 0.3, 0.2
% Reduction in area (%R) : 30%, 60%, 90%
Fillet radius (r) : sharp, 1/64", 1/16", 1/8"

Die contact surface fracture, as expected, was primarily controlled by the punch corner radius. Smaller radii promoted the occurrence of fracture. The 1/8th inch radius case did not exhibit any die contact surface fracture.

The preform aspect ratio indicated some correlation to the occurrence of side intrusion defects. In general, the occurrence was increased with decreasing preform aspect ratios and % reduction in area. For single rib shapes, bottom intrusion occurs for low preform aspect ratios but higher % reduction in area. For opposed rib shapes, these same conditions influence internal fracture. The scatter band of the data was too wide to derive any quantitative correlations.

The rather premature occurrence of free surface fracture led to a closer examination of the growth of strain at the surface during deformation. The strains were measured and are plotted in Figure 22, for a thin, single rib.[33]

For the two punch corner radii indicated, the strain increases very rapidly and tapers off at larger punch displacements. The workability limit for the material is shown, and it is evident as to why fracture was exhibited. The rapid growth and subsequent tapering off suggests a corner radius influence. Specifically, that as the material is rounding the corner, the free surface undergoes excessive strain. To control the initial strain effects, a preform with the corner built in is inferred. Such a preform was

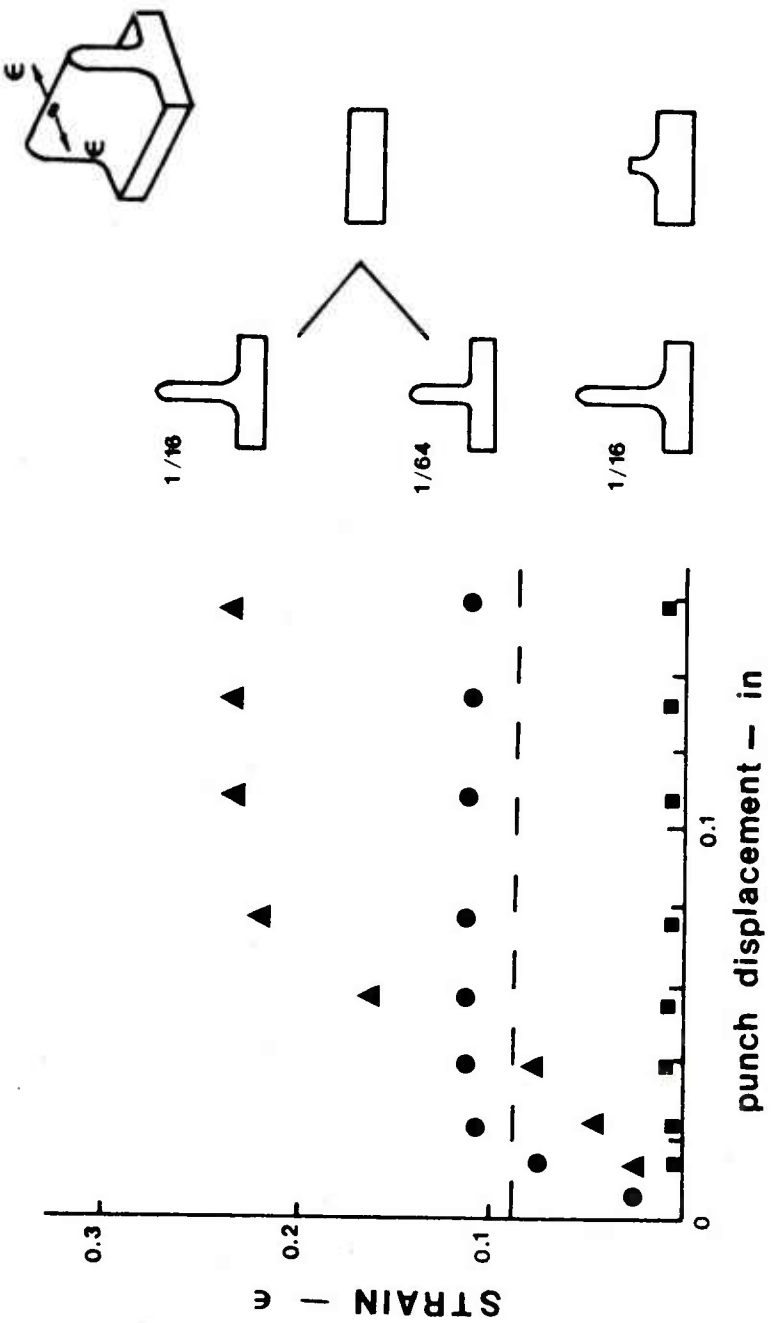

Figure 22. Strain history at free surface of back-extruded, 6061AB aluminum alloy preform during forging.

subsequently used, and the results are shown. The importance of preform design is once again demonstrated. Note that the ribs are draftless. The presence of a draft angle increases the influence of friction and the strain at the free surface will continously increase with increasing deformation.

Densification of thin ribs was good, due to the large amounts of lateral flow at the rib base. As the thickness increases, greater density gradients are to be expected across the thickness of the rib. This implies that thick ribs have to undergo some amounts of repressing to fully densify it. Consequently, the forging of thick ribs, if possible, is to be preferably done by upsetting.

4.5 Overview of CAD of Preforms

The computer-aided design of preforms to powder forge a complex part consists of two major activities, namely, (i) Part Geometry Description and (ii) Preform Design. The two may be independent of each other, however, for a coherent transition from one to another requires that the part description be compatible and complete to the extent required by the preform design phase. A general part description is not the goal of this research. Any part description simplifications that result due to limitations in the preform design stage are expolited. Simplicity, without loss of accuracy, was the emphasis for the design of the part

description program.

Conceptually, the preform design phase may be roughly classified to consist of the following subtasks:

(1) Sub-division of a complex part into regions.

(2) Identification of basic deformation modes.

(3) Determination of preform shapes for each mode.

(4) Assembly of individual preform shapes.

The sub-division of a complex part into regions may be accomplished either by the designer explicitly specifying the regions or the program determining the region sub-divisions automatically according to some set of rules. At this stage, there is not enough experience to be able to define completely the region sub-division rules for the latter process. Consequently, region sub-division is delegated to the designer. The regions are explicitly specified, during part description, according to guidelines which need to be adhered to, to prevent possible design failures at a later stage.

Assuming that the complex part has been sub-divided into regions, two routes may be stipulated towards the determination of the preform shape. The first route is the automatic preform design, wherein, generic deformation modes are identified according to the region configuration; and for each mode a specific preform shape, that is established as optimum, is automatically determined. This process would require no user intervention. The complexity and the

relative inexperience in the vast possibilities preclude such an ideal scheme. The second route, is the interactive approach approach, where the preform shape is arbitrarily specified for each region by the designer. Depending upon the specification, the generic modes are isolated and the specified shape is evaluated for consistency, densification, fracture etc., by the program. The preform profile is then interactively manipulated by the designer till a satisfactory preform is determined. Some experience is required to judge whether the preform is satisfactory from a practical standpoint. However, in this approach, additional decision making functions can be built in as further knowledge and experience is obtained in preform design. The accuracy of the program will have to evolve through constant additions in the future.

Figure 23 illustrates the overall structure of the present CAD program. The part description phase is a seperate activity, primarily because of the probability of error being higher. The preform design phase is in an interactive graphics environment to allow for a rapid evaluation of trial preforms. The details are now considered in the appropriate sequence.

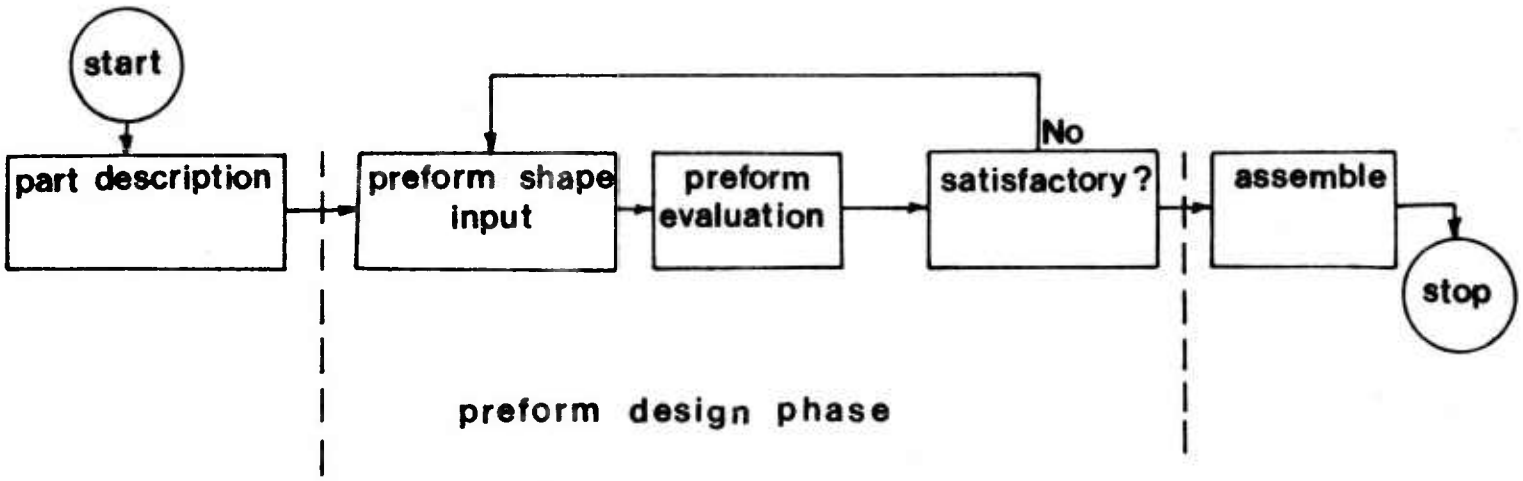

Figure 23. Overall structure of computer-aided preform design program.

4.6 Part Geometry Description

A part geometry description program was developed to describe a 3-dimensional part in a form that is suitable for subsequent processing by the preform design phase. The program emphasizes simplicity and, hence, limitations have been imposed to accomplish the description. The choice of APT for part description was rejected. Firstly, because it is designed for use in machining, and an APT description would require considerable reprocessing to convert to a form that is suitable for forging preform design. Secondly, it needs considerable user training. Thirdly, the size of the APT program is much too large as it contains features completely unrelated to forging.

The program that was developed is called "PADEL" (PArt DEscription Language). It is tailored to specifically meet the requirements of powder forging. In addition to being able to describe the part, region sub-divisions may be readily accomplished, forging directions specified, volumes calculated etc., which are features peculiar to powder forging. It is not generalized to describe all possible components. Nevertheless, it is capable of describing a large class of parts that are currently being powder forged.

4.6.1 Description Space

The part description is done in the first octant of a 3-dimensional Carthesian space, called the description space, Figure 24. The coordinate planes are referred to as XYPLN, YZPLN and ZXPLN. The forging plane is implicitly fixed as XYPLN, hence, the forging direction is the negative Z-direction.

Prior to description, the part is oriented so that it is wholly in the description space and has the desired forging direction. If the part has any plane of symmetry, then the appropriate plane is made to coincide with a coordinate plane. The coordinate plane is then explicitly identified as being a plane of symmetry. In this event, only that portion of the part in the description space need be defined.

4.6.2 Zone Description

A zone is defined as a volume that is generated by translating or rotating about an axis a representative cross-section. The translation or rotation is bounded by two planes, called the primary and secondary definition planes. Hence, in effect, a zone is describable by defining the primary and secondary definition planes, along with the cross-section profile in the primary definition plane.

Any part that is describable by PADEL is assumed to be decomposable into zones. The decomposition of a part in

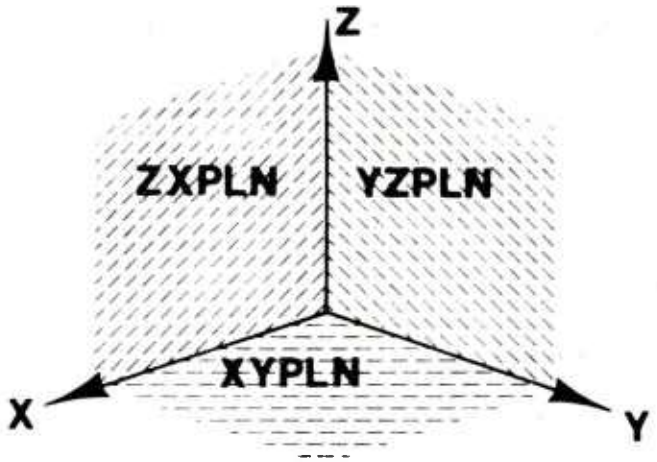

Figure 24. Definition of the part description space.

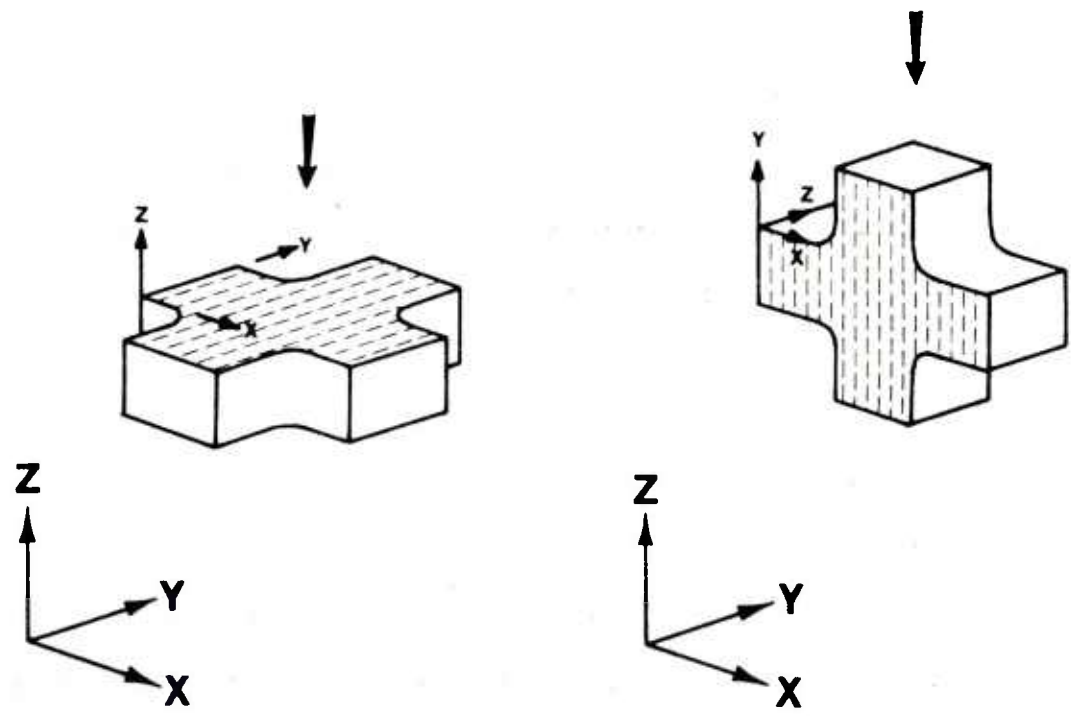

Figure 25. Primary definition plane orientations possible for the definition of zones.

description space is accomplished by defining "cut planes" that intersect the part, thereby isolating the zones. The cut planes are always normal to the forging plane, and furthermore, do not permit any metal flow from one zone to another through itself. The pair of definition planes that define any zone may be either parallel or normal to the forging plane, Figure 25.

By definition of a zone, a restriction is placed on the geometric complexity of the part that can be described. Specifically, variation in the cross-section profile during translation or rotation cannot be represented. The advantage of this restriction is that a complex 3-dimensional part may be considered as a series of cross-sections. Preform design is considerably simplified when done on a cross-section level. However, small features in the part, which cannot be decomposed into zones, can be indirectly input as an excess volume to be added on to the appropriate zone.

4.6.3 Cross-Section Description

Any zone is completely defined by its definition planes and the cross-section profile in the primary definition plane. The cross-section profile is described by two contours, whose ends are connected by straight lines to close the profile. Such a description serves to distinguish the surfaces of the zone that contact the punches, die side walls and adjacent zones.

In the case where the primary definition plane is normal to the forging plane, the contours that are described represent intersections of the primary definition plane with the upper and lower punch surfaces. The ends of the contour, which are connected by straight lines, in turn, represent the intersection of the definition plane with either the die wall surfaces or cut planes.

In the case where the primary definition plane is parallel to the forging plane, the contours represent intersection of the primary plane with the die wall surfaces. The cross-sections on the definition plane, in themselves, are surfaces that are coincident with the upper and lower punches respectively.

Each of the two contours are described using statements borrowed from APT. The contour is assumed to be a contiguous sequence of line segments and circular arcs. Each of these segments are first explicitly defined by the respective APT geometric statements for lines and circles and then the sequence is specified by other statements.

4.6.4 Region Description

Once the two contours of a cross-section are defined, the region sub-division is accomplished according to changes in the contour. The sub-division is done by specifying the interface locations. The interfaces are strictly plane surfaces, which upon intersection with the primary definition

plane, result in a line that intersects the two contours only once. The interface lines are defined so that the lateral metal flow is approximately normal to the interface line.

1.6.5 Structure of PADEL

The part description program, PADEL, is implemented as a two stage processor. The input to the processor is a source program consisting of legal statements (Appendix C), that describe the part.

Stage I processing is essentially a syntax check on the validity of the source program statements. Each statement has a rigid syntax that must be adhered to. Any syntax errors detected during processing will prevent entry into stage II.

Stage II processing is the arithmetic processing stage. The part is internally reconstructed by the program as an assembly of regions. The surfaces of each region are identified with punch surfaces, die wall surfaces, cut planes etc. Any errors detected at this stage will cause PADEL to abort. On successful processing, the part is stored on a zone by zone basis in a disk file for use by the preform design phase.

4.7 Preform Design Methodology

Preform design is accomplished on a region by region basis. The flow of metal in the regions is determined by the relative shape difference between the tooling and the preform. Tooling profiles are established in the part description stage. Hence, once an approximate preform shape is provided, metal flow may be inferred and evaluated.

The description by PADEL reduces a complex component to a set of zones. The cross-section of each zone consists of two contours, called the TOP and BOTtom contour respectively, which are connected at its end points by straight lines. Each zone is further decomposed into regions, the interfaces being represented in the cross-section plane by interface lines that intersect the contour at points. These intersection points between the region interface lines and the contours are called "nodes". Note that the end points of the two contours also become nodes. By virtue of these definitions, the number of nodes on either contour is one more than the number of regions defined in the zone; the number of nodes on both contour being equal. Figure 26 illustrates these definitions.

The specification of a preform shape is a user function, done in an interactive graphics environment. Recall that the contours of a cross-section represent the intersection of the primary definition plane with the tooling surfaces at the end

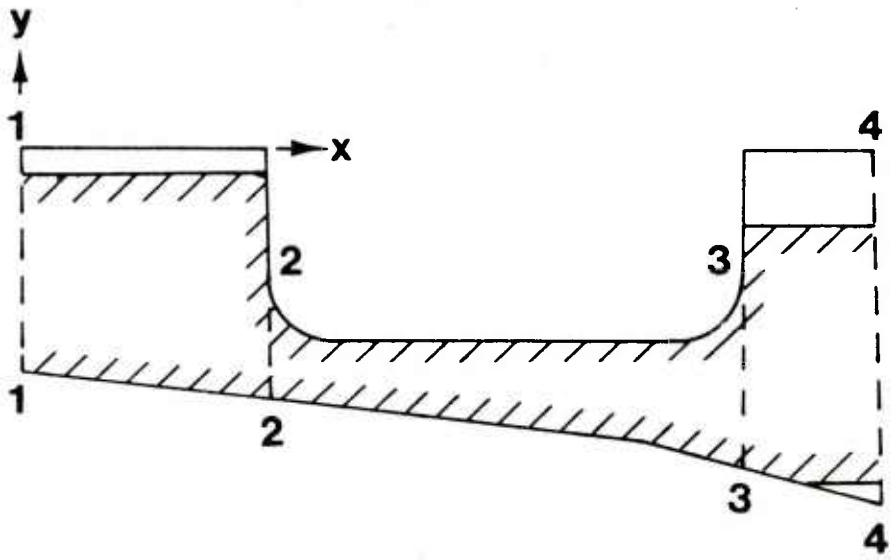

FILL / TOP,21,FROM,2,8.0
FILL / TOP,34,FROM,3,5.0
FILL / BOT,34,FROM,3,5.0

Figure 26. Definition of nodes on the 'TOP' and 'BOT' contour of a zone cross-section. The result of a preform specification by the user, with respect to the contours, is shown.

of the forging stroke. The preform shape input is done with respect to the contours, and in effect, represents the contact configuration of the tooling with the preform at the start of the forging. Preform design then entails a proper seperation of the user input preform shape profiles, so that proper weight control and distribution is obtained, and the evaluation for non-aggravating metal flow and full densification.

4.7.1 Preform Shape Description

The contours of a zone are defined in a local x-y plane. The nodes are ordered left to right by increasing values of its x-coordinates. Between a pair of nodes is the tooling profile for the region(s), Figure 26.

Preform shape description may be accomplished in two directions. The first is the "filling of cavities" of the top and bottom contours. The second is the specification of a clearance with respect to the end lines of the contours. The terms 'top' and 'bottom' are relative, and are defined according to the physical format of the display on the CRT. It is recommended that they correspond to the top and bottom punches. The present version of the preform shape evaluation program assumes this correspondence.

Consider an arbitrary cross-section, each of whose contours have M nodes ordered in increasing x-coordinates.

(i) The level of any node is defined as the value of the y-coordinate of the node, with respect to the local reference frame.

(ii) The minimum base level of a contour is defined according to

$$\begin{aligned} (\underline{y}_B) &= \text{Min}\{y_i\}_{i=1}^{M} \\ (\underline{y}_B) &= \text{Max}\{y_i\}_{i=1}^{M} \end{aligned} \tag{4-1}$$

(iii) Any profile between two nodes on either contour is referenced by the ordered node pair IJ; where strictly, I ≠ J.

(iv) Any interface line that connects nodes on the top and bottom contours is referenced by the node pair IJ, where strictly, I = J.

(v) A cavity is said to exist between the nodes I and J of a contour if the maximum (minimum) of the profile, y_p, is

$$\begin{aligned} y_p &> y_B \quad \text{--TOP Contour} \\ y_p &< y_B \quad \text{--BOT Contour} \end{aligned} \tag{4-2}$$

where y_B is the current base level for the profile. The cavity depth, H, is measured from the base level by

$$H = |y_p - y_B| \tag{4-3}$$

With these definitions the preform shape input scheme may be introduced. The shape input is based on appropriate manipulations of the base level of each contour, from the minimum level, by means of explicit commands. By progressively updating the base level, various preform shapes may be input. Three commands are available, namely, the FILL/ command, the FLOAT/ command and the NOFLOW/ command. Their description and function follow.

Filling of cavities is accomplished by a command of the form

FILL/[TOP,BOT],IJ,FROM,[I,J],k

where [TOP,BOT] represent an explicit identification for the top and bottom contour respectively.

IJ references the node pair, I=J.

FROM,[I,J] explicitly changes the base level to the referenced node I or J.

k is the degree of fill, measured from the base level, that is desired and $0<k<10$. A unit degree of fill is arbitrarily defined as H/10.

Specification of k=0 will result in the preform shape between the nodes I and J to be a horizontal line through the reference node. For k=10, the preform shape matches the tooling profile, i.e., no clearance is provided. Intermediate values of k will result in a clearance.

Once a profile is 'filled' by the command, it can only be 'refilled' or 'unfilled' by restarting the shape input. However, other profiles of a contour may be addressed and manipulated. The current base level is used to automatically define the preform shape for those profiles not addressed by an explicit command. Figure 26 illustrates the result of a FILL/ specification. Note that the FILL/ command is exclusively used to describe the preform shape with respect to the top and bottom contours only.

Floating of the preform from the end lines of the contours is accomplished by a command of the form

FLOAT/II,k

where II represents the node pair corresponding to the end line.

k is the degree of float, measured from the end line, that is desired and, 0<k<10. A unit degree of float is defined arbitrarily as 1/10-th the distance from the end line to the interface line.

Specification of k=0, will result in the preform being flush with the end line. For k=10, the preform is flush with the interface line, and hence, is completely absorbed in the adjacent region.

To provide for flow in a direction normal to the definition plane, the command

NOFLOW/II

where II represents an interface line, is used. The preform design program always attempts to provide flow in one direction. Hence by properly constraining flow in the definition plane and a judicious use of NOFLOW/, flow in the normal direction may be achieved.

The use of the above commands is illustrated in a later section where the preform shape is specified for a weapon component.

4.7.2 Preform Shape Evaluation

The evaluation of the shape input by the user is done in two stages. First, the stroke is computed by appropriate mass balances and second, the overall metal flow that occurs in the regions is checked for consistency with predetermined allowable conditions. Inconsistent metal flow will lead to undensified regions. These situations are rectified by the user by appropriate manipulations on the input shape.

The bottom punch is assumed to be stationary. The initial preform density is assumed to be constant for all regions in the part. The program attempts to determine a single stroke for the upper punch that is required to size the preform. In the case of hot repressing of multi-level parts with preforms of uniform initial density, a single

stroke will result in undensified regions. In such cases, split punches are used where each punch has a stroke that provides for full densification of a region.[5] A single stroke option for repressing is applicable only in the case where the preform has a non-uniform initial density in various regions. In contrast, presence of metal flow during upset forging of preforms allows for a single stroke and uniform initial preform density. This necessitates that proper clearances for metal flow be provided so that a proper preform weight distribution is achieved to form a fully densified part.

Any region of the part consists of 6 surfaces, as shown in Figure 27. Each region exhibits a characteristic metal flow during forging, according to the relative shape difference (and hence clearance) between the preform and the tooling. Table 2 illustrates the various metal flow possibilities that occur in a region during forging. These flow possibilities are for regions derived from a parent zone, whose primary definition plane is normal to the forging plane. Consequently, region interfaces are coincident with the Left and Right surfaces. The presence of metal flow across interfaces is used to classify a region as a member of an extrusion deformation mode (or extrusion group). No metal flow across interfaces classifies a region as a member of an upset deformation mode (or upset group). Note that similar metal flow possibilities exist for regions derived from a

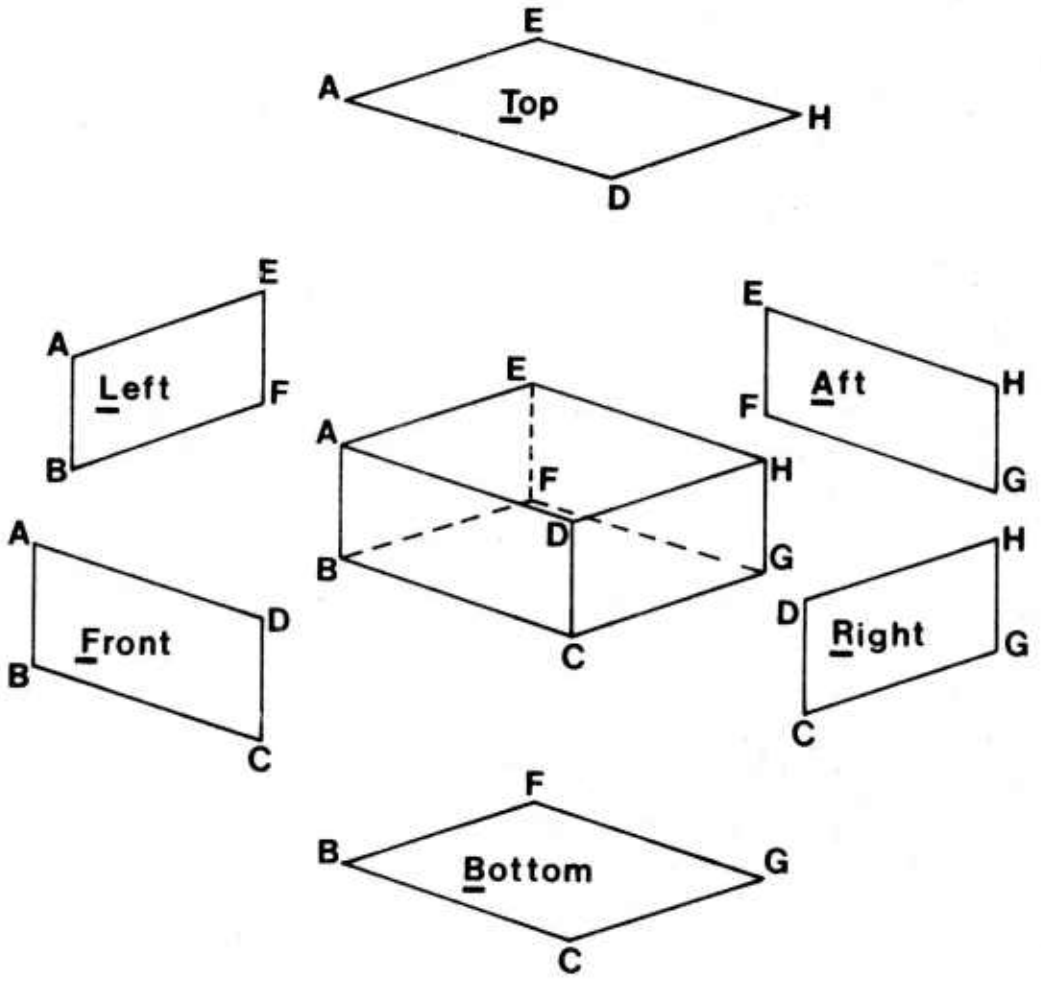

Figure 27. Illustrations of surface descriptions for a region, for preform design.

Table 2. Metal flow directions in regions during forging.

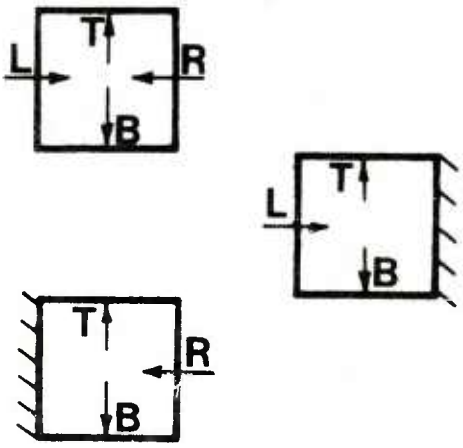

DUAL EXTRUSION

Interface flow into region

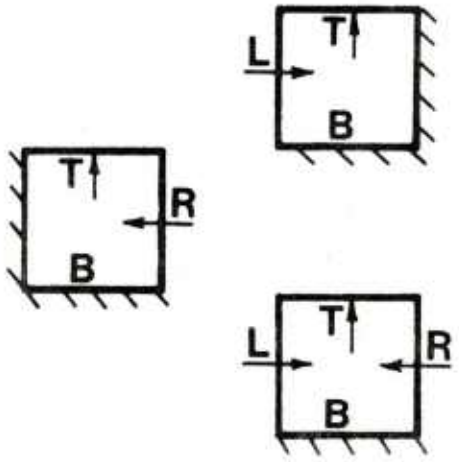

BACK EXTRUSION

Interface flow into region

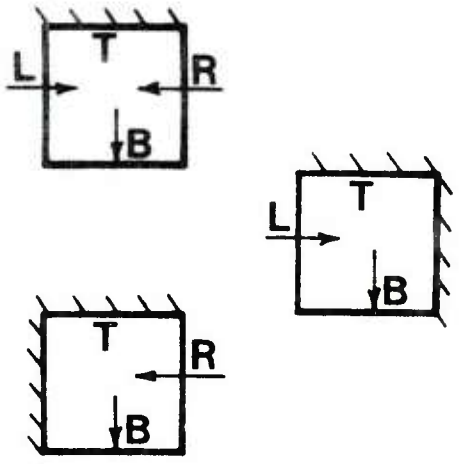

FORWARD EXTRUSION

Interface flow into region

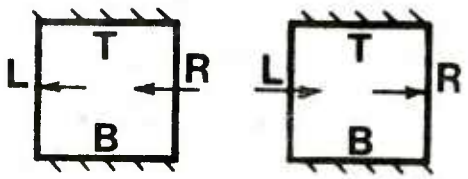

LATERAL (normal) EXTRUSION
Interface flow into region

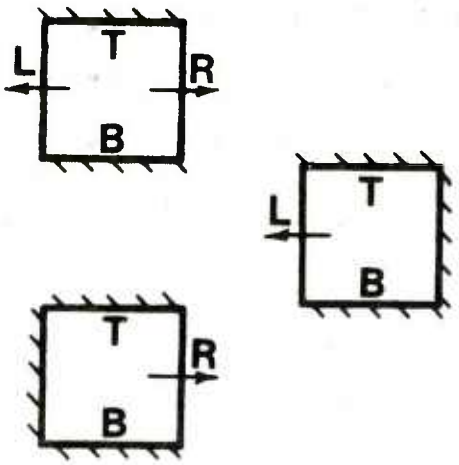

LATERAL (normal) EXTRUSION
Interface flow out of region

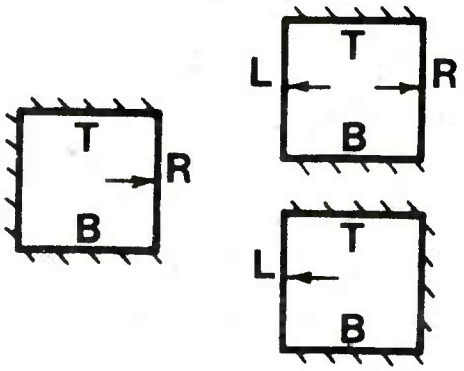

UPSET
Contained flow, towards Left / Right surfaces

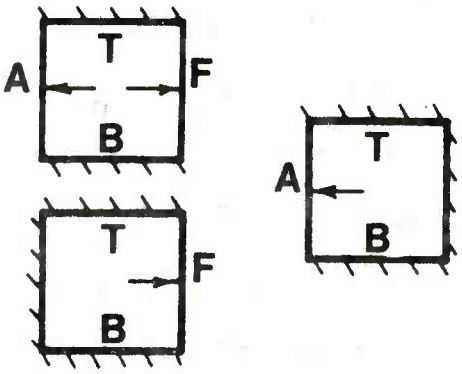

UPSET
Contained flow, towards Front / Aft surfaces

parent zone whose primary definition plane is parallel to the forging plane. These possibilities are not incorporated in the present shape evaluation program. The extension is a future task, and may be readily appended by following procedures analogous to those currently implemented.

The mass balance strategy for a region is dependent upon whether the region is a member of an extrusion group or an upset group. For an arbitrary region, the mass of material in the region at the finished forged state, M_f, is given by

$$M_f = \rho_f (A_f . D_f + \Gamma_f) \qquad (4-4)$$

where ρ_f = theoretical density of the material.

A_f = cross-sectional area of the region.

D_f = depth of region in the normal direction.

Γ_f = additional volume for the region, due to a feature that could not be input via PADEL.

The mass of preform material required in the region need not be equal to M_f. This is true when the region belongs to an extrusion group and exchanges mass across interfaces. However, if it belongs to an upset group, there is no mass exchange, in which case the mass of preform material is equal to M_f. Recall that the preform shape is input with respect to the tooling profiles at the end of the stroke. Hence, the cross-section area enclosed by the preform input shape for a region, A_p, is less than or equal to A_f. This depends upon the shape specified by the user. Figure 28 illustrates three possible cases of shape (clearance) specification.

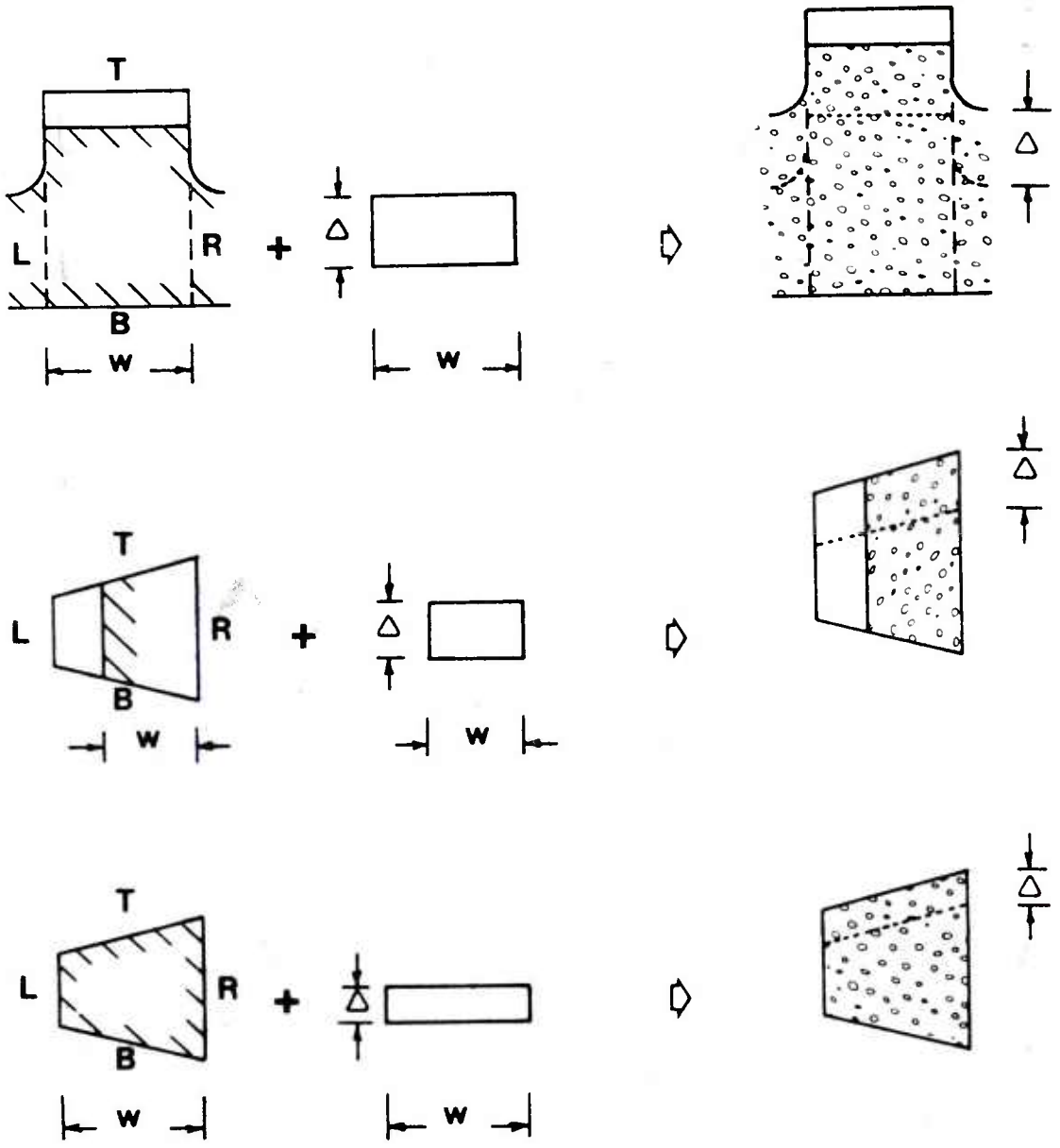

Figure 28. Schematic representation of stroke computations for regions with clearances in each of the three directions.

For a stroke, Δ, the mass of the preform material in a region is given by

$$M_p = \rho_p(A_p.D_p) - \rho_p(\Delta.w_p)D_p \qquad (4\text{-}5)$$

where w_p is the width as shown in Figure 28. The subscript 'p' corresponds to quantities defined for the preform. Hence, for the region in an upset group, $M_p=M_f$. For the region in an extrusion group, $M_p = M_f$. Exchange of mass is postulated to occur out of a region through interfaces if $M_p > M_f$. Conversely, if $M_p < M_f$, mass exchange is into the region.

A region that is a member of an extrusion group must be paired with another region of the same group, across the interface that permits metal flow. The direction of metal flow is from a region of excess mass to a region of deficit mass. The total mass of preform material in an extrusion group, must equal that required by the group in the finished part. This mass balance is given by

$$\rho_f \sum_{i=K}^{L} (A_f D_f + \Gamma_f)_i = \rho_p \{ \sum_{i=K}^{L} (A_p D_p)_i + \Delta \sum_{i=K}^{L} (w_p D_p)_i \} \qquad (4\text{-}6)$$

By definition of the group, $(D_p)_i = (D_f)_i$, and the stroke, Δ, for the group is

$$\Delta = \{ \Sigma(V_f)_i / D - \Sigma(A_p)_i \} / \Sigma(w_p)_i \qquad (4\text{-}7)$$

where $\rho = \rho_p / \rho_f$ is the fractional density of the preform.

$D = D_p = D_f$ is the depth of the extrusion group.

$(V_f)_i = (A_f . D_f + \Gamma_f)_i$

Once the stroke is computed, the metal flow directions across interfaces may be readily determined by computing the excess or deficit mass for each region from (4-4) and (4-5). For a valid preform, the direction of metal flow must be consistent with the allowable flow configurations listed in Table 2. An inconsistent flow pattern will imply the possibility of under densification, this situation is rectified by appropriate modification of the input shape by the user.

A region that belongs to an upset group has no mass exchange with an adjacent region. The required mass is fully contained in the preform. The stroke, Δ , is directly related to the clearance. The mass balance for the region is given by

$$\rho_f(A_f D_f + \Gamma_f) = \rho_p\{A_p D_p + (\Delta . w_p) D_p\} \qquad (4\text{-}8)$$

Hence, the stroke, Δ , is

$$\Delta = \{V_f / \rho D_p - A_p\} / w_p \qquad (4\text{-}9)$$

Clearances can occur in two directions, as shown in Figure 28. Firstly, it can be in the lateral direction and secondly, it can be in a direction normal to the cross-section plane. In the first case, we have $D_p = D_f = D$, and the clearance 'c' is given by $c = (w_f - w_p)$. The stroke is then given by

$$\Delta = (V_f / \rho D - A_p) / (w_f - c) \qquad (4\text{-}9a)$$

where A_p is an implicit function of c.

In the second case, we have $w_p = w_f = w$, and consequently $A_p = A_f$. The clearance 'c' is defined by $c = (D_f - D_p)$. The stroke is

$$\Delta = \{V_f / \rho (D_f - c) - A_p\} / w_p \qquad (4\text{-}9b)$$

In both equations (4-9a) and (4-9b), the stroke is dependent upon the clearance. We can define a stroke range that varies between a minimum value corresponding to a zero clearance and a maximum value corresponding to a maximum allowable clearance. The maximum allowable clearance is strictly to be determined from workability considerations. Presently it is set to be half the total length in the direction of flow.

Consider a zone, which is an assembly of regions that belong to the upset group. Each region of the zone will yield a stroke range if no clearances are specified explicitly. On the other hand, if clearances are explicitly specified, then each region will yield a unique stroke according to (4-9a) or (4-9b). These strokes need not be the same, and we have a situation that is found in repressing. If instead of specifying explicit clearances, suppose only the desired clearance directions are specified. Then for each region, a maximum stroke and a minimum stroke may be

obtained. If the stroke for the zone is chosen as the largest of the minimum strokes, then only the region whose minimum stroke corresponds with the chosen stroke undergoes repress. The other regions have clearances, which may be determined by solving (4-9a) and (4-9b). It is for this reason that a specification of k=-1 in the FLOAT/ command is available. In such cases, the program computes the clearances for the regions.

If the zone has an extrusion group, the stroke is explicitly computed by (4-7). This stroke then forms the basis for calculating the clearances for all the upset group regions.

In the case of a multi-zone part with only upset group regions, the optimum stroke is chosen from the optimum for each zone. If two zones have extrusion groups with different strokes, then user intervention is necessary in choosing the stroke and the appropriate shape modification required to obtain a single stroke value.

During preform shape input, the program monitors each profile description as it is input by the user and attempts to define and classify the regions. If an extrusion group necomes defined, an attempt to change to an upset group by the use of the NOFLOW/ command will be foiled. Being an interactive program, various preform shapes may be readily input and evaluated. Upon successful design, the preform is stored on a zone by zone basis for subsequent compaction.

4.8 Application to a Weapon Component

The computer-aided design approach is applied to a non-axisymmetric weapon component. This serves to determine the feasibility of the approach and provide the framework for improvement of the interaction between the designer and the program.

The part drawing for the component is shown in Figure 29. The first task is the description of the component, along with identification of a forging direction and a schematic sub-division into zones and regions. The second task is the design of a preform using the CAD approach. The third and final task is the trial forging of the preform(s) to evaluate for occurrence of defects and undensified regions.

4.8.1 Geometry Description

The weapon component has a plane of symmetry. The part is shown in isometric, Figure 30, properly oriented in the description space. Note that the plane of symmetry is made coincident with a coordinate plane, hence only half the part need be described.

The orientation of the part, as shown in Figure 30, implies that the forging direction has been decided. For this component, this is the only orientation that will permit ejection of the part after forging. The presence of a

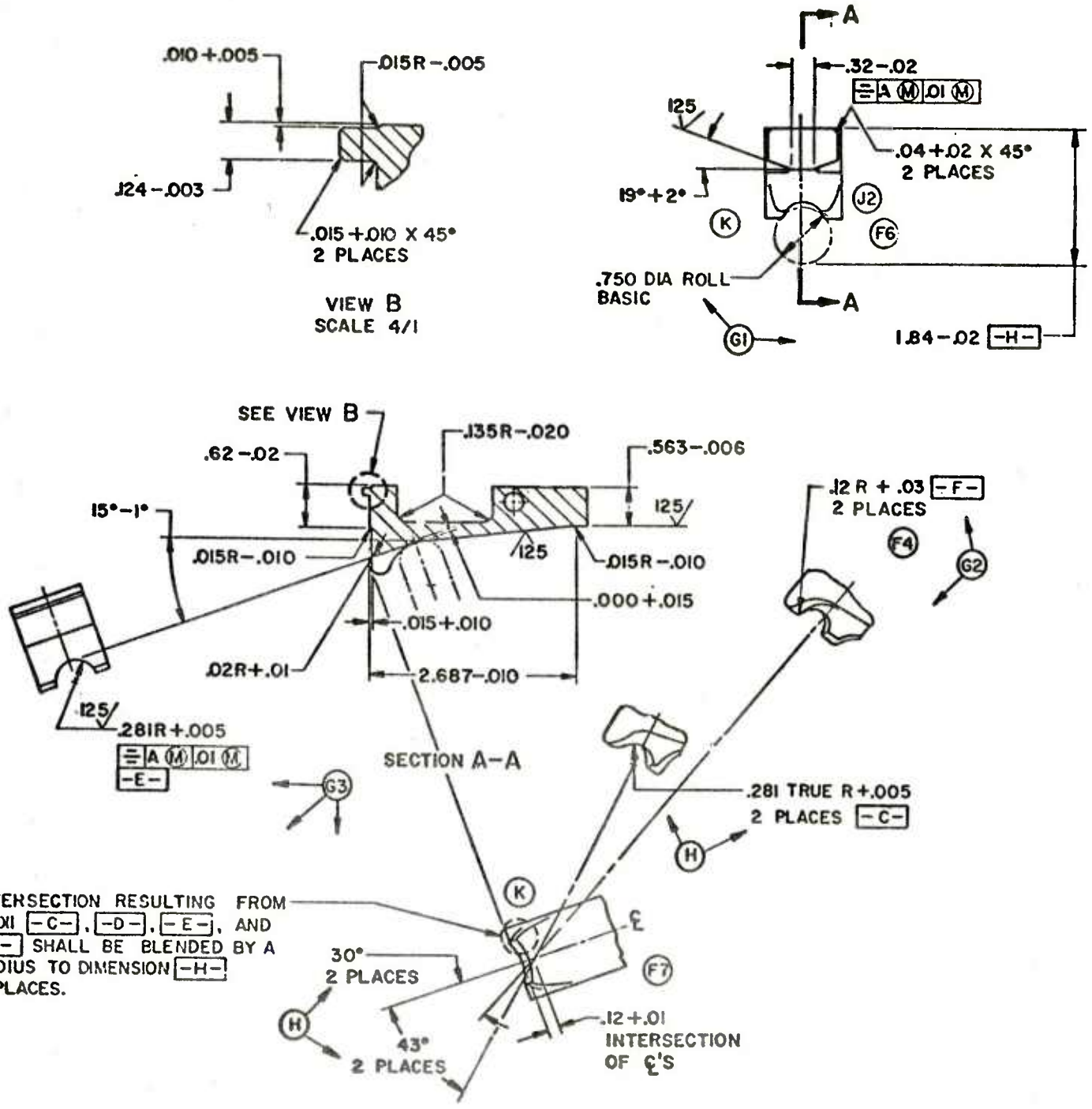

Figure 29. Part drawing for a non-symmetric weapon component.

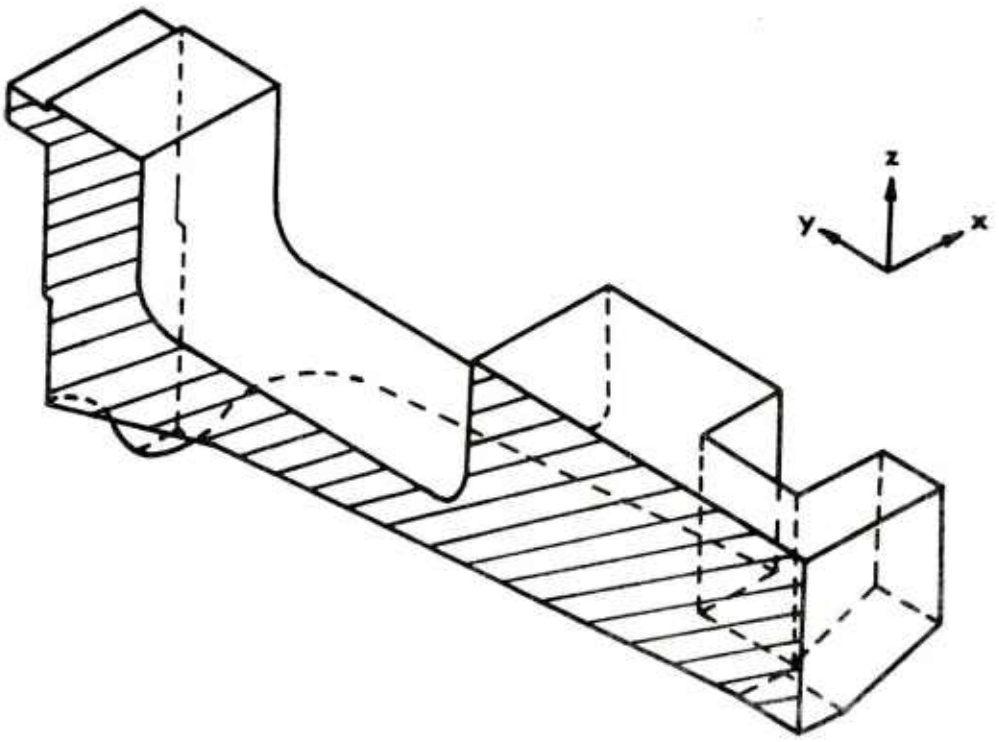

Figure 30. Half isometric view of the part oriented in description space. Note the plane of symmetry, and hence only half the part is described.

protrusion, called lug, at the bottom left precludes forging in the X-direction. However if, for the current orientation, a suitable preform cannot be obtained then the forging direction may be changed with subsequent machining of the lugs. In the present orientation, only the hole in the center, Figure 29, needs to be drilled.

Figure 31 illustrates the decomposition of the part into zones by slicing with cut planes, CTPL1 and CTPL2. The cut planes are normal to the forging plane. The part is shown in an exploded view, with the zones isolated, in Figure 32. The definition planes and the local coordinate planes are easily identified.

At this point, it is evident that the lug cannot be described as a zone since it does not have a characteristic cross-section. Therefore, the part is modified for description by removing the lug. The removed volume of metal is then input seperately, to zone 1.

The contours of each zone, Figure 33, are now described. Each contour is assumed to consist of a contiguous sequence of line segments and circular arcs. These are described using statements to define the lines and circles and then the connectivity is established. The statements are similar in format to those of APT, and are listed in Appendix C.

The PADEL source program that describes the weapon component is given in Appendix D. Figures 31, 32 and 33 used in conjunction with the source program will clarify the

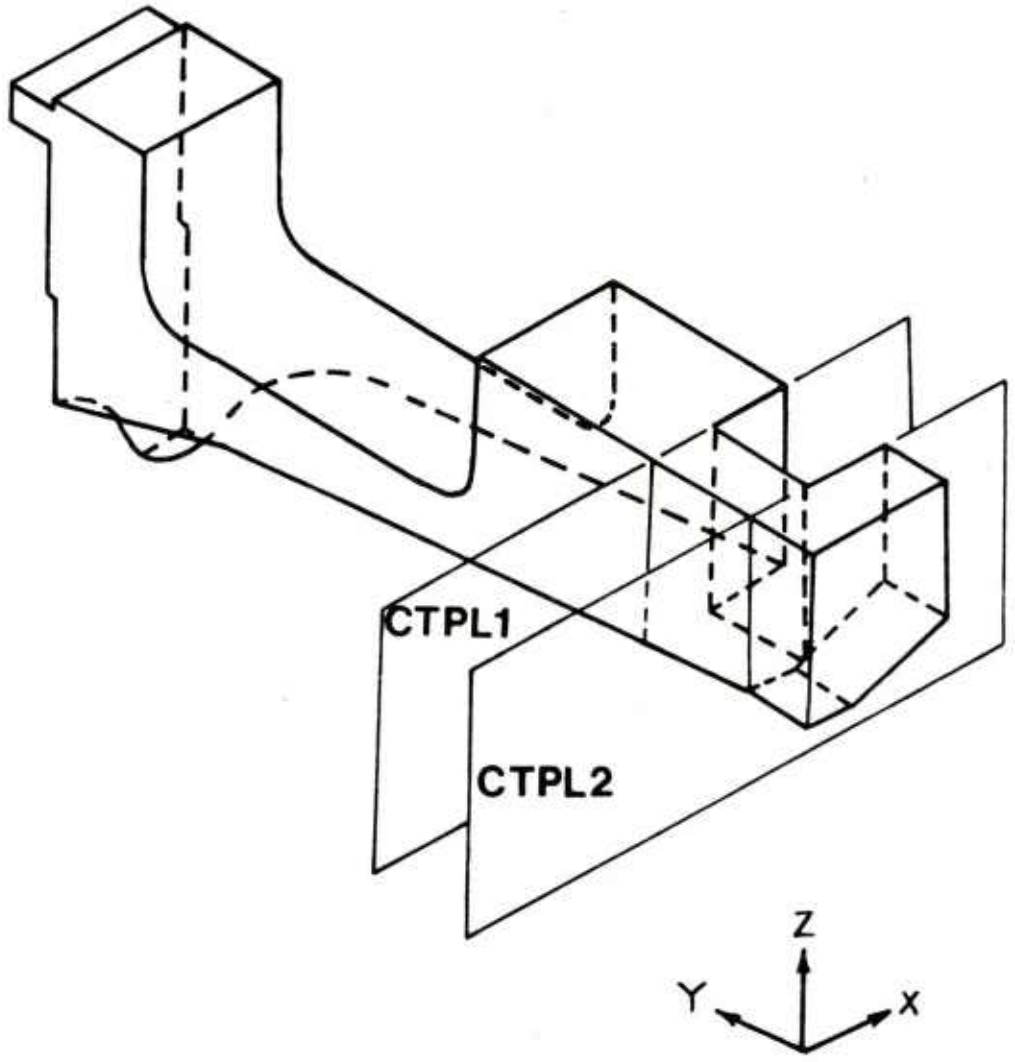

Figure 31. Decomposition of the part into zones using 'cut planes'.

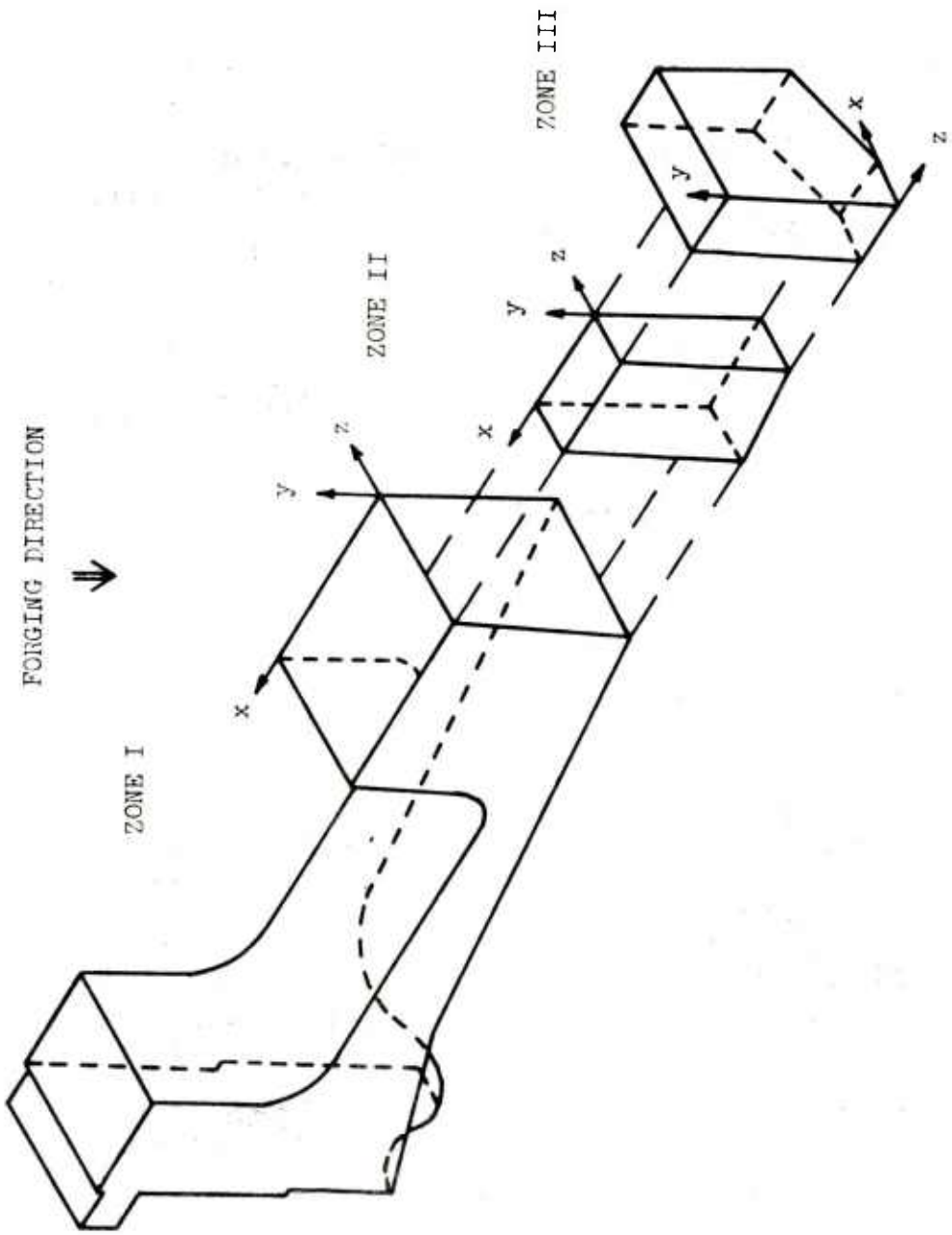

Figure 32. Exploded view of the part showing the zones and the definition planes.

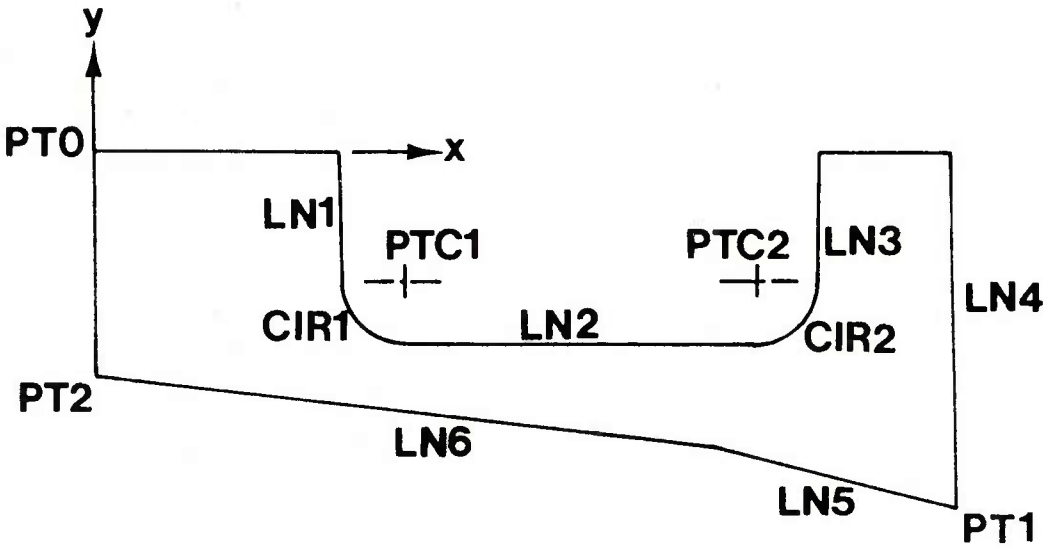

Zone - 1

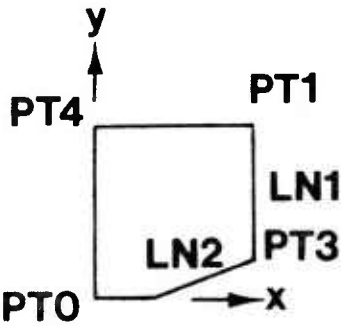

Zone - 3

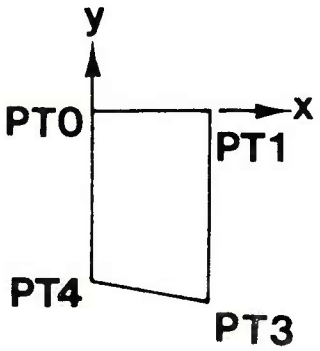

Zone - 2

Figure 33. Geometric elements for the contour description of the zones.

description scheme. Note that the lines in the source program that begin with a semi-colon are comment lines which are ignored by PADEL. The results of processing are stored in a disk file for input to the preform design phase. Graphics verification of the input is available.

4.8.2 Preform Design

The output from PADEL is the input for the design phase. Each zone of the part is explicitly called by the user, preform shapes are input and evaluated. Final assembly of the individual preforms to provide the overall preform is then automatically accomplished.

When a zone is explicitly called for preform shape input, the top and bottom contours are displyed on the CRT along with the nodes and the schematic region sub-sivision as shown if Figure 34. The preform shape input commands, to be entered by the user, are also indicated.

Consider zone 1. This zone is divided into 3 regions, which are ordered left to right. The minimum base levels for the two contours are computed. For the top contour, the minimum base level corresponds to the level of nodes 2 or 3. For the bottom contour, the minimum base level corresponds to the level of node 1. Filling of the shape is done with respect to these defined base levels. If no commands are specified, the base levels are used to compute the preform shape. Specifically, for the top contour, the preform shape

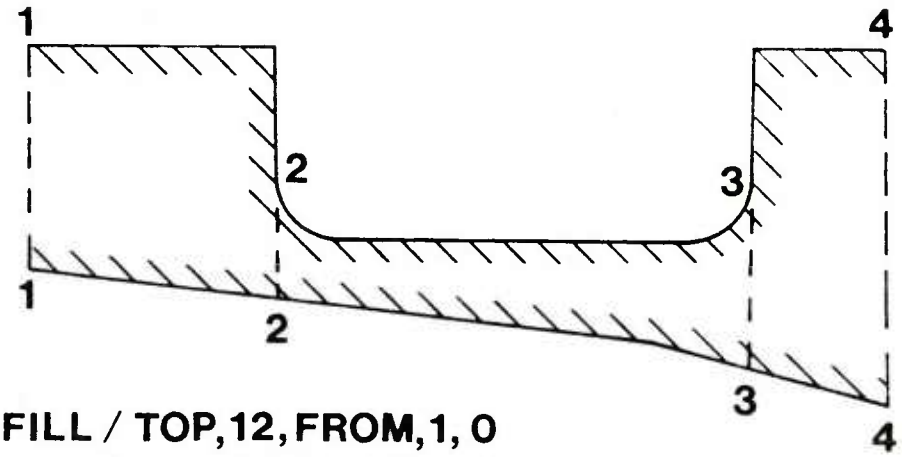

FILL / TOP,12,FROM,1,0
FILL / BOT,34,FROM,3,10
NOFLOW / 22
NOFLOW / 33

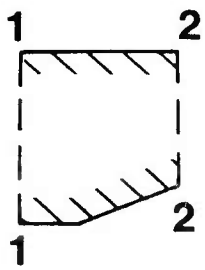

FLOAT / 22,-1

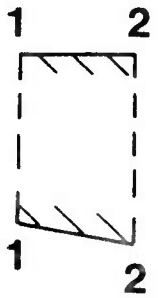

FILL / BOT,12,FROM,2,0

Figure 34. Shape input commands for the design of the preform for the part under consideration.

in region 1 a horizontal line through node 2; follows the contour from node 2 to node 3 in region 2 and is a horizontal line at level of node 3 in region 3.For the bottom contour, the shape is a horizontal line through node 1 for all the regions as the base level does not intersect the contour. The region interfaces 22 and 33 are assumed to permit flow unless explicitly stated otherwise with a NOFLOW/ command.

The first FILL/ command of Figure 34 addresses the TOP profile of region 1. Note that the fill reference level node is now node 1, hence the base level is changed to the level of node 1. If the shape is to match the contour in region 3, there is no necessity to specify another FILL/ command. This is true only if the contour in region 3 is lower than the established base level. The FILL/ command for the bottom contour has the same effect. The result of this specification is shown shaded in Figure 34. The result of a different specification for the same zone is illustrated in Figure 26.

Suppose that the NOFLOW/ command is not given. Then, the regions of zone 1 constitute an extrusion group. The stroke is calculated from a mass balance. The calculated mass is compared with the mass required in each region in the finished part. For an initial preform density of 80% theoretical, the calculated stroke is 0.15 inches. The computed masses for the regions are:

	Region 1	Region 2	Region 3
Required mass	0.2202	0.1568	0.1947
Preform mass	0.2172	0.2028	0.1517
Difference	-0.0030	0.0460	-0.0430

The interface metal flow is from region 2 to both regions 1 and 3. However, most of the flow is from region 2 to region 3, with very little flow from region 2 to region 1. Region 1, then, is approximately under repress with about 20% height reduction. For this stroke it is improbable that region 3 will be fully densified.

Specifying the NOFLOW/ commands to the above preform changes the mode of deformation. As a result, metal flow in each region is contained and, the direction of flow is normal to the plane of the paper. Each region then becomes a member of the upset group. For an initial preform density of 80% theoretical, the stroke is computed to be 0.48 inches and this stroke corresponds to the largest of the minimum strokes for the regions. Furthermore, it corresponds to the minimum stroke of region 3. Hence, now region 3 undergoes a repress. Recall that region 3 contains the lug at the bottom and a lip at the top; so some metal flow is bound to occur to fill these undefined features. Regions 1 and 2 have clearances from the die walls and lateral metal flow is present during forging.

Table 3. Volumes of regions in the weapon component.

Total measured volume of part = 21.52 cc = 1.3132 in^3
Volume of central hole = 0.0505 in3
Total volume of finished part = 1.3132 + 0.0505
= 1.3637 in^3

Computed volumes for the described part:

Zone 1------	Region 1 = 0.2202 in^3	
	Region 2 = 0.1568 in^3	
	Region 3 = 0.1622 in^3	
Zone 2------	Region 1 = 0.04729 in^3	
Zone 3------	Region 1 = 0.06294 in^3	
Total described volume (1/2 part)		= 0.6494 in^3
Described volume of finished part		= 1.2988 in^3
Volume of features not described		= 1.3637 - 1.2988
		= 0.0649 in^3
Volume to be added to Zone 1		= 0.03245 in^3

Since each region of the preform has the required mass of the finished shape, densification problems are avoided. Die wear at the corners is avoided as there is no substantial flow around them. Free surface fracture occurrence is also inhibited due to the presence of compression over the entire volume of the preform. Hence, this is a desirable preform.

The clearances for all the regions in the part are computed for a stroke of 0.5 inches. This was explicitly chosen to allow for a small clearance in region 3 to permit the preform to fall into the dies before forging. The assembled preform is shown in Figure 35. The broken lines indicate the die walls.

The preform shown in Figure 35 will lead to lap defects due to the sharp transition in the profile from one region to another. Generous blending is required to prevent this defect. This is done externally. The blended preform is shown, Figure 36, in isometric. The overall metal flow during forging is shown in Figure 37. The dimensioned preform drawing is given in Figure 38. This is the preform that is trial forged.

4.8.3 Prototype Forging

Six preforms were machined according to the preform drawing, Figure 38. The material was 4640 steel powder, compacted to 80% density and sintered at 2050F. Each machined preform was coated with graphite, reheated to 1800F

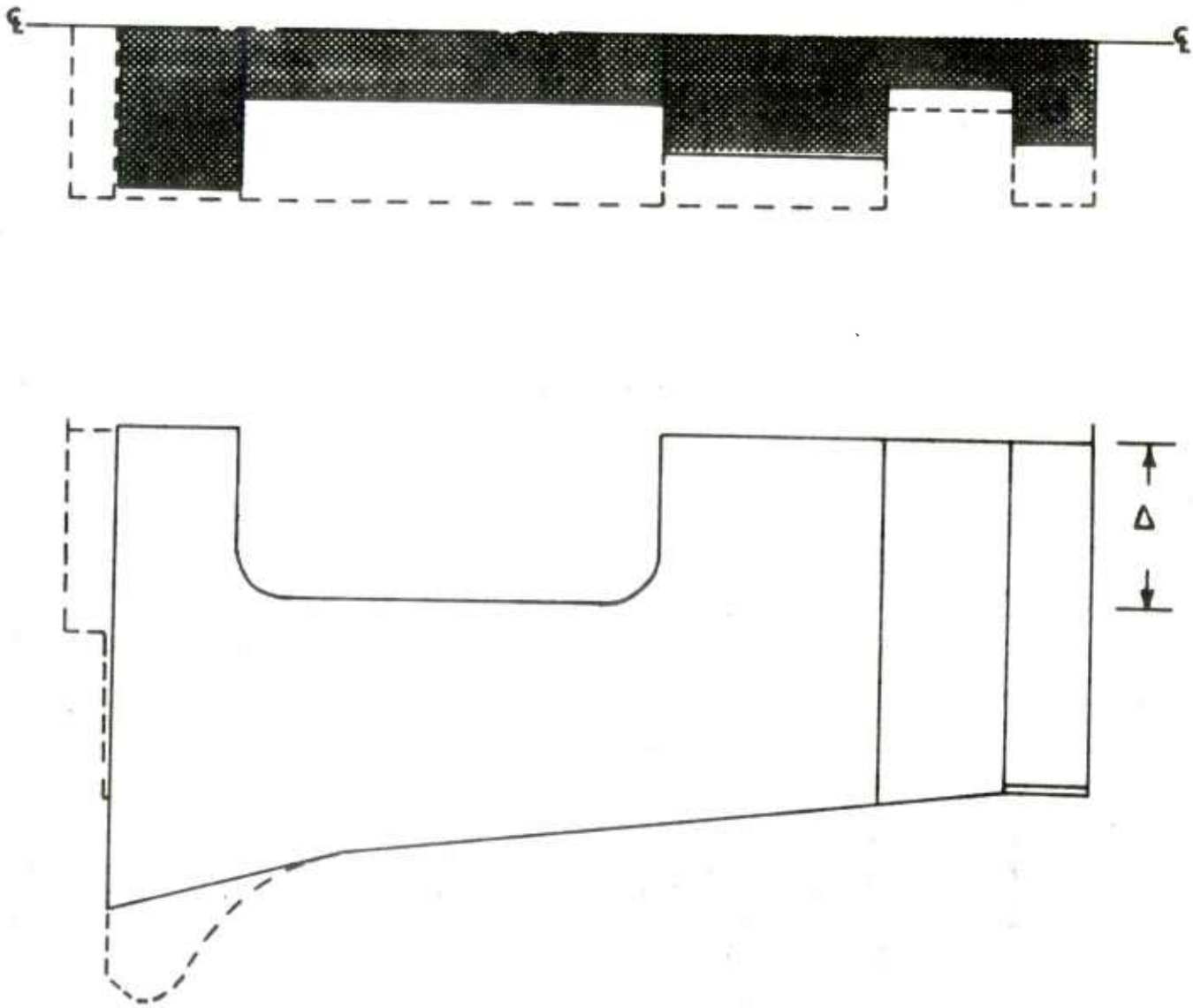

Figure 35. Assembled preform (unblended) showing the respective clearances.

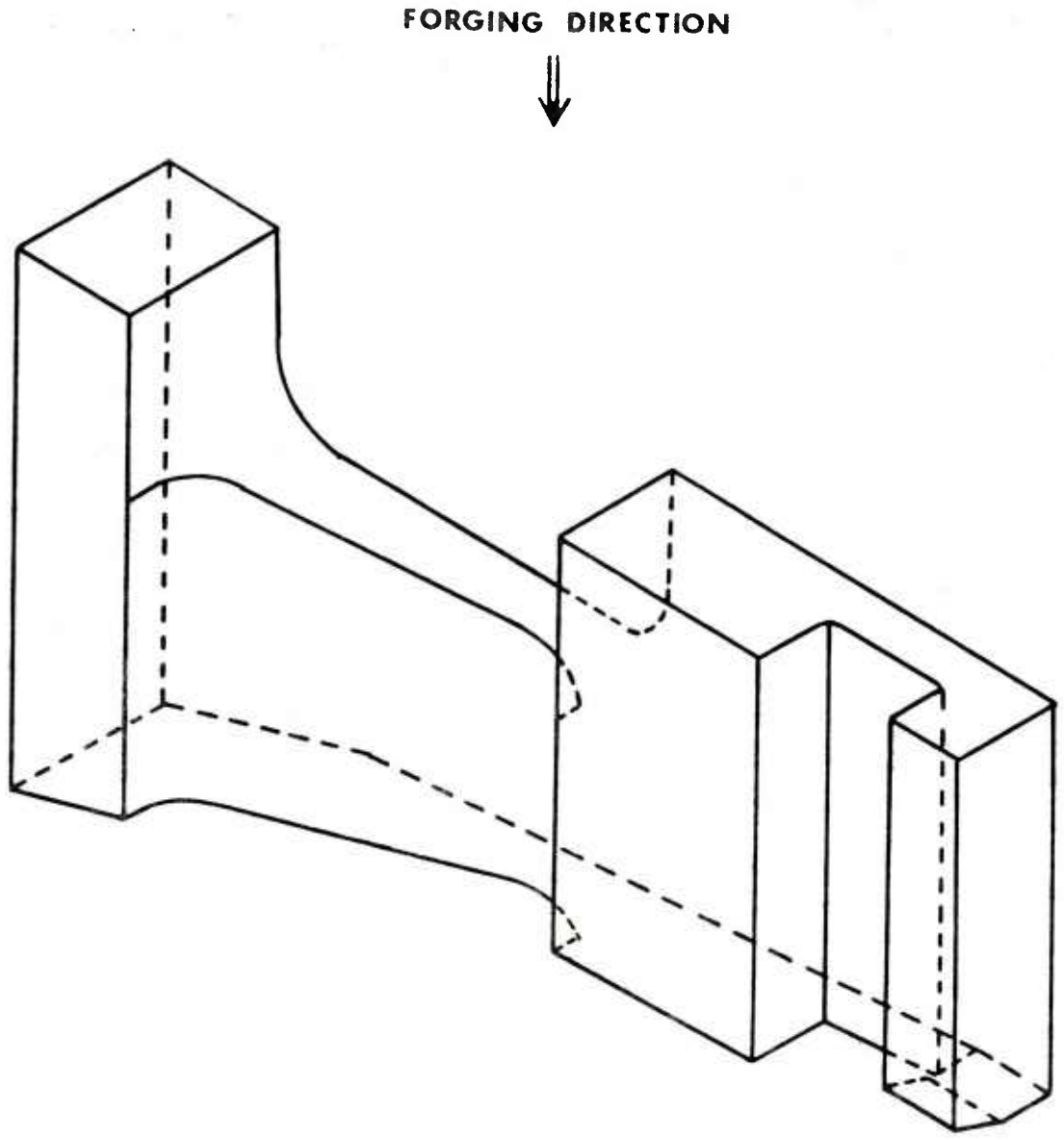

Figure 36. Half isometric view of the designed preform. The sharp corners have been blended externally.

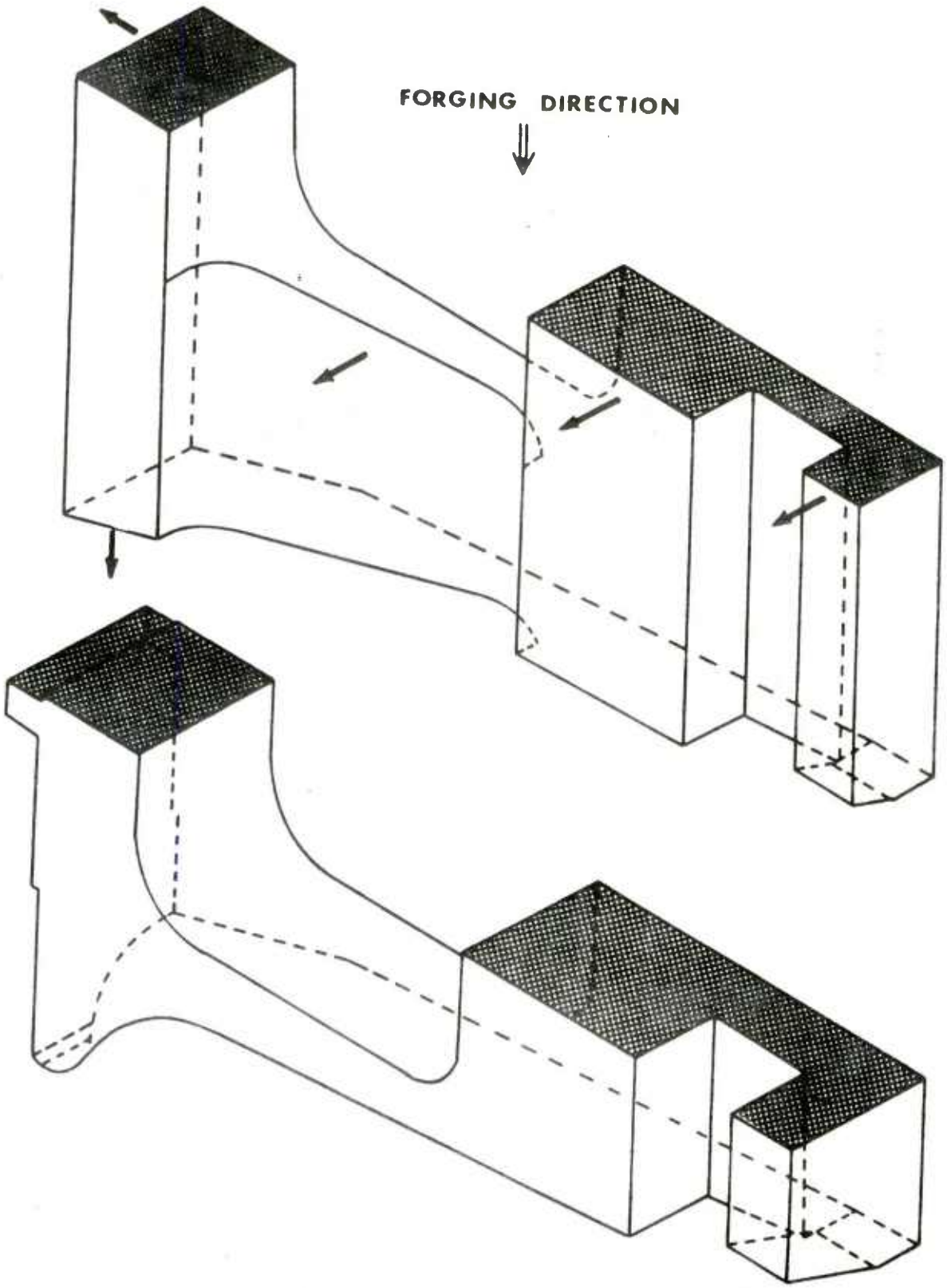

Figure 37. Metal flow directions in the designed preform during forging.

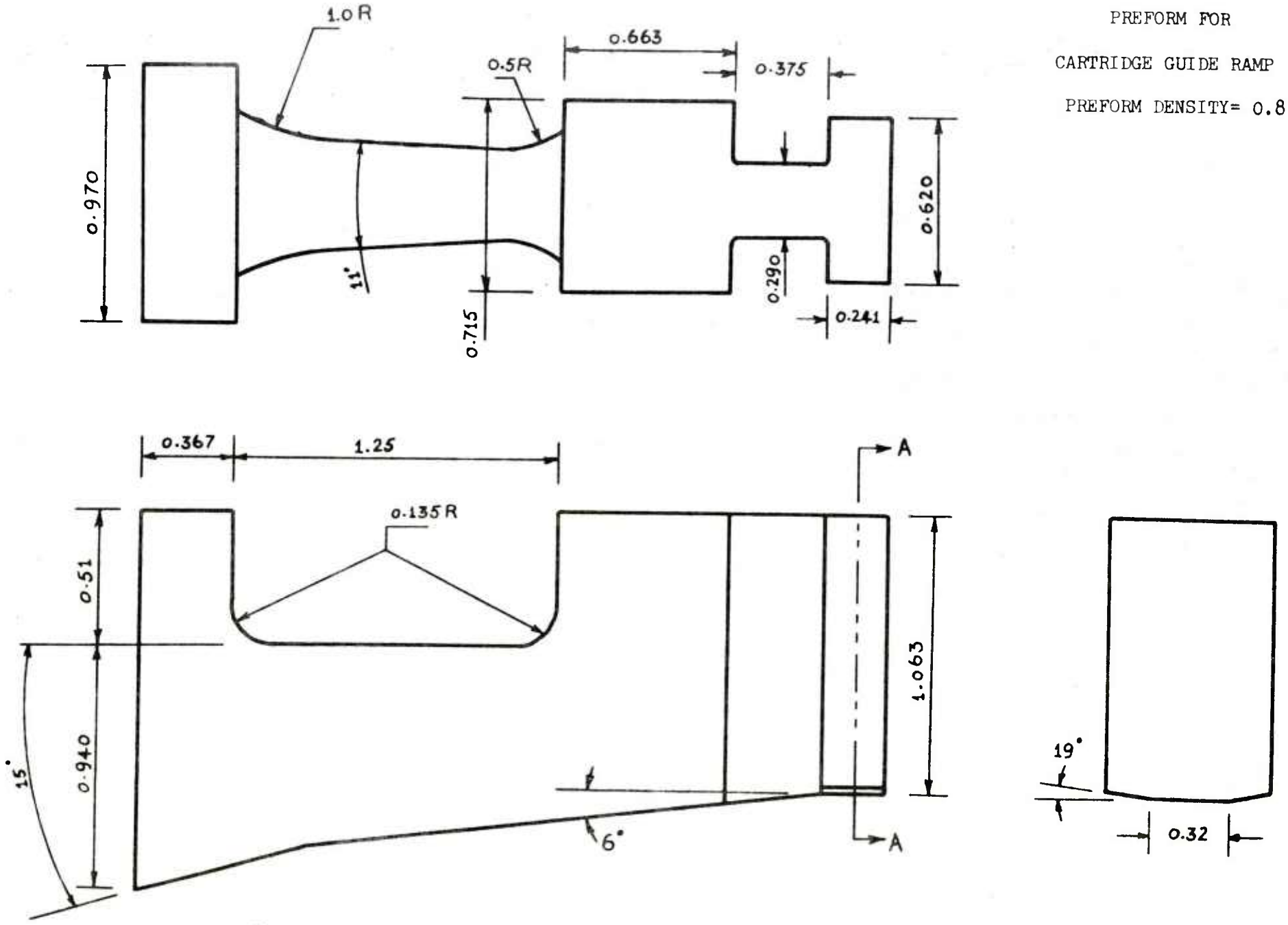

Figure 38. Dimensioned preform drawing for prototype forging of the part.

and forged in a hydraulic press. Prior to forging,graphite in water was sprayed on the dies for lubrication.

The forging trials were successful.[34] There were no defects in the forgings. The lugs, lip etc. were fully formed. Macrographs taken at various sections indicated good densification, except for some residual porosity at the surfaces.[35]

A flat preform was also forged to ascertain the defect formation. As expected, it resulted in considerable fractures and lap defects. This experiment served to confirm the importance of preform design in powder forging.

5.0 CONCLUSIONS AND RECOMMENDATIONS

A computer-aided preform design technique has been developed and applied to obtain a preform for a weapon component. The designed preform was forged to a fully densified, defect free part. The goals, set out in the project have been achieved. Specifically, the goals were to develop a general approach, as far as possible, to input the data regarding the shape of the finished part and material; develop a preform design scheme for the part; design the preform for a specific part using the CAD approach; forge the preform designed; and critique the merit and limitations of this approach.

The CAD program developed consists of two phases. The first phase is the description of the part geometry, by a simple but efficient method. Currently available techniques for geometry description include sophisticated drafting packages (IBM/Lockheed CADAM) and the NC part description program APT. The use of these were rejected due to the considerable training required for the potential user. A part description scheme, called PADEL, was developed for this project. PADEL has features which are suited to forging applications. Specifically, forging direction specification, sub-division to regions and the identification of punch/die profiles. It is relatively simple to use. However, it has limitations on the complexity of part geometry that can be

described. These limitations are justifiable, as the goal of this research was not toward the development of another "complete" geometry description scheme.

The second phase is the preform design phase. Preform design is accomplished on an interactive basis where the user supplies trial preform shapes which are evaluated by the program for densification and optimum metal flow modes. By interactively manipulating the preform shapes, a desirable preform is obtained. The computer evaluation is based on empirical guidelines developed through experience with powder preform forging. The interactive approach eliminates most of the trial-and-error involved in preform design as is commercially practiced.

The effects of all process parameters on metal flow and fracture in powder preform forging is too complex to be incorporated into this program. As a result, an exact definition of the preform is impossible. Some minor adjustments may be necessary after a few forging trials. Evolution of the program through user experience and increased understanding of the mechanics of metal flow is expected to lead to constant improvements.

An immediate extension that can be considered is the extension of the current approach to axi-symmetric parts. The present program can also be used, with some modifications, to determine the punch strokes required for

hot repressing of preforms. In this case, user shape input can be bypassed as the preform shape conforms closely to the finished shape. A further extension is the design of die compaction processes, where extensive shape manipulation capabilities are not required.

The present program is implemented on a DEC-10 computer. Graphics capability is required, and the TEKTRONIX PLOT-10 software is used for this purpose. All programming is in FORTRAN-10, except for some specialized routines which are coded in assembly language. Some modifications will be required to execute on a different computer.

The state of analytical techniques was reviewed for application to the computer-aided design program. Two techniques were developed, the slab analysis and the energy method, in its simplest form. This development led to some interesting observations. Specifically, the influence of friction at the die/part interface on the densification behavior. Perhaps a fundamental experimental and analytical study is warrented at this stage. The energy method developed, can be extended using two-dimensional elements to obtain detailed density distributions in a deforming preform. Furthermore, it appears to be a promising technique for the application of workability analysis to preform design. Considerable research activity is foreseen in this area.

To start an analytical evaluation of preforms, the preform must be defined. The CAD approach, using empirical guidelines, can be used to specify the approximate preform that is subjected to analytical evaluation. Thus future activity should be directed along two fronts. First, the improvement of the empirical approach to yield a fairly reliable preform. Second, the development of the energy method of a similar technique capable of detailed results towards the evaluation of fracture and densification of preforms. Once these objectives are accomplished, an integrated powder forging process design may be assembled.

APPENDIX A

Radial Stress Distribution for Axisymmetric Slab

Consider the n-th slab or zone, as shown in Figure 10. The slab is located between the radial position r_n , r_{n+1} . The pressures acting on an infinitesmal element are also indicated. Taking force equilibrium along the coordinate directions, we have

Radial:

$$(p_r+dp_r)hrd\theta - p_r(r+dr)(h+dh)d\theta - \tau_u(r+dr/2)Cos\alpha_u d\theta\ dS_u$$
$$- \tau_l(r+dr/2)Cos\alpha_l d\theta\ dS_l - p_u(r+dr/2)Sin\alpha_u d\theta\ S_u$$
$$- p_l(r+dr/2)Sin\alpha_l d\theta\ S_l - 2p_\theta(h+dh/2)Sin(d\theta/2)\ dr$$
$$= 0$$

Assuming that Sin $d\theta/2 = d\theta/2$ and $p_\theta = p_r$, neglecting higher order differentials the above can be simplified to

$$dp_r/dr = \{p_r\ dh/dr + (\tau_u+\tau_l) + (p_u tan\alpha_u + p_l tan\alpha_l)\ \} / h \qquad (A-1)$$

Axial:

(i) Upper Interface.

$$p_z(r+dr/2)d\theta\ dr = p_u(r+dr/2)\cos\alpha_u d\theta\ dS_u - \tau_u(r+dr/2)\sin\alpha_u d\theta\ dS_u$$

which simplifies to

$$p_u = p_z + \tau_u \tan\alpha_u$$

(ii) Lower interface.

$$p_l = p_z + \tau_l \tan\alpha_l$$

Now by the geometry of the element,

$$-dh/dr = (\tan\alpha_u + \tan\alpha_l)$$

Eliminating p_u, p_l and dh/dr from (A-1), and changing pressures to stresses according to $\sigma_r = -p_r$, $\sigma_z = -p_z$ we have

$$d\sigma_r/dr = -\{(\sigma_r-\sigma_z)(\tan\alpha_u+\tan\alpha_l) + (\tau_u\sec^2\alpha_u + \tau_l\sec^2\alpha_l)\} / h$$

with

$$r = r_{n+1} \ ; \ (\sigma_r)_{n+1} = (\sigma_r)_{r=r_{n+1}} \qquad \text{(A-2)}$$

The interface shear is represented by a friction factor according to

$$\tau = mk \qquad \text{(A-3)}$$

where k :Shear yield of the porous compact.

m : friction factor.

APPENDIX B

Rectangular Element Equations for Energy Method

Consider the m-th element flanked by sides i and j. Then,

(i) Velocity vector interpolation.

$$\underset{\sim}{u}^{*}_{(m)} = G^{T}\,\underset{\sim}{v}_{(m)} \tag{B-1}$$

where

$$\underset{\sim}{v}^{T}_{(m)} = \lfloor \underline{\ } v_i \quad v_j \underline{\ } \rfloor \quad ; \quad G^{T} = \lfloor q_i \quad q_j \rfloor$$

$$q_i = (1+s)/2 \; ; \; q_j = (1-s)/2 \; ; \quad -1 < s < 1$$

(ii) Coordinate Transformation.

$$r = q_i r_i + q_j r_j \tag{B-2}$$

(iii) Strain-rate vector.

$$\dot{\underset{\sim}{\varepsilon}}_{(m)} = B\underset{\sim}{v}_{(m)} = \begin{matrix} \partial u/\partial r \\ u/r \end{matrix} \tag{B-3}$$

where

$$B = \begin{matrix} -1/r_{ji} & 1/r_{ji} \\ q_i/r & q_j/r \end{matrix}$$

(iv) Equivalent Strain-rate.

Simplifying (3-25) we get

$$\dot{\varepsilon}^2_{eq(m)} = \frac{2}{3(1+\nu)} \dot{\underset{\sim}{\varepsilon}}^T A \dot{\underset{\sim}{\varepsilon}} + \frac{1}{3(1-2\nu)} \dot{\underset{\sim}{\varepsilon}}^T C \dot{\underset{\sim}{\varepsilon}} + \frac{2\nu}{(1+\nu)(1-2\nu)} c^T \dot{\underset{\sim}{\varepsilon}} + \frac{1-\nu}{(1+\nu)(1-2\nu)} \dot{\varepsilon}^2_z$$

where

$$A = \begin{matrix} 1.0 & -0.5 \\ -0.5 & 1.0 \end{matrix} \quad ; \quad c = \begin{matrix} 1.0 \\ 1.0 \end{matrix} \quad ; \quad C = \begin{matrix} 1.0 & 1.0 \\ 1.0 & 1.0 \end{matrix}$$

Substituting (B-3) and simplifying

$$\dot{\varepsilon}^2_{eq} = \underset{\sim}{y}^T X \underset{\sim}{y} + 2\alpha_1 c^T B \underset{\sim}{y} + \alpha_0 \qquad \text{(B-4)}$$

where the element subscript (m) is dropped and

$$X = \frac{2}{3(1+\nu)} B^T A B + \frac{1}{3(1-2\nu)} B^T C B$$

$$\alpha_1 = \frac{\nu}{(1+\nu)(1-2\nu)} \dot{\varepsilon}_z$$

$$\alpha_0 = \frac{1-\nu}{(1+\nu)(1-2\nu)} \dot{\varepsilon}^2_z$$

(v) Element level functional.

The functional at the element level is

$$\phi = \int_V \sigma_{eq} \dot{\varepsilon}_{eq} \, dV - \int_{S_F} \tau \, G^T \underset{\sim}{v} \, dS$$

Substituting (B-4), we have

$$\phi = \int_V \sigma_{eq} (\underset{\sim}{y}^T X \underset{\sim}{y} + 2\alpha_1 c^T B \underset{\sim}{y} + \alpha_0)^{\frac{1}{2}} \, dV - \int_{S_F} \tau G^T \underset{\sim}{y} \, dS$$

and hence,

$$\partial\phi/\partial \underset{\sim}{y} = \int_V \sigma_{eq} (X\underset{\sim}{y} + \alpha_1 B^T c)/(\dot{\varepsilon}^2_{eq})^{\frac{1}{2}} \, dV - \int_{S_F} \tau G \, dS \qquad \text{(B-5)}$$

(vi) Linearization.

At the n-th iteration on velocity components, suppose

$$\underset{\sim}{y}_{(n)} = \underset{\sim}{y}_{(n-1)} + \Delta \underset{\sim}{y}_{(n)} \qquad \text{(B-6)}$$

Substituting (B-6) into (B-4) and retaining first order terms in $\Delta y_{(n)}$,

$$\dot{\varepsilon}^2_{eq(n)} = \dot{\varepsilon}^2_{eq(n-1)} + 2(\underset{\sim}{y}^T X^T + Q^T) \Delta \underset{\sim}{y}_{(n)}$$

$$= \dot{\varepsilon}^2_{eq(n-1)} + 2a^T_{(n-1)} \Delta \underset{\sim}{y}_{(n)}$$

where

$$Q = \alpha_1 B^T c \quad \text{and} \quad a_{(n-1)} = X \underset{\sim}{y}_{(n-1)} + Q$$

Hence,

$$\dot{\varepsilon}^{-1}_{eq} = (\dot{\varepsilon}^2_{eq})^{-\frac{1}{2}} = \dot{\varepsilon}^{-1}_{eq} - \dot{\varepsilon}^{-3}_{eq} a^T_{(n-1)} \Delta \underset{\sim}{y}_{(n)} \qquad \text{(B-7)}$$

The volume integrand of (B-5) at the n-th iteration is

$$= \sigma_{eq} \dot{\varepsilon}^{-1}_{eq(n)} \quad (X\underset{\sim}{v}_{(n)} + Q)$$

Substituting (B-6) and (B-7) we have,

$$= \sigma_{eq} \dot{\varepsilon}^{-1}_{eq(n-1)} \quad a_{(n-1)} + \{X - \dot{\varepsilon}^{-2}_{eq(n-1)} \; a_{(n-1)} a^{T}_{(n-1)} \} \Delta\underset{\sim}{v}_{(n)} \}$$

Defining $\Gamma = \int_{S_F} \tau G \, dS$, (B-5) becomes

$$\partial\phi/\partial\underset{\sim}{v} = \sigma_{eq} P_{(n-1)} \; \Delta\underset{\sim}{v}_{(n-1)} + \sigma_{eq} H_{(n-1)} - \Gamma \qquad \text{(B-8)}$$

where

$$P_{(n-1)} = \int_{V} \dot{\varepsilon}^{-1}_{eq(n-1)} \{ X - \dot{\varepsilon}^{-2}_{eq(n-1)} \; a_{(n-1)} \; a^{T}_{(n-1)} \} \, dV$$

$$H_{(n-1)} = \int_{V} \dot{\varepsilon}^{-1}_{eq(n-1)} \; a_{(n-1)} \, dV$$

Assembling (B-8) we have

$$\sum_{m=1}^{M} \partial\phi / \partial v = 0$$

The integrals are numerically evaluated using a 2-point Gaussian quadrature. The coefficient matrix of the system of linear equations is tri-diagonal and is solved using recursion relationships.

APPENDIX C

PADEL STATEMENT FORMATS

C.1 Part description space statements

(i) Point statements.

PPOINT / X, Y, Z

PPOINT / plane 1, plane 2, plane 3

(ii) Plane statements.

PLANE / ppoint, PARLEL, plane

PLANE / ppoint 1, ppoint 2, PERPTO, XYPLN

PLANE / PARLEL, plane, [XLARGE, XSMALL, YLARGE, YLARGE, ZLARGE, ZSMALL], d

The keyword "CUTPLN" may be substituted for "PLANE" to define cut planes. Note that the positive unit normals for the relative plane definitions are in the same sense as the parent plane. For the second definition, the sense of the normal is defined by

$$n \times v = k$$

where, n = positive unit normal.

v = unit vector from ppoint 1 to ppoint 2 projected on XYPLN.

k = positive unit normal of XYPLN.

C.2 Primary definition plane statements

(i) Point statements.

POINT / x, y

POINT / INTOF, line 1, line 2

POINT / [XLARGE, XSMALL, YLARGE, YSMALL], INTOF, line, circle

POINT / [XLARGE, XSMALL, YLARGE, YSMALL], INTOF, circle 1, circle 2

(ii) Line statements.

LINE / x, y, x, y

LINE / point 1, point 2

LINE / [XAXIS, YAXIS]

LINE / point, [LEFT, RIGHT], TANTO, circle

LINE / point, [PARLEL, PERPTO], line

LINE / point, ATANGL, θ ,line

LINE / PARLEL, line, [XLARGE, XSMALL, YLARGE, YSMALL], d

(iii) Circle statements.

CIRCLE / x, y, r

CIRCLE / point 1, point 2, point 3

CIRCLE / CENTER, point, RADIUS, r

CIRCLE / CENTER, x, y, RADIUS, r

CIRCLE / CENTER, point 1, point 2

CIRCLE / CENTER, point, TANTO, line

CIRCLE / CENTER, point, [LARGE, SMALL],
TANTO, circle

CIRCLE / TANTO, line, [XLARGE, XSMALL, YLARGE,
YSMALL], point, RADIUS, r

C.3 Non-definition statements

PARTNAME/ (user defined name)

FINISH/

ZONE/n

ENDZON/n

SYMMETRY/ plane 1, plane 2, plane 3

BETWEEN/ plane 1, plane 2

FRAME/ plane 1, plane 2

REVERSE/ plane 1, plane 2, plane 3

INCLUDE/ plane 1, plane 2

TOP/ point

BOT/ point

REGION/ line 1, line 2,...

GOFWD/ line 1, line 2,...

GOFWD/ line 1, line 2,...circle

GOCLK/ circle 1, circle 2

GOCLK/ circle 1, line

GOACLK/ circle 1, circle 2

GOACLK/ circle 1, line

ADD/

APPENDIX D

PADEL SOURCE STATEMENTS FOR A PART

```
;***** TYPICAL SOURCE FILE FOR PADEL *****
;
;PART TITLE (MAX 30 CHARACTERS)
;
     PARTNAME/WEAPON-COMPONENT
;
;ORIENT PART IN DESCRIPTION SPACE.
;SPECIFY THE DEGREE OF SYMMETRY; IF ANY.
;
     SYMMETRY/YZPLN
;
;SUB-DIVISION INTO ZONES.
;DEFINE APPROPRIATE CUT PLANES.
;
     CTPL1=  CUTPLN/PARLEL,ZXPLN,YLARGE,0.616
     CTPL2=  CUTPLN/PARLEL,ZXPLN,YLARGE,0.241
;
;THE CUT PLANES ARE DEFINED WITH RESPECT TO THE
;PART COORDINATE SYSTEM.  NOW FOR EACH INTENDED ZONE,
;IDENTIFY THE FOLLOWING:
;  (1) PRIMARY AND SECONDARY DEFINITION PLANES.
;  (2) LOCAL COORDINATE PLANES.
;THE COORDINATE PLANES UPON INTERSECTION WITH THE
;PRIMARY DEFINITION PLANES DEFINE THE X-AXIS AND
;Y-AXIS FOR THE ZONE CONTOURS.  IT IS IMPERATIVE
;THAT THE PROGRAMMER KNOW THE SENSE OF THE POSITIVE
;UNIT NORMALS OF THE PLANES SINCE THEY REPRESENT
;THE POSITIVE AXES OF THE ZONE FRAME.
;
;THE PERTINENT PLANES FOR THE ZONES ARE:
;
;ZONE 1.
;
;PRIMARY PLANE...PRIM1
;
     PRIM1=  PLANE/PARLEL,YZPLN,XLARGE,0.515
;
;SECONDARY PLANE...YZPLN
;LOCAL X-AXIS PLANE...CTPL1
;LOCAL Y-AXIS PLANE...LOCY
;
     LOCY=  PLANE/PARLEL,XYPLN,XLARGE,4.0
```

```
;ZONE 2.
;
;PRIMARY PLANE...PRIM2
;
     PRIM2=   PLANE/PARLEL,YZPLN,XLARGE,0.215
;
;SECONDARY PLANE...YZPLN
;LOCAL X-AXIS PLANE...CTPL2
;LOCAL Y-AXIS PLANE...LOCY
;
;
;ZONE 3.
;
;PRIMARY PLANE...ZXPLN (REVERSED)
;SECONDARY PLANE...CTPL2
;LOCAL X-AXIS PLANE...YZPLN
;LOCAL Y-AXIS PLANE...LOCY3
;
     LOCY3=   PLANE/PARLEL,LOCY,ZSMALL,0.563
;
;
;END OF ALL PLANE DEFINITIONS.
;
;
;START DEFINITION OF ZONES.
;
     ZONE/1
;
;INDICATE THE DEFINITION PLANES.
;
     BETWEEN/PRIM1,YZPLN
;
;INDICATE THE COORDINATE PLANES.
;
     FRAME/CTPL1,LOCY
;
;INDICATE INTERFACE PLANES.
;
     INCLUDE/CTPL1
;
;START OF CONTOUR DEFINITION.
;
     PT0=   POINT/INTOF,XAXIS,YAXIS
     LN1=   LINE/PARLEL,YAXIS,XLARGE,0.663
     PTC1=   POINT/0.798,-0.375
     PTC2=   POINT/1.798,-0.375
     CIR1=   CIRCLE/CENTER,PTC1,RADIUS,0.135
     CIR2=   CIRCLE/CENTER,PTC2,RADIUS,0.135
     LN2=   LINE/PARLEL,XAXIS,YSMALL,0.51
     LN3=   LINE/PARLEL,LN1,XLARGE,1.25
     PT1=   POINT/2.268,-0.935
```

```
      LN4=   LINE/PT1,PARLEL,YAXIS
      LN5=   LINE/PT1,ATANGL,-15,XAXIS
      PT2=   POINT/0.0,-0.61
      LN6=   LINE/PT2,ATANGL,-6,XAXIS
;
;CONTOUR SEQUENCE SPECIFICATION.
;
      TOP/PT0
      GOFWD/XAXIS,LN1,CIR1
      GOACLK/CIR1,LN2
      GOFWD/LN2,CIR2
      GOACLK/CIR2,LN3
      GOFWD/LN3,XAXIS,LN4
;
      BOT/PT2
      GOFWD/LN6,LN5,LN4
;
;REGION DEFINITION FOR ZONE
;
      REGION/LN1,LN3
;
;DOES ANY MASS HAVE TO BE USER INPUT? IF YES THEN:
;
      ADD/
;
;ALL INPUT FOR ZONE I COMPLETE : TERMINATE.
;
      ENDZON/1
;
;
;INPUT FOR ZONE II.
;
      ZONE/2
      BETWEEN/PRIM2,YZPLN
      FRAME/CTPL2,LOCY
      INCLUDE/CTPL1,CTPL2
;
      PT0=   POINT/0.0,0.0
      PT1=   POINT/0.375,0.0
      PT3=   POINT/0.375,-0.61
      PT4=   POINT/0.0,-0.563
;
      TOP/PT0
      GOTO/PT1
;
      BOT/PT4
      GOTO/PT3
;
      ENDZON/2
;
```

```
;INPUT FOP ZONE III.
;
      ZONE/3
      BETWEEN/ZXPLN,CTPL2
      REVERSE/ZXPLN
      FRAME/YZPLN,LOCY3
      INCLUDE/YZPLN
;
      PT0=   POINT/0.0,0.0
      PT1=   POINT/0.499,0.563
      LN1=   LINE/PT1,PARLEL,YAXIS
      PT2=   POINT/0.16,0.0
      LN2=   LINE/PT2,ATANGL,19.0,XAXIS
      PT3=   POINT/INTOF,LN2,LN1
      PT4=   POINT/0.0,0.563
;
      TOP/PT4
      GOTO/PT1
;
      BOT/PT0
      GOTO/PT2
      GOTO/PT3
;
      ENDZON/3
;
;
;DESCRIPTION COMPLETE.
;
      FINISH/
;
;
```

BIBLIOGRAPHY

1. Hirshhorn, J. S., Introduction to Powder Metallurgy, American Powder Metallurgy Institute, New York, 1969.

2. Kuhn, H. A. and Lawley, A., eds., Powder Metallurgy Processing - New techniques and Analysis, Academic Press, 1978, pp 99-138.

3. Downey, C. L., "Powder Preform Forging - An Analytical and Experimental Approach to Process Design" (Ph.D. dissertation, Drexel University, 1972).

4. Suh, S. K., "Prevention of Defects in Powder Preform Forging" (Ph.D. dissertation, Drexel University, 1976).

5. Lally, F. T. and Toth, I. J., Forged Metal Powder Products (TRW Inc. and U.S. Army Weapons Command, August 1972).

6. Kuhn, H. A. and Lawley, A., Op. Cit., pp 139 - 171.

7. Ibid., p. 141.

8. Ibid., p. 149.

9. Keeler, S. P., "Understanding Sheet Metal Formability", Machinery, May 1964.

10. Kuhn, H. A., "Forming Limit Criteria - Bulk Deformation Processes", Proceedings of 21st Sagamore Army Materials Research Conference, Advances in Deformation Processing (Syracuse University Press, 1973).

11. Lee, P. W. and Kuhn, H. A., "Fracture in Cold Upset Forging - A Criterion and Model", Metallurgical Transactions, Vol. 4, 1974, pp 969 - 974.

12. Kuhn, H. A. and Downey, C. L., "Deformation Characterictics and Plasticity Theory of Sintered Powder Materials", Int. J. Powder Metallurgy , Vol 7, 1971, pp 15-25.

13. Shima. S., "A Study of Forming of Metal Powders and Porous Matals", (Ph.D. Dissertation, Kyoto University, Japan, 1975).

14. Honess, H., "Über das Plastiche Verhalten von Sintermetallen bei Raumtemperatur", (Ph.D. Dissertation, Stuttgart University, W. Germany, 1976).

15. Hill, R., "The Mathematical Theory of Plasticity", Clarendon Press, 1950, p. 31.

16. Lee, C. H. and Kobayashi, S., "New Solutions to Rigid-Plastic Deformation problems using a Matrix Method".ASME Transactions, J. Engg. Industry, Vol. 95, 1973, pp 865-873.

17. Thomsen, E. G., Yang, C. T. and Kobayashi, S., "Mechanics of Plastic Deformation in Metal Processing", Macmillan Co., New York, 1965, p. 162.

18. Rooyen, G. T. and Backofen, W. A., "Study of Interface Friction in Plastic Compression", Int. J. Mech. Science, Pergamon Press, Vol. 1, 1960, pp 1-27.

19. Hill, R., op. cit., p. 66.

20. Ibid, p. 67.

21. Male, A.T. and Cockcroft, M. G., "A Method for the Determination of the Coefficient of Friction of Metals under Conditions of Bulk Plastic Deformation", J. Inst. Metals, Vol. 93, 1964, pp 38-46.

22. Halter, R. F., "Pilot Production for Hot Forming Powder Metallurgy Preforms",Modern Developments in Powder Metallurgy - Processes, Vol. 4, Plenum Press, New York, 1971, pp 385-394.

23. Bockstiegel, G. and Bjork, U., "The Influence of Preform Shape on Material Flow, Residual Porosity and Occurrence of Flaws in Hot Forged Powder Compacts". Powder Metallurgy, Vol. 17, No. 33, 1974, pp 126-139.

24. Griffiths, T. J., Jones, W., Lundgren, M. and Bassett, M.B., "Pilot Study of Preform Design for Sinter Forging", Powder Metallurgy, Vol. 17, No. 33, 1974, pp 140-156.

25. Suh, S. K., Kuhn, H. A. and Downey, C. L., "Metal Flow and Fracture in Extrusion Forging Processes", Transactions ASME, J. Engg. Matls and Tech., Vol. 98, 1976, pp 330-336.

26. Kuhn, H. A. and Suh, S. K., "Emperical Models of Die Contact Surface Fracture and Central Burst in Forging", Proceedings: Fourth North American Metal Working Conference, 1976.

27. Downey, C. L. and Kuhn, H. A., "Application of a Forming Limit Concept to the Design of Powder Preforms for Forging", Transactions ASME, J. Engg. Matls. and Tech., April 1975, pp 121-125.

28. APT Part Programming, IIT Research Institute, 1967.

29. Akgerman, N., Subramanium, T. L. and Altan, T., "Manufacturing Methods for a Computerized Forging Process for High Strength Materials", Battelle Columbus Laboratories, Final Report, Air Force Materials Laboratory, Wright Patterson Air Force Base, Ohio, January 1974.

30. Billhardt, C. F., Akgerman, N. and Altan, T., "CAD/CAM for Closed Die Forging of Track Shoes and Links", Battelle Columbus Laboratories, Final Report for AMMRC, Watertown, Mass., July 1976.

31. Akgerman, N. and Altan, T., "Application of CAD/CAM in Forging Turbine and Compressor Blades", Transactions ASME, J. Engg. Power, April 1976, pp 290-296.

32. Chung, H., Unpublished Research, University of Pittsburgh, 1978.

33. Brinkmeyer, L., "Prevention of Defects in Powder Preform Forging", (Unpublished M.S. Thesis, University of Pittsburgh, 1979).

34. Kuhn, H. A., University of Pittsburgh, private communication.

35. Solanki, M., Rock Island Arsenal, private communication.

DISTRIBUTION

	Copies
A. Department of Defense	
Defense Documentation Center ATTN: TIPDR Cameron Station Alexandria, VA 22314	12
B. Department of the Army	
Commander US Army Materiel Development and Readiness Command ATTN: DRCMT 5001 Eisenhower Avenue Alexandria, VA 22333	1
Commander US Army Materiel Development and Readiness Command Scientific and Technical Information Team - Europe ATTN: DRXST-STL, Dr. Richard B. Griffin APO New York 09710	1
Commander US Army Armament Materiel Readiness Command ATTN: DRSAR-RDP DRSAR-SC DRSAR-QAE DRSAR-IRW Rock Island, IL 61299	1 1 1 1
Commander US Army Armament Research & Development Command ATTN: DRDAR-PMP, Mr. Donald J. Fischer Dover, NJ 07801	1
Director US Army Materials and Mechanics Research Center ATTN: DRXMR-M Watertown, MA 02172	2
Commander US Army Maintenance Management Center ATTN: DRXMD-A Lexington, KY 40507	1
Commander US Army Electronics Research and Development Command ATTN: DRSEL-PA-E Fort Monmouth, NJ 07703	1

DISTRIBUTION

	Copies
Commander US Army Missile Research and Development Command ATTN: DRDMI Redstone Arsenal, AL 35809	1
Commander US Army Tank-Automotive Materiel Readiness Command ATTN: DRSTA-Q Warren, MI 48090	1
Commander US Army Tank-Automotive Research and Development Command ATTN: DRDAR-UL DRDTA-RKA Warren, MI 48090	1 1
Commander US Army Aviation Research and Development Command ATTN: DRDAV-EXT P.O. Box 209 St. Louis, MO 63166	1
Commander US Army Troop Support and Aviation Materiel Readiness Command ATTN: DRSTS-PLE 4300 Goodfellow Blvd. St. Louis, MO 63120	1
Commander Ballistic Research Laboratories ATTN: DRXBR-X Aberdeen Proving Ground, MD 21005	1
Commander Harry Diamond Laboratories ATTN: DRXDO-RCD 2800 Powder Mill Road Adelphi, MD 20783	1
Commander New Cumberland Army Depot ATTN: SDSNC-QA New Cumberland, PA 17070	1
Commander Pueblo Army Depot Activity ATTN: DRXPU Pueblo, CO 81001	1

DISTRIBUTION

	Copies
Commander Red River Army Depot ATTN: SDSRR-QA Texarkana, TX 75501	1
Commander Sacramento Army Depot ATTN: SDSSA-QA Sacramento, CA 95813	1
Commander Seneca Army Depot ATTN: SDSSE-R Romulus, NY 14541	1
Commander Sharpe Army Depot ATTN: SDSSH-QE Lathrop, CA 95330	1
Commander Sierra Army Depot ATTN: SDSSI-DQA Herlong, CA 96113	1
Commander Tobyhanna Army Depot ATTN: SDSTO-Q Tobyhanna, PA 18466	1
Director US Army Industrial Base Engineering Activity ATTN: DRXIB-MT Rock Island Arsenal Rock Island, IL 61299	2
Director USDARCOM Intern Training Center ATTN: SDSRR-QA Red River Army Depot Texarkana, TX 75501	1
Commander US Army Tropic Test Center ATTN: STETC-TD Drawer 942 Fort Clayton, Canal Zone	1

DISTRIBUTION

	Copies
Commander Anniston Army Depot ATTN: SDSAN-QA Anniston, AL 36202	1
Commander Corpus Christi Army Depot ATTN: SDSCC-MEE Mail Stop 55 Corpus Christi, TX 78419	1
Commander Fort Wingate Army Depot Activity ATTN: DRXFW Gallup, NM 87301	1
Commander Letterkenny Army Depot ATTN: SDSLE Chambersburg, PA 17201	1
Commander Lexington-Blue Grass Army Depot Activity ATTN: SDSLX Lexington, KY 40507	1
Commander Tooele Army Depot ATTN: SDSTE-QA Tooele, UT 84074	1
Commander Holston Army Ammunition Plant ATTN: SARHO Kingsport, TN 37660	1
Commander Indiana Army Ammunition Plant ATTN: SARIN Charleston, IN 47111	1
Commander Iowa Army Ammunition Plant ATTN: SARIO Middletown, IA 52601	1

DISTRIBUTION

	Copies
Commander Joliet Army Ammunition Plant ATTN: SARJO Joliet, IL 60434	1
Commander Lone Star Army Ammunition Plant ATTN: SARLS Texarkana, TX 75501	1
Commander Louisiana Army Ammunition Plant ATTN: SARLA P.O. Box 30058 Shreveport, LA 71161	1
Commander Milan Army Ammunition Plant ATTN: SARMI Milan, TN 38358	1
Commander Radford Army Ammunition Plant ATTN: SARRA Radford, VA 24141	1
Commander Riverbank Army Ammunition Plant ATTN: SARRB Riverbank, CA 95367	1
Commander Scranton Army Ammunition Plant ATTN: SARSC Scranton, PA 18501	1
Commander Twin Cities Army Ammunition Plant ATTN: SARTC New Brighton, MN 55112	1
Commander Volunteer Army Ammunition Plant ATTN: SARVO-T P.O. Box 6008 Chattanooga, TN 37401	1

DISTRIBUTION

	Copies
C. Department of the Navy	
Commander US Navy Materiel Industrial Resources Office	
ATTN: Code 044, CPT L. C. Dictmar	1
Code 227	1
Philadelphia, PA 19112	
D. Department of the Air Force	
Commander Air Force Materials Laboratory	
ATTN: LTM	1
Wright-Patterson AFB, OH 45433	

AO _____ Accession No._____

Commander, Rock Island Arsenal
ATTN: SARRI-EN
Rock Island, IL 61299

COMPUTERIZED POWDER METALLURGY (P/M) FORGING TECHNIQUES, by Suresh Pillay and Howard Kuhn

Report EN-80-02, Sep 80, 150 p. Incl. Illus. tables, (AMS Code 3297.16.6785) Unclassified report.

Forging of sintered powder preforms is an attractive manufacturing alternative to convention forging as it combines the cost and material saving advantages of conventional, press-and-sinter, powder metallurgy and the property enhancement of forging. The preforms contain a dispersion of voids and forging of such materials into finished shapes must be accomplished such that no defects are formed and all residual porosity is eliminated. These objectives can be achieved through the proper design of the powder preform. The design currently is accomplished through a lengthy trial-and-error procedure.

UNCLASSIFIED

1. Computer-alded design
2. Preform design
3. Powder metallurgy
4. Powder forging

i

DISTRIBUTION
Copies available from DDC.

AO _____ Accession No._____

Commander, Rock Island Arsenal
ATTN: SARRI-EN
Rock Island, IL 61299

COMPUTERIZED POWDER METALLURGY (P/M) FORGING TECHNIQUES, by Suresh Pillay and Howard Kuhn

Report EN-80-02, Sep 80, 150 p. incl. Illus. tables, (AMS Code 3297.16.6785) Unclassified report.

Forging of sintered powder preforms is an attractive manufacturing alternative to convention forging as it combines the cost and material saving advantages of conventional, press-and-sinter, powder metallurgy and the property enhancement of forging. The preforms contain a dispersion of voids and forging of such materials into finished shapes must be accomplished such that no defects are formed and all residual porosity is eliminated. These objectives can be achieved through the proper design of the powder preform. The design currently is accomplished through a lengthy trial-and-error procedure.

UNCLASSIFIED

1. Computer-aided design
2. Preform design
3. Powder metallurgy
4. Powder forging

i

DISTRIBUTION
Copies available from DDC.

AO _____ Accession No._____

Commander, Rock Island Arsenal
ATTN: SARRI-EN
Rock Island, IL 61299

COMPUTERIZED POWDER METALLURGY (P/M) FORGING TECHNIQUES, by Suresh Pillay and Howard Kuhn

Report EN-80-02, Sep 80, 150 p. Incl. Illus. tables, (AMS Code 3297.16.6785) Unclassified report.

Forging of sintered powder preforms is an attractive manufacturing alternative to convention forging as it combines the cost and material saving advantages of conventional, press-and-sinter, powder metallurgy and the property enhancement of forging. The preforms contain a dispersion of voids and forging of such materials into finished shapes must be accomplished such that no defects are formed and all residual porosity is eliminated. These objectives can be achieved through the proper design of the powder preform. The design currently is accomplished through a lengthy trial-and-error procedure.

UNCLASSIFIED

1. Computer-aided design
2. Preform design
3. Powder metallurgy
4. Powder forging

i

DISTRIBUTION
Copies available from ODC.

AD _____ Accession No._____

Commander, Rock Island Arsenal
ATTN: SARRI-EN
Rock Island, IL 61299

COMPUTERIZED POWDER METALLURGY (P/M) FORGING TECHNIQUES, by Suresh Pillay and Howard Kuhn

Report EN-80-02, Sep 80, 150 p. incl. Illus. tables, (AMS Code 3297.16.6785) Unclassified report.

Forging of sintered powder preforms is an attractive manufacturing alternative to convention forging as it combines the cost and material saving advantages of conventional, press-and-sinter, powder metallurgy and the property enhancement of forging. The preforms contain a dispersion of voids and forging of such materials into finished shapes must be accomplished such that no defects are formed and all residual porosity is eliminated. These objectives can be achieved through the proper design of the powder preform. The design currently is accomplished through a lengthy trial-and-error procedure.

UNCLASSIFIED

1. Computer-aided design
2. Preform design
3. Powder metallurgy
4. Powder forging

i

DISTRIBUTION
Copies available from ODC.

Empirical design rules have been established, from simple model experiments, to facilitate the proper design of preforms. Application of these rules to complex components requires an understanding of the behavior of porous materials with respect to densification, flow and fracture and the effects of die design, lubrication and temperature.

An interactive computer-aided design approach was developed to facilitate the design and evaluation of preforms. The design was accomplished in two phases. The first phase described the part to be forged together with a schematic subdivision of the part into regions. The second phase involved the specification of trial preform shapes for the part. The program evaluated the input shape for densification and non-aggravating metal flow. This was accomplished by recognizing characteristic deformation modes in the input shape for which available design rules have been programmed. By interactively manipulating the preform shape, a proper preform may be obtained rapidly. The program determines the size and mass distribution required in the preform to achieve full densification.

The present program was implemented for non-axisymmetric parts with a reasonably complex geometry. The procedure developed was applied to a weapon component wherein the designed preform was trial forged and metallurgically evaluated. The success of the forging encourages further study to extend the accuracy and capabilities of the present approach to other part configurations.

Empirical design rules have been established, from simple model experiments, to facilitate the proper design of preforms. Application of these rules to complex components requires an understanding of the behavior of porous materials with respect to densification, flow and fracture and the effects of die design, lubrication and temperature.

An interactive computer-aided design approach was developed to facilitate the design and evaluation of preforms. The design was accomplished in two phases. The first phase described the part to be forged together with a schematic subdivision of the part into regions. The second phase involved the specification of trial preform shapes for the part. The program evaluated the input shape for densification and non-aggravating metal flow. This was accomplished by recognizing characteristic deformation modes in the input shape for which available design rules have been programmed. By interactively manipulating the preform shape, a proper preform may be obtained rapidly. The program determines the size and mass distribution required in the preform to achieve full densification.

The present program was implemented for non-axisymmetric parts with a reasonably complex geometry. The procedure developed was applied to a weapon component wherein the designed preform was trial forged and metallurgically evaluated. The success of the forging encourages further study to extend the accuracy and capabilities of the present approach to other part configurations.

Empirical design rules have been established, from simple model experiments, to facilitate the proper design of preforms. Application of these rules to complex components requires an understanding of the behavior of porous materials with respect to densification, flow and fracture and the effects of die design, lubrication and temperature.

An interactive computer-aided design approach was developed to facilitate the design and evaluation of preforms. The design was accomplished in two phases. The first phase described the part to be forged together with a schematic subdivision of the part into regions. The second phase involved the specification of trial preform shapes for the part. The program evaluated the input shape for densification and non-aggravating metal flow. This was accomplished by recognizing characteristic deformation modes in the input shape for which available design rules have been programmed. By interactively manipulating the preform shape, a proper preform may be obtained rapidly. The program determines the size and mass distribution required in the preform to achieve full densification.

The present program was implemented for non-axisymmetric parts with a reasonably complex geometry. The procedure developed was applied to a weapon component wherein the designed preform was trial forged and metallurgically evaluated. The success of the forging encourages further study to extend the accuracy and capabilities of the present approach to other part configurations.

Empirical design rules have been established, from simple model experiments, to facilitate the proper design of preforms. Application of these rules to complex components requires an understanding of the behavior of porous materials with respect to densification, flow and fracture and the effects of die design, lubrication and temperature.

An interactive computer-aided design approach was developed to facilitate the design and evaluation of preforms. The design was accomplished in two phases. The first phase described the part to be forged together with a schematic subdivision of the part into regions. The second phase involved the specification of trial preform shapes for the part. The program evaluated the input shape for densification and non-aggravating metal flow. This was accomplished by recognizing characteristic deformation modes in the input shape for which available design rules have been programmed. By interactively manipulating the preform shape, a proper preform may be obtained rapidly. The program determines the size and mass distribution required in the preform to achieve full densification.

The present program was implemented for non-axisymmetric parts with a reasonably complex geometry. The procedure developed was applied to a weapon component wherein the designed preform was trial forged and metallurgically evaluated. The success of the forging encourages further study to extend the accuracy and capabilities of the present approach to other part configurations.